Electric space-charge measurements in convective and other weather conditions

Ogden, Trevor, L.

ELECTRIC SPACE-CHARGE MEASUREMENTS IN CONVECTIVE AND OTHER WEATHER CONDITIONS

by

TREVOR L. OGDEN, B.Sc.

A Thesis Presented In Candidature for the Degree of Doctor of Philosophy in the University of Durham

August 1967.

FOREWORD

The main part of this thesis describes the investigation of space-charge movements in convective weather. Measurements in other weather conditions, which were made as the opportunity allowed, are described in chapters 7 to 9. All the experiments, however, were concerned with the movement of space charge.

Throughout the thesis, the sign of the atmospheric potential gradient is taken as positive if a small positive charge would tend to move towards the Earth. The term "field" is not used where its sign is important. Currents are taken as positive if they tend to neutralize the Earth's charge, i.e. transfer positive charge downwards or negative charge upwards, and space-charge density gradients as positive if the positive charge density increases upwards or negative charge density increases downwards. These conventions are consistent in that a positive potential gradient gives a positive conduction current, and a positive density gradient a positive convection current. The usual fine-weather day-time conditions give a positive conduction current and probably a negative convection current. In dynamic meteorology, the upwards direction is taken as positive.

The term "convection current" is only used to denote the transfer of electric charge by convection. Readers unfamiliar with the subject of turbulent transfer may find the reviews by Priestley (1959) and Webb (1964) useful introductions.

Rationalized MKS units are used exclusively in the theoretical work, and in most other cases, although I have broken this rule where common sense demanded, e.g. to express a length in cm. I have also respected the custom in ice work of measuring charges in electrostatic units. The following conversion factors may be found useful.

1 e cm^{-3}	=	0.16 pC m^{-3}
125 e cm^{-3}	=	20 pC m^{-3}
250 e cm^{-3}	=	40 pC m^{-3}
1 esu	=	3.33×10^{-10} C
1 esu gm^{-1}	=	0.33 μC kgm^{-1}

"Vibrating-Reed Electrometer" is usually abbreviated to "V.R.E."

I wish to express my debt to my supervisor for the last two years, Dr. W.C.A. Hutchinson, for his help and advice, and also to the late Professor J.A. Chalmers, who supervised the first year of the work, and continued to take an active interest up to the time of his death. It

is a pleasure to thank Professor G.D. Rochester for the provision of research facilities in the Department, the Departmental Technical Staff for their assistance, especially Mr. Jack Moralee, and the Science Research Council for a maintenance and equipment grant. Without the willing co-operation of local landowners and farmers, much of the work would have been impossible, and I am especially grateful, for permission to use the site at Mordon West Farm, to the land agent of the Eldon Estates, Mr. R.H. Scrope, F.L.A.S., Eldon Estate Office, Eldon, Bishop Auckland. In addition, I wish to express my thanks to Dr. M. Stone, Reader in Mathematical Statistics in this University, for his advice on section 6.4.5.

I also have to thank my fellow research students in the Atmospheric Physics Group, who have never hesitated to point out shortcomings in the work, and have occasionally suggested ways of overcoming them. In this respect I am particularly indebted to Mr. I.M. Stromberg, who gave generous and valuable help with electronics. His particular contributions are acknowledged in the text.

Finally, the typescript was prepared by Miss Elaine Bunton, to whom I am very grateful for her speed and efficiency.

T.L.O.

ABSTRACT

Theories of convection below cloud-base are reviewed, together with experimental techniques and evidence. It is concluded that, over land in sunny weather, a forced convection layer is probably overlain by one in which the heat flux is carried by buoyant plumes which may change their form at a few hundred metres.

If space charge is considered as carried by air movement, the convection current i_2 in forced convection is given by

$$i_2 = k^2 z^2 \frac{\partial u}{\partial z} \frac{\partial \sigma}{\partial z}$$

where k is von Karman's constant, z the height, u the mean horizontal wind-speed, and σ the space-charge density. In free convection

$$i_2 = \left(\frac{h^2 H g}{T \rho C_p} \right)^{\frac{1}{3}} z^{4/3} \frac{\partial \sigma}{\partial z}$$

where h is a number equal to about 0.9, H the heat flux, T the absolute temperature, Cp the specific heat and ρ the density of air, and g the acceleration due to gravity. Buoyant plumes will probably have space-charge density excesses, of magnitude much less than 1 pC m^{-3}.

Measurements of space-charge density with filtration apparatus show pulses lasting about 40 s, and about

40 pC m^{-3} high: these seem to be associated with free convection, but are probably not coincident with buoyant elements. The horizontal diameters and separations of the pulses are proportional to wind-speed.

The turbulence theory could be used to determine the charge given to the air by melting ice by measuring the space-charge density gradient over melting snow. A calculation from earlier results gives a charge of about 0.16 μC kgm^{-1} melted, similar to values obtained by other methods.

Measurements of potential gradient near a small group of deciduous trees in stormy weather are provisionally explained in terms of point discharge, starting at about 1000 V m^{-1} and reaching 0.5 μA at 1650 V m^{-1}.

Observations in fog show negative space charge originating at power lines, confirming earlier work, and suggest the use of space charge measurements to study atmospheric diffusion from a point source.

CONTENTS

PAGE

LIST OF SYMBOLS

Constants without particular significance are not listed. Where the meaning of a symbol changes from chapter to chapter, the chapter number is given in brackets before the meaning.

$\bar{B}$	Buoyancy factor
C	(5) Field mill stator-earth capacitance
Cp	Specific heat at constant pressure
D	(4) Diffusion coefficient of ions
d	(8) Horizontal distance of field mill from discharging point
e	Electronic charge
F	(1) Radial turbulent potential heat flux; (2-) Potential gradient
f	Field mill signal frequency
g	Acceleration due to gravity
H	Heat flux
H^*	Dimensionless heat flux
h	(8) Height of discharging point
I	Stator-earth current
i	Total air-earth current; (8) Point-discharge current
i_1	Conduction current
i_2	Convection current
K_m	Momentum turbulent transfer coefficient
K_q	Charge turbulent transfer coefficient
k	(2 & 7) Von Karman's constant; (4) Boltzmann's constant; (8) $\frac{\text{radius of diffusing plume}}{\text{distance from origin}}$

w	(1) Velocity in z direction; (4) Mobility of ions
w_1	Mobility of positive small ions
w_2	Mobility of negative small ions
x	Horizontal measurement
z	Vertical measurement
z_o	Roughness length
Γ	Dry adiabatic lapse rate
ε_o	Permittivity of free space
θ	potential temperature
μ	Ratio of horizontal and vertical radii in a bubble
ν	Kinematic viscosity of air
ρ	Density of air
σ	Space-charge density
τ	Vertical turbulent shear stress (= momentum flux)
ϕ	Angle
χ	Nuclei concentration
ω	Angular signal frequency

SUFFIXES

e	environmental value
m	maximum value
'	excess over environment

This page should come after the next.

L	(1 & 2) Obukhov's length scale; (7) latent heat of melting of ice
l	(4) Length of tube; (6) Intersection length of pulse
n	(5) Field-mill frequency in r.p.m.
n_1	Density of all positive ions
n_2	Density of all negative ions
n_{s1}	Density of positive small ions
n_{s2}	Density of negative small ions
P	Columnar resistance of atmosphere
Q	(2) Radial space-charge flux; (4) Gas flow-rate
R	(1 & 2) Horizontal radius of buoyant element; (5) Stator-earth resistance
R_i	Richardson's number
R_o	(1 & 2) Most probable value of R
r	(1 & 2) Horizontal distance from centre of buoyant element; (8) Radius of diffusing plume
S	Charge released per kilogram of melting snow ("specific charge")
T	Absolute temperature
T_*	Temperature scale value
t	(6) Half-peak duration of pulse
u	Velocity in x direction
u_r	Radial velocity
$\bar{u}$	Mean wind-speed over half hour
u_*	Friction velocity
V	(2) Potential of Electrosphere; (5) Signal voltage on stator; (8) Plate-earth voltage
V_o	(8) Threshold value of V
V_∞	(5) Stator signal voltage at $\omega = \infty$

CHAPTER 1

CONVECTION BELOW CLOUD-BASE

1.1 Introduction

The recognition of convection as a mode of heat transfer in fluids came eight years after Montgolfier's first use of it for flight. Archimedes was traditionally the first to understand why an object placed in a liquid rises to the surface if its weight is less than that of an equal volume of water, but it was not until 1797 that Rumford (1870) discovered that this phenomenon could transfer heat through a fluid, when the "immersed body" was a volume of the same fluid at a different temperature. We now call this form of heat transfer "buoyant convection" or "free convection". It is to be distinguished from "forced convection", which is also heat transfer by bulk movement of the fluid, but occurring when the motion is imposed not by buoyancy but by some other force, such as shear stress, when a velocity gradient occurs in the fluid. As will be shown, forced convection is also an important factor in atmospheric heat transfer, but for the remainder of this chapter the word "convection" on its own will be used to mean free convection.

The problem of atmospheric convection is basically this:

Of the sun's radiation incident on the Earth, only about 13% is directly absorbed by the troposphere, compared with about 48% which is absorbed by the ground. Part of this 48% is used in evaporating moisture, or in photosynthesis, but much is transferred to the first few metres of the atmosphere by radiation and conduction. This heat is distributed to the rest of the atmosphere by free and forced convection: what is the relative importance of these modes, what is the form of the buoyant convective elements, and what factors affect them?

This chapter reviews the methods of investigation and the present evidence on these questions. The experimental study described in later chapters concerns only the lowest few metres of the atmosphere, but this survey is necessary not only to set the measurements made in their context in regard to the rest of the troposphere, but also because similar measurements made by other workers have been interpreted in terms of, for example, cellular structure in the whole region below cloud-base, and this must therefore be reviewed.

1.2 The Nature of the Evidence

Direct measurements of the most important two parameters in determining convective structure, temperature gradients and vertical air velocity, can only be made from

instruments on an aircraft or on a structure attached to the ground, although much information can be gained from indirect methods. Before the main theories of convection are compared, the methods of gaining evidence for them must be mentioned.

1.2.1 Powered aircraft

These provide the best evidence available of atmospheric structure above a few tens of metres. Temperature and humidity can be measured with probes, and vertical air velocity by detecting the vertical acceleration of the aircraft. By using quick-response apparatus, features two or three metres in diameter can be resolved. This method has the advantage of allowing a survey of a fairly large area quickly, and comparisons can be made of the thermal structure over different surfaces, for example. Although the measurements are reliable, the picture a flight gives is basically one-dimensional, along the line of flight. Attempts have been made to overcome this. It is possible, for example, to try to detect the same thermal structures at several heights by flying along a constant heading, and then returning to a point more or less above the starting-point while allowing the aircraft to drift with the wind, and then flying back along the original heading. (This method was adopted, for example, by

Grant (1965)). Also, a very limited picture in a horizontal plane can be obtained by putting instruments on different parts of the aircraft (Warner and Telford (1963)). Where a very large number of results is available, statistical analysis can yield a fuller picture.

1.2.2 Gliders

Much information on "thermals" (i.e. regions of buoyant rising air) can be obtained from sailplane pilots, who rely on them to gain height. (A glider is any engineless aeroplane; a sailplane is one designed to gain height by "soaring" in thermals or wave-clouds behind ridges). Such information is, however, unsystematic and limited. The pilot usually measures air-speed and vertical speed, and can therefore report on such factors as the distribution and strength of thermals, the altitudes at which they become apparent and die away, and their relation to clouds. Likely "hot-spots" - features on the ground which act as sources of thermals - and their variation with time of day and other factors are well-known to the pilot. However, the glider moves with the air, and the information is limited by this. If lift ceased suddenly, for example, it would be difficult for the pilot to tell whether he had flown out of the side of a "plume" or dropped through the bottom of a "bubble" of rising air. For this reason, most

glider pilots, when questioned specifically about structure of thermals, tend to support whatever theory of convection is currently popular. For example, Rainey (1947), interpreted his flights in terms of cellular convection, which was favoured at that time. On the other hand, Yates (1953) accounted for gliding data in terms of the "eroding bubble" theory published that year, but Scorer (1957) and Woodward (1959) both felt the gliding evidence supported the "entraining bubble" theory.

It might be expected that more valuable information might be gained by "reading between the lines" in more informal literature designed for fellow enthusiasts rather than meteorologists. For this reason, the author has tried to read widely in gliding magazines and other literature. The results of this are reported in section 1.4.

One tool which might possibly be applied to exploring thermals, which does not yet seem to have been used, is one of the powered sailplanes now available. These carry a small engine which enables them to fly like any other powered aircraft, but when the engine is switched off, they have sufficiently good aerodynamic performance to soar. This should overcome the limitation imposed on gliders of having to adapt their flight path to maintain height, and should allow more systematic work.

1.2.3 Birds and insects

Many species of bird take advantage of thermal upcurrents, and some types, such as vultures and cheels, rely on thermals to soar. Woodcock (1940) observed the soaring of herring-gulls over the sea, and his observations of the relation of different methods of soaring to wind and temperature conditions were later explained very neatly by Priestley (1956) in terms of the plume theory. The eroding bubble theory was also supported from the bird and insect observations of Hankin (1913) by Scorer (1954b). To some extent, soaring birds make convection currents visible, and can give useful information on their distribution, strength and vertical extent.

1.2.4 Fixed-site investigations

Observations of atmospheric parameters from towers on the ground have been used to make deductions about convective processes. The advantages of this method are attractive: the instruments do not move relative to the ground, of course, the construction and installation of measuring equipment, of power supplies, and of recording apparatus are relatively easy, and the whole operation is cheaper. However, measurements are usually limited to the bottom few score metres of the atmosphere. The plume

theory is based on tower measurements, but the height limitation has so far prevented detailed extrapolation upwards. This limitation has been overcome by using moored balloons (Jones and Butler 1958), but the greater the height of the support for the instruments, the greater the danger that it will interfere with the phenomena it is to investigate.

1.2.5. Water-tank experiments

The extension to the atmosphere of observations made in liquids was the basis of the theory of cellular convection, and these experiments will be mentioned in section 1.3.1. In more recent years water-tank experiments have been used to provide valuable information for the bubble theory (section 1.3.2). However, the differences between a water-tank and the atmosphere do not need emphasis. The effects of boundaries, the large differences between air and water of density, surface tension, viscosity, thermal conductivity, and specific heat make interpretation difficult. In a liquid, viscosity decreases with temperature; in a gas it increases. Moreover, conditions in water-tank experiments are generally much steadier than they are in the atmosphere. Information can be obtained from these experiments on general hydrodynamic processes which may take place in the atmosphere, but care must be exercised in drawing conclusions.

1.2.6 Cloud observations

Photographic and visual observations of turrets growing from the top of cumulus clouds have been used as evidence about the behaviour of similar rising masses of air below cloud-base. However, these turrets frequently grow into stably-stratified air, and they may also be cooled at the outside by evaporation of the cloud droplets, and so the conditions are considerably different from those of masses of air rising from the ground. In recent years, more valuable information has been gained from satellite photographs of large-scale cloud patterns indicating some organised convective behaviour. This will be dealt with more fully below (section 1.3.1), as will the familiar phenomenon of "cloud-streets" - long rows of cumulus cloud.

1.2.7 Radar

Radar is now a familiar tool in disturbed-weather meteorology, but in the last few years it has become apparent that centimetre-wavelength radar can be useful in tracking refractive index changes in fine weather. The results do not at the moment fit in very well with any of the currently-favoured theories of convection, but they will be discussed under the bubble theory, which they seem to support most closely. It is to be hoped that

this method, which alone seems to offer the chance of simultaneous observations over a wide area and depth of atmosphere, will yield more information in future.

1.3 Convection Models

As has already been indicated, theories of atmospheric convection are based on three models: the cell, the bubble, and the plume. The evidence for these interpretations, and the relations between them, will now be considered.

1.3.1 The cell theory

Cellular convection may be defined as a horizontally periodic arrangement of upcurrents of warm fluid and downcurrents of cooler fluid. An example is the Bénard cellular structure. A cooling liquid breaks up into a pattern of polygonal cells in which an upcurrent is surrounded by a region of downcurrents, usually when the liquid is in a thin layer uniformly heated from below. This phenomenon is observed in many liquids, and is particularly striking when the liquid carries a suspension of elongated particles which line themselves along the direction of flow, and are therefore more obvious where the flow is parallel to the surface than where it is perpendicular. Aluminium paint thinned with turpentine,

whose evaporation at the surface causes the temperature gradient, gives a good illustration. Cellular structure also occurs in layers of gases, but here the downcurrent is at the centre and the upcurrent at the edges of the cells. When a shear is applied to the fluid, the cells change shape, usually forming long strips parallel to the direction of shear. Thomson (1881) first described the phenomenon, but it was first thoroughly investigated by Bénard (1900). Rayleigh (1916) carried out the original theoretical analysis and showed that the way in which the viscosity changes with temperature determines the direction of motion in the cell, accounting for this difference between gases and liquids.

The suggestion that similar cellular convection occurs in the atmosphere was made by Brunt (1925), who pointed out the modifications that would be necessary to Rayleigh's theory. However, the much more complicated situation of the atmosphere, with such effects as wind-shear, turbulent rather than molecular diffusion, and the lack of a firm upper limit has made analysis difficult. Most writers seem to be concerned with whether or not cellular convection could occur in a fluid like air on a scale comparable with the atmosphere, rather than with whether or not it does occur in practice. It seems fair to say that a firm conclusion from the theoretical standpoint has

not yet been reached. A comprehensive account and bibliography of attempts are given by Chandrasekhar (1961).

It may be remarked that Priestley (1959) took the condition for cellular convection in still air obtained by Rayleigh (1916) and Jeffreys (1928), and showed that, in the atmosphere near the ground, free convection is found to set in long before this condition is fulfilled, indicating strongly that Benard cellular convection is unlikely in wind over land.

For many years after Brunt's suggestion, experimental evidence of atmospheric cellular convection was small. The familiar dapples and billows which commonly occur in layer clouds were compared with the patterns in liquids, and it was suggested that they were due to cellular motion in the cloud layer (Mal 1930, Brunt 1937). These billows form along the wind direction, and must be distinguished from transverse rolls, which are due to a vorticity effect.

It was also suggested that similar rolls between cloud-base and ground would account for cloud-streets, but this is clearly an over-simplification. Kuettner (1959) has outlined a more convincing explanation, which is based on what may still be broadly described as cellular convection. According to Kuettner, cloud-streets, long rows of cumulus aligned roughly in the direction of the wind,

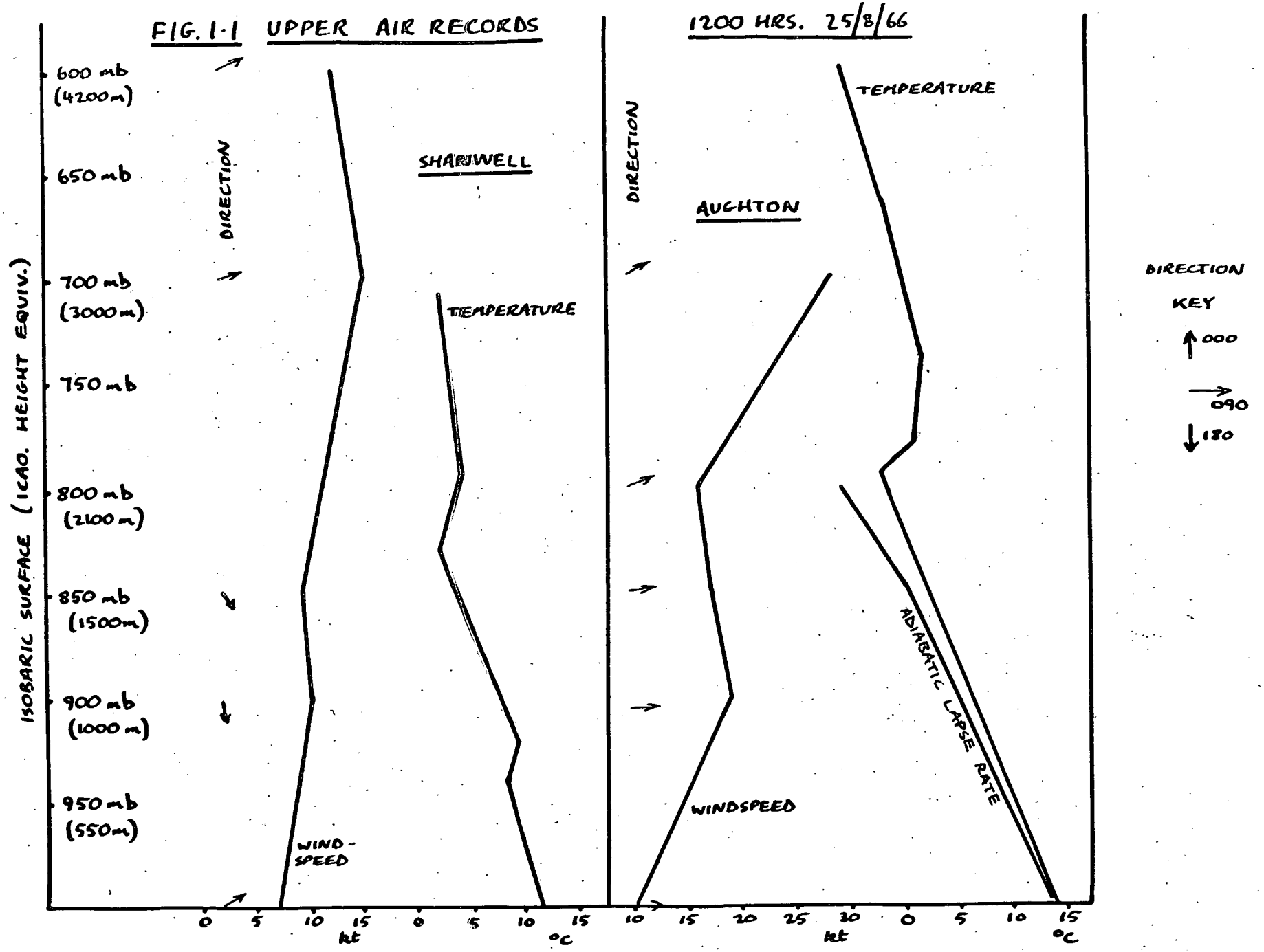
FIG. 1·1 UPPER AIR RECORDS
1200 HRS. 25/8/66
600 mb (4200m)
650 mb
700 mb (3000m)
750 mb
800 mb (2100m)
850 mb (1500m)
900 mb (1000m)
950 mb (550m)
ISOBARIC SURFACE (ICAO. HEIGHT EQUIV.)
DIRECTION
SHAWWELL
TEMPERATURE
WIND-SPEED
0 5 10 15 kt
0 5 10 15 °C
DIRECTION
AUGHTON
TEMPERATURE
ADIABATIC LAPSE RATE
WINDSPEED
10 15 20 25 30 kt
0 5 10 15 °C
DIRECTION KEY
000
090
180

are common over a large part of the earth's surface, and in some are the predominant type of convective cloud. From inspection of many cases, he concluded that streets outside the tropics occur when a polar high irrupts into the temperate zone, and is heated from below. The resulting air-flow is from cold to warm, with the high pressure on the right. Kuettner showed that the result will be a maximum windspeed in the convective layer - not at the surface - and little change of direction with height. He suggested that the curvature of the wind gradient will mean that ascending and descending parcels of air will have opposing vorticities, and that this will inhibit convective circulations in the wind direction in favour of circulations perpendicular to it, giving cloud-streets.

Confirmation of this theory has come from Japan in a study of banded cloud and snowfall by Higuchi (1963). It is interesting to note that, due to the easterly progression of weather in the north temperate zone, the irruption of a polar high is much more likely on the eastern side of a continental mass, such as in Japan or the north-east United States, than on the western. This may account for the comparative rarity of cloud-streets in the British Isles. The author has noted three examples at Durham in the last two years (16.6.65., 15.10.65, and 28.8.66. all near midday), of which only the last, the most marked, occurred

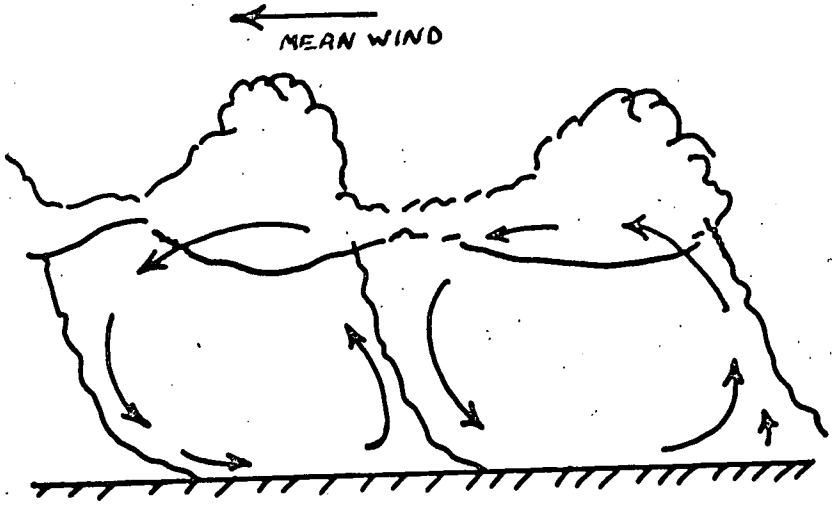

(a) SECTION

FIG. 1·2 DURST CELLS

(b) PLAN

in the conditions described by Kuettner, with a polar anticyclone over the Norwegian sea giving a ridge of high pressure over the British Isles. Figure 1·1 shows the upper-air records taken at Shanwell (Fife) and Aughton (Liverpool) at 1200 hours on August 25th. In both cases there is a maximum windspeed in the first 1500 m (although the paucity of readings makes it difficult to be more specific about the height), and a backing of windspeed with height above the maximum. The other two examples occurred in confused synoptic situations, with no clear distinguishing features.

Durst (1932) interpreted measurements of windspeed variations in terms of a rolling cellular structure (Fig. 1·2). The passage of a cell wall ("gust front") would be marked by the appearance of air from a higher level, i.e. colder, with higher speed, and less turbulent. Although this account was well-supported by the evidence presented in the paper, there seems to have been no substantial supporting evidence found since.

Until high-altitude cloud-photographs became available, the evidence for atmospheric cellular convection, other than in cloud layers, was very small, but when satellite photographs began to be commonplace, cellular cloud patterns were at once noticed. It soon became apparent that these were common, and covered

large areas. They had presumably previously escaped attention because their size was too great to be obvious to an individual observer, but too small to appear on a synoptic chart. Typically, they consisted of cumulus clouds arranged in rings 30 to 50 miles in diameter, cloud groups, or cloud bands. A simple Bénard structure seemed to be precluded both by the diameter-height ratio (an order of magnitude larger than that usually supposed) and by the fact that the rings, bands and groups were composed of distinct individual clouds rather than cloud masses.

Krueger and Fritz (1961)* described the patterns and analysed the conditions for their occurrence. These seemed to be a layer of moist air about 1700 m deep over an ocean surface warm enough to maintain the adiabatic lapse-rate through the layer. Through this layer there was little variation with height of windspeed or direction. The layer was superposed by a more stable air-mass. Frenzen (1962) interpreted these results in terms of two superimposed Bénard patterns of slightly different wavelengths. In the case of the cloud groups, the patterns would be in the unstable layer, interfering to give reinforced upcurrents at intervals much larger than in the simple Bénard case. Frenzen also accounted for the presence of

individual clouds rather than a mass. For the cloud rings, one of the patterns would be in the unstable, and the other in the overlying layer.

Cells had already been indicated under similar conditions by the results of Woodcock and Wyman (1947) and Langwell (1948), who all worked in the trade wind zone, where cool air was blowing over a warmer sea. It is interesting to note that of all atmospheric conditions this corresponds most closely to the circumstances for the production of cells in a liquid: steady and uniform heating from below, and little shear in the convective layer.

Although the exact form of the mechanism has yet to be elucidated, it seems probable that some form of cellular convection is taking place in this case. However, there is very little evidence that cellular convection of the Bénard or Durst type occurs over the land below cloud-base: the presence of wind-shear, surface height irregularities, and non-uniform heating make some other form much more likely.

1.3.2 The bubble theory

Early glider pilots (e.g. Hirth 1933) saw thermals as bubbles of warm air rising from near the surface towards cloud-base. The support given to the cell model by such

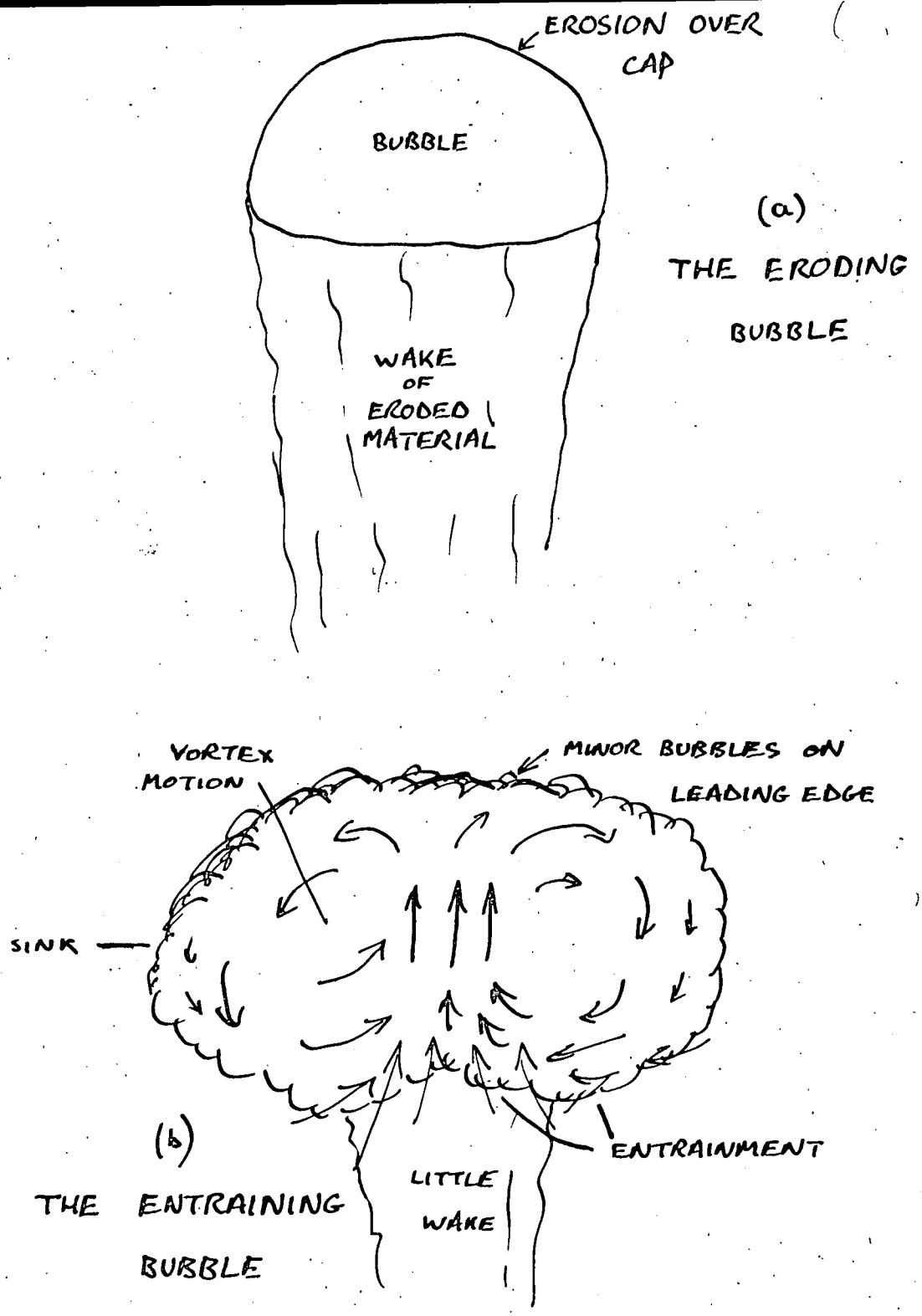

FIG. 1·3 THE BUBBLE THEORIES

authorities as Brunt led later pilots to interpret thermals according to this picture, but the bubble model was formally revived by Scorer and Ludlam(1953). This formulation imagined the bubbles as having a spherical top and a flat base, like an air bubble rising in water (Fig. 1.3a). Little air penetrated the top, although mixing took place over this surface, and the bubble was therefore eroded as it rose. (In this thesis, this is referred to as the "eroding bubble" theory.) The bubble tended to sweep smaller ones in behind it, and these, and eroded cap material, gave a wake cooler than the bubble itself, but warmer than its surroundings. When it had risen a distance equal to one or two diameters, the bubble was all eroded away, but the warm wakes of successive bubbles heated an increasingly deep layer of air, which could then break away as a larger bubble. In this way, successively larger bubbles rose from a heat source, until they were big enough to reach cloud-base.

This model was postulated to explain reports of glider pilots, and gained support from observations of cumulus turrets (Malkus and Scorer 1955). However, experiments in water-tanks (Scorer and Ronne 1956), soon showed that this type of bubble would only occur if a

buoyant air-mass penetrated stably stratified surroundings. Although this happens above clouds, it is not, of course, relevant to convection below cloud-base in unstable conditions, and except for one recent piece of evidence, warrants no further discussion.

The evidence concerned comes from observations of anomalous radar echoes - "angels" - at centimetre wavelengths, whose diurnal and annual variation follow convective activity. Short-term variations show frequency increasing with higher surface temperature and decreasing with higher wind-speed. No echoes are obtained for a surface windspeed greater than 10 m s^{-1}. These features indicate some kind of convective disturbance, causing refractive index changes which give rise to the echoes. However, the echoes obtained are such that they must arise either from point objects, or from large smooth hemispherical reflectors with horizontal bases - the objects are only in focus at the zenith, although results at small angles to the vertical indicate the hemispheres may have rough edges. The objects have vertical velocities between +3 and -3 m s^{-1}, with a mean of +1 m s^{-1}. The important discrepancy with the eroding bubble model is, however, the size: the hemispheres have diameters of 1-3 km (at heights of 1½ - 3 km). This is an order of magnitude larger than the thermals of glider

pilots, and is difficult to fit in with other data on bubbles. Perhaps it is best to reserve judgement on this phenomenon until simultaneous measurements of the hemispheres and temperature traverses in the air are available. A survey of results is given by Atlas (1964).

The results of Scorer and Ronne, developed by Scorer (1957) and Woodward (1959), showed that a bubble rising through an unstratified environment would have a vortex-like motion with mixing at the front surface, some entrainment behind, and little wake (Fig. 1.3b). This is referred to here as the "entraining bubble" model. The vertical velocity of the core is about twice the velocity of the bubble as a whole, and at the edges, the motion is actually downwards, recalling the observations of some glider-pilots that "sink" sometimes surrounds a thermal. By dimensional analysis, Scorer (1957) found the vertical velocity w to be related to the radius of the largest horizontal section of the bubble R and the buoyancy $g\bar{B}$ by

$$w = D(g\bar{B}R)^{\frac{1}{2}} \qquad (1.1)$$

$\bar{B}$ has the form density difference divided by total density. D is a dimensionless constant found by experiment in the water tank to be about 1.2, and cloud observations give a similar value.

The radius of the bubble is also found to be proportional to its distance z from an ideal origin,

$$z = nR \qquad (1.2)$$

and n is found to vary from one thermal to another, but is approximately equal to 4.

Scorer (1958, p.174) shows that these relationships give the potential temperature lapse-rate found experimentally in the free-convection regime,

$$\frac{\partial \theta}{\partial z} \propto z^{-4/3} \qquad (1.3)$$

but this is, of course, a characteristic of any free convection model that makes the similarity assumption (Priestley 1954).

Experimental evidence that bubbles of the postulated form occur in the atmosphere is small. There is some evidence from glider pilots (section 1.4), but this is subject to the doubts expressed in section 1.2.2. The evidence from powered aircraft is more useful, and is surveyed in section 1.5.

As will be seen from the next section, measurements on towers generally favour the plume model, but mention must be made of the results of Bunker (1953) who measured temperature and vertical velocity at 25 m and 100 m on a mast, and interpreted his results in terms of bubbles. It is difficult to see from Bunker's paper

whether or not his results are consistent with the plume theory. He found a typical bubble at 25 m to have a diameter of 90 m, a temperature excess of ½°C, and a vertical velocity of 0.9 m s^{-1}. At 100 m, the bubbles were less frequent, but more easily separated from the surrounding air, and commonly had a diameter of 500 m, temperature excess of 0.6°C., and vertical velocity of 1 - 1.4 m s^{-1}. Apart from the diameter at 100 m, which is rather large, these measurements accord well with data from aircraft.

In conclusion, the bubble theory would provide a satisfactory picture of buoyant convection, but conclusive evidence of its widespread applicability to the atmosphere is lacking. A comparison of critical evidence with the plume theory will be made in section 1.6.

1.3.3 The plume theory

It has already been mentioned that temperature gradient measurements near the ground indicate that in the free convection region, $\partial\theta/\partial z \propto z^{-4/3}$, and that this proportionality can be derived from dimensional analysis without specifying the structure of the buoyant elements. Below this zone, heat transfer is by turbulent transfer alone. Qualitatively, it may be considered that the

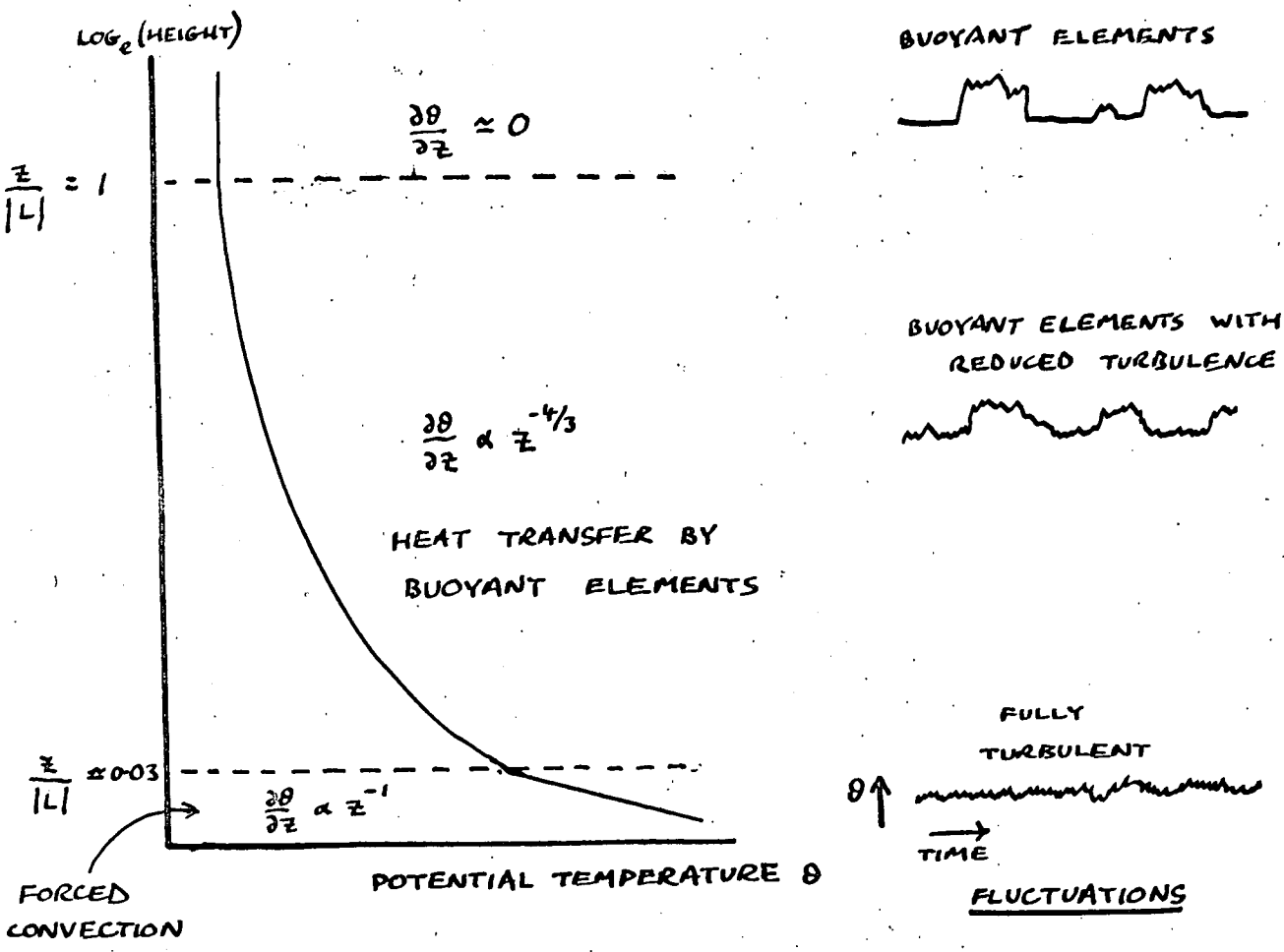

FIG. 1·4 TEMPERATURE STRUCTURE IN THE FIRST FEW TENS OF METRES (AFTER WEBB 1964)

THE DIAGRAMS ON THE RIGHT SHOW HOW CONTINUOUS MEASUREMENTS OF TEMPERATURE OR VERTICAL VELOCITY REVEAL A PULSE STRUCTURE MOVING WITH THE WIND, DUE TO BUOYANT ELEMENTS.

heat flux reaching the ground from the sky by radiation must be removed from the surface by forced and free convection. (In fact, transfer of heat from the ground to the air by long-wave radiation takes place over the first two or three metres, and much heat is absorbed at the surface in evaporation). Close to the ground, wind-shear, and hence turbulence, is high, and the turbulence produced is sufficient to carry the upward heat flux by forced convection. Higher up, wind-shear is less, and the more powerful mechanism of free convection must supplement the reduced turbulence. Turbulence tends to dissipate the buoyant elements, which therefore cannot survive for any appreciable time in the lowest layer (Webb 1962). Webb (1958) detected a second transition at which the potential temperature gradient becomes very small, and beyond which the buoyant elements penetrate with negligible dissipation or heat transfer by turbulence (Fig. 1.4). The height of the transitions increases with windspeed and surface roughness. Over grassland with a windspeed of 5 m s^{-1}, the first will occur at about 1½ m, and the second at about 50 m.

Although the form of the temperature gradients is not uniquely determined by the type of convective element, it seems that some progress can be made by

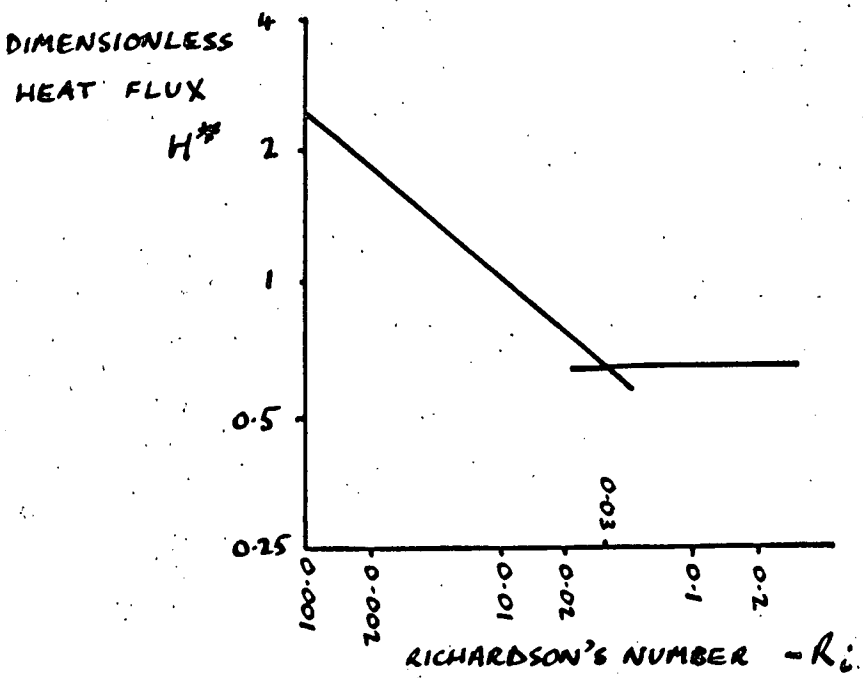

FIG. 1·5 SWINBANK'S HEAT-FLUX

RESULTS

considering the transitions, and it is in this that the plume theory has had some success. Priestley (1955), analysing the results of Swinbank, obtained the relation between H* and Ri shown in Figure 1.5, where dimensionless heat flux $H^* = H/\left[C_p\rho\left(\frac{g}{T}\right)^{\frac{1}{2}}\left(\frac{\partial\theta}{\partial z}\right)^{3/2}z^2\right]$

and Richardson's number $R_i = \left(\frac{g}{T}\right)\frac{\partial\theta}{\partial z}\Big/\left(\frac{\partial u}{\partial z}\right)^2$

(H = heat flux per unit area, Cp = specific heat at constant pressure, T = absolute temperature, ρ = density, u = horizontal wind velocity). The results plotted on log scales appeared to lie on two intersecting straight lines, meeting at H* = 0.69, and R_i = -0.03. If this is so, the obvious interpretation is that these represent the free and forced convection regimes, for simple analysis shows that in the forced convection zone, H* will depend on height (i.e., on R_i), but in the free convection zone it will be constant. The values of R_i and H* at the transition remain to be explained.

Priestley (1956) considered which type of buoyant element would be most efficient at removing heat from the lowest layer, and concluded that a long upward moving curtain would be most efficient, because its heat and momentum would be dissipated in only one dimension, whereas a plume would lose heat in two dimensions, and a bubble, the least efficient, in three. However, a long

curtain was far less likely to be initiated in nature than a plume, which might be triggered by any hot-spot or mechanical disturbance. Priestley therefore applied the treatments of Priestley and Ball (1955) and Morton, Taylor and Turner (1956) of an axially symmetric plume rising from a hot-spot. Using r as the radius of an annular element, the equations of continuity, vertical motion and heat conservation are, respectively,

$$\frac{\partial}{\partial z}(r w \rho) + \frac{\partial}{\partial r}(r u_r \rho) = 0 \qquad (1.4)$$

$$\frac{\partial}{\partial z}(r w^2 \rho) + \frac{\partial}{\partial r}(r u_r w \rho) = r \frac{\vartheta'}{\vartheta_e} \rho g + \frac{\partial}{\partial r}(r \tau) \qquad (1.5)$$

$$\frac{\partial}{\partial z}(r w \vartheta \rho) + \frac{\partial}{\partial r}(r u_r \vartheta \rho) = -\frac{1}{c_p} \frac{\partial}{\partial r}(r F) \qquad (1.6)$$

(u_r = radial velocity, τ vertical turbulent shearing stress, F radial potential turbulent heat flux. Primed values are the excess over the environmental values, indicated by suffix $_e$. Suffix $_m$ denotes value of the excess at the centre of the plume. R is the radius of the plume).

When substitution is made for the lapse-rate in the free convection regime (equation 1.3), these give a solution which, for z = 0, gives R = 0 and $R^2 w_m^2 \vartheta_m^2 = 0$,

indicating that, once a plume is triggered by a suitable source, it is self-maintaining. Physically, it can be visualised drifting with the wind, merely drawing air from the lowest layer. The solution, in the form given by Priestley (1959) is

$$R = \left(\frac{3a}{8b - 9a}\right) c z \tag{1.7}$$

$$w_m = \left(\frac{3ad}{16}\right)^{\frac{1}{2}} \left(\frac{gC}{\theta_a}\right)^{\frac{1}{2}} z^{1/3} \tag{1.8}$$

$$\theta'_m = \left(\frac{1}{2}d\right) C z^{-1/3} \tag{1.9}$$

a,b,c,d and C are constants, of which the first four depend on the form of the radial profiles of γ, w, and θ' assumed in the plume. Priestley (1959), also obtained equations for the dimensionless heat flux maxima and means:

$$H_m^* = \left(\frac{3ad^3}{64}\right)^{\frac{1}{2}} \tag{1.10}$$

and

$$H^* = H_m^* \beta \tag{1.11}$$

where

$$\beta = \frac{q\,\overline{w\theta'}}{w_m \theta'_m} + \frac{q^2}{p^2} \frac{\overline{w}\,\overline{\theta'}}{w_m \theta'_m} \tag{1.12}$$

P and q are the relative masses of descending and ascending air respectively. The barred values are averages over the plume. Assuming Gaussian profiles of θ', and w, Priestley obtained a = d = 2, b = 3; and, from measurement, p = 0.53, q = 0.47. Hence, at the transition to free convection, H* = 0.48. By another method, Priestley (1956) obtained $-R_i = 0.035$. These values compare with the experimental results of Swinbank of H* = 0.69 and $R_i = -0.03$. On the basis of improved

measurements, Priestley (1959) suggested $H^* = 0.9$ as closer to the true value.

These values were obtained assuming a Gaussian cross-section for the plume. Experimentally, however, Vul'fson (1964) showed atmospheric buoyant elements to have the temperature profile

$$T' = T_m' \left(1 - \frac{r^2}{R^2}\right)^{\frac{1}{2}}$$

It is shown in section 2.4.3 that this gives $d = \frac{4}{3}$, and a similar calculation shows that $a = \frac{4}{3}$. Also,

$$\overline{w} = \frac{\int_0^R 2\pi r w_m \left(1 - \frac{r^2}{R^2}\right)^{\frac{1}{2}} dr}{\pi R^2}$$

$$\overline{\theta'} = \frac{\int_0^R 2\pi r \theta_m' \left(1 - \frac{r^2}{R^2}\right)^{\frac{1}{2}} dr}{\pi R^2}$$

These can be integrated directly to give $\overline{w} = \frac{2}{3} w_m$, and $\overline{\theta'} = \frac{2}{3} \theta_m'$. Similarly,

$$\overline{w\theta'} = \left[\int_0^R 2\pi r \left(1 - \frac{r^2}{R^2}\right)^{\frac{1}{2}} w_m \theta_m' \, dr\right] \Big/ \pi R^2$$

This can be integrated using the substitution $r = R\cos\theta$ giving

$$\overline{w\theta'} = \frac{1}{2} w_m \theta_m'$$

Using these relations, $\beta = 0.42$, and $H^* = 0.16$, which is considerably further from the experimental value than the result from the Gaussian profile.

Priestley also calculated the values for the transition to linear convection ("curtains"), which, if there were a suitable triggering mechanism, would take

place at lower values of lapse rate, and obtained H^* = 1.02 and $-R_i$ = 0.011.

Woodcock (1940) delineated the conditions of windspeed and lapse rate in which seagulls soared linearly or in circles, and Priestley showed that his values agreed well with these conditions.

Vul'fson (1964) found experimentally that $R \propto z^{1/3}$ which disagrees with equation (1.7). This is a serious discrepancy, and indicates a fault in Priestley's argument. In the light of this, it is not surprising that Priestley's derivation of H^* does not agree better with experiment, and that an attempt to graft Vul'fson's temperature profile onto Priestley's derivation should only make matters worse. Vul'fson also carried out a theoretical analysis, which yielded the same form of variation with z for θ'_m and w_m as Priestley's, but also gave $R \propto z^{1/3}$. He did not proceed to obtain H^*.

Although these treatments show the plume model explains the experimental facts fairly well, it does not show it to be the only one which satisfies the results. A similar calculation does not seem to have been done for the bubble model, but until it is, we cannot be sure that it would not give as good a result. The conclusive evidence, however, has been provided by

Taylor (1958) who measured temperature fluctuations simultaneously at several levels, and found that the same pulse could be detected at all levels. The pulses reached the higher thermometers before the lower, showing that the structure was a plume leaning in the direction of the wind, with a moving source. Because the warmer air would move to the upper side of a leaning plume, it is to be expected that the back edge of a temperature pulse on a record would look sharper than the leading edge, and this is the case with Taylor's records. A rising bubble would probably not impinge on all heights, and would certainly not do so in the order observed.

Mention may be made here of the results of Bent and Hutchinson (1966), who measured space charge and other parameters at 1 and 19 m on a mast. They found, in convective weather, pulses of charge correlating with increases in temperature and decreases in windspeed closely resembling the records of Taylor and those illustrated by Priestley (1959, P.68). Bent and Hutchinson suggested some form of cellular convection might explain their results, but it seems clear a better explanation is provided by the plume theory. If this is correct, the result is important for two reasons:

firstly because the space-charge pulses appear to give very clear indications of plumes, and secondly because these results were obtained over quite broken country, whereas most previous sites have been chosen for exceptional flatness. The main object of the work described in this thesis is the further investigation of these pulses.

At higher levels, as has already been remarked, the evidence is ambiguous. The only attempt to correlate vertical velocities at different levels seems to be that of Angell (1964), who worked at 200, 530 and 860 m on a barrage-balloon cable, and correlated the cospectra and quadrature spectra between levels. He found that the spectra were related in a way which certainly indicated the plume theory rather than the bubble, although again the evidence is not conclusive.

In conclusion, there is strong evidence that free plumes, i.e. plumes whose sources move with the wind, occur in the first 50 m. At higher levels, the evidence is weaker.

1.4 Informal Gliding Evidence

As mentioned in section 1.2.2, it is difficult to form a consistent picture of thermals from the formal reports of glider pilots, perhaps because conditions in

the atmosphere are so variable anyway. However, despite all the contradictions, certain general patterns can be seen from the mass of incidental mentions of thermal conditions in accounts of flights.

As regards the formation of thermals, the features on the ground which act as sources of rising air are well known, and easily explained. The most marked of these is variation of slope of the ground, because slopes facing the sun get hotter than flat ground or shaded slopes. For this reason, unlevel ground gives stronger thermals earlier in the day than flat ground (MacCready 1961; Welch 1953). Soil type is important: for example, patches of chalky ground are said to act as thermal sources, perhaps because of their lower thermal conductivity (Scorer 1958, P.176). Smith (1963), discussing the effects of thermal updraughts on gas-filled balloons, remarks that the balloonist "must realize that a lake passing beneath him will tend to lower his height in the daytime ..... A wood will have the same effect, and so will marshland and sea. On the other hand, a town will send him up, just as a hot cornfield will, or a stretch of tarmac." Most of these examples can be attributed to high or low thermal

conductivity. Scorer (1958; P.176) suggests that cornfields act as thermal sources because ripe corn does not absorb heat in transpiration. A strong source of thermals, such as a power station or a south-facing slope, may continually initiate thermals which are therefore found spread out in a line downwind. Such thermal streets may also arise without an obvious source. These appear to be common, and may form a large number of parallel lines (Welch 1953), presumably resembling cloud-streets (section 1.3.1).

However, most thermals encountered by pilots cannot be attributed to any particular source, and appear to arise spontaneously.

Kearon (1965) relates how a retrieval crew drove backwards and forwards on the ground below the glider "in an attempt to trigger off the thermal". It is difficult to understand this, although the idea may derive from Scorer (1954a). Perhaps it is not meant to be taken too seriously.

Pilots report that thermals carry with them all the expected characteristics of air originating near the ground, even as far as smell. (It has been suggested that soaring birds use this to find thermals (Slater 1965)). The structure of turbulence inside a thermal is said to

resemble that near the ground, and to be readily distinguished by the pilot (Welch 1953). It has been suggested that some of these characteristics might be used to detect thermals at a distance. Especially relevant to the present work is the suggestion that the excess space charge of the rising air might give rise to horizontal electric fields detectable some distance away (e.g. James 1960). A method commonly proposed is to have probes on the nose and tail of the sailplane and to fly in the direction which gives the greatest difference in potential between the two (or the greatest rate of change of potential of one of them). A spherical bubble of air of excess charge 40pC m^{-3} (250 e cm^{-3}) and radius 100 m would give a field 200 m from the centre of about 40 V m^{-1}, so this method may be feasible, but much would depend on the size of the space-charge excess, and the response-time of the probes.

As would be expected, there is more confusion about the shape and other characteristics of individual thermals. It is generally agreed they begin at about 200 - 300 m above the ground with a diameter of perhaps 150 m, and increase in size with height. Bold pilots will look for lift down to 100 m, however, and the limit seems to be set by the necessity for the pilot to look for a landing-

place before he gets too low. Most thermals are reported to have a temperature excess of 1 - 2°C, and have an upward velocity of up to 5 m s^{-1} (Yates, 1953). Wills (1961) says a thermal "can be most easily (but rather inaccurately) visualized as a column of warm air rising", but most pilots today pay lip service at least to the bubble theory. There seems to be little firm evidence on the vertical extent of individual thermals. It is usually difficult to say whether or not two gliders at different heights are in the same thermal, because a continuous plume will have a considerable lean in wind-shear, even if the bottom of the thermal is not fixed on the ground. If a collection were made of photographs taken when many sailplanes were in flight near to one-another - for example at national championship meetings - it might be possible to come to some conclusions on this point. The author has seen only two relevant photographs. One ("Sailplane and Gliding" 16 (6, Dec. 1965 - Jan. 1966), 556) shows eighteen gliders circling in the same thermal, but apparently all at the same height. The other ("Sailplane and Gliding" 16 (4, Aug. - Sept. 1965), 312) shows eleven sailplanes at different heights apparently in a column at an angle to the vertical. (Since the camera was looking up through the column, and no horizon is shown, it is difficult to be sure.) By comparison of the wing-

span with the distribution of gliders, the diameter of the areas of lift can be estimated: in the first case it is about 480 m, and in the second about 290 m. These values are consistent with those usually suggested by pilots, but much higher than the average dimensions given by Vul'Fson (1964), discussed in section (1.5). Pearson (1966), writing of the "different" qualities of thermals in Rhodesia, remarks how many times in the 1966 national championships pilots would "slide in a few hundred feet under, or over, another pilot who was obviously in 4 - 5 m s^{-1} lift, yet all they could find was sink no matter where they looked". With the reservation mentioned above, this seems clear evidence for "bubbles". It is not out of the question for Rhodesian thermals to be "different", since the nature of the rising element might well depend on the properties of the surface. For example, the special type of fast-rotating plume which gives a "dust-devil" if it travels over a dusty surface seems to form only in very high lapse rates; such as occur over a desert surface. Vul'fson's (1964, section 3.10) aircraft measurements have shown an inverse relationship of temperature and velocity of thermals with latitude.

Pearson also describes the thermals as being "in a

large area of surrounding sink". Buoyant elements obviously rise through air generally subsiding to preserve the mass balance, but there seems some evidence that the sink may be concentrated immediately round the thermal. Yates (1953) describes this zone as being narrower and weaker than the upcurrent. However, Williamson (1966), says regions of sink are not necessarily closely associated with upcurrents. As has been seen in section 1.3.2, the entraining bubble theory predicts a region of sink immediately surrounding the rising air.

Findlater (1959) compared pilots' reports of soaring conditions over nine years with wind-shear and surface wind found from meteorological reports and found that a shear greater than about three knots per thousand feet made thermals "distorted or difficult to use", although surface windspeed appeared also to affect the conditions in a rather complicated way.

There are few reports of thermal spacing, but Garrod (1966) studied his own records and concluded that the thermal diameter and spacing increased with the depth of the convective layer, and the ratio of the spacing to the depth of convection was about 4.65.

In conclusion, it may be said that the most consistent attribute of glider pilots' "thermals" seems

to be their variety. They seem to form at about 200 - 300 m, to rise at a few metres a second to cloud-base or an inversion, and to have diameters of a few hundred metres. The evidence about the depth of individual thermals is not conclusive, but there is some limited evidence of considerable vertical continuity. The rising air sometimes seems to be surrounded by sink. The size and speed of the air in the thermals both seem much greater than the average values measured by Vul'fson (1964), reviewed in the next section, and this is all the more surprising when his finding that the smaller thermals are generally warmer is taken into account. In view of this, the fact that glider pilots usually report thermals to be much rarer than Vul'fson's results indicate is not surprising: they would seem to be operating right at the tail-end of both the size and vertical-velocity distributions.

1.5 Powered Aircraft Measurements

Aircraft traverses show that, in convective conditions, there are discrete zones, like the pulses in Fig. 1.4, in which temperature, humidity, turbulence, and vertical velocity are all distinctly different from the average. These are clearly buoyant elements. Various workers have investigated them, but only Vul'fson (1964)

has measured enough for a clear pattern to emerge. This section is largely a summary of some of his results, with which the measurements of other workers are broadly consistent.

Vul'fson measured temperature in traverses at various standard heights (100, 300, 500, 1000 m, and then at 500 m intervals until the temperature pulses were no longer distinct; in later flights, 50 m was also made a standard height, and in some conditions measurements were also made at 10 and 30 m). On each flight, measurements were made successively at all standard heights, and the data were only accepted for processing if measurements at all heights were satisfactory. Despite this condition, acceptable measurements were made of about 50,000 pulses.

This large number allowed proper statistical treatment of the data, overcoming the draw-back mentioned in section 1.2.1, that measurements are made along a chord of the plume of bubble, but must be related to the diametric properties. Vul'fson processed his data in this way for two possible models, the plume, and an oblate spheroidal bubble. Direct distinction of the models could not therefore be made from the data, although it could be inferred.

The temperature profile of 400 pulses was found to be fitted well by

$$T' = T_m' \left(1 - \frac{r^2}{R^2}\right)^{\frac{1}{2}}$$

This profile was the same along a chord as along a diameter, and did not change with height. It is, of course, considerably different from the normal distribution assumed by Priestley (1956) and others, and, as has been shown, this considerably affects the calculated values of H* and R_i for free convection. No fine structure, such as might be expected from the entraining bubble theory, was noticed.

Up to 300 m, it was found for both the bubble and plume models that

$$R \propto z^{1/3}$$

and beyond that height R increased much more slowly. As Vul'fson notes this variation is the same as that found for refractive index anomalies from radar observation by Norton, Rice and Vogler (1955). At any particular height, the distribution of R was given by

$$F(R) = a\left(R/R_o\right)^b e^{b\left(1 - \frac{R}{R_o}\right)}$$

where R_o was the most probable horizontal radius at the height, and a and b were constants depending on z. The mean values of R at 100 m were 30.5 and 23 m for plumes and bubbles respectively.

The average maximum temperature excesses of the pulses was inversely proportional to the third power of the height, decreasing from about 0.6°C at 10 m to about 0.1°C at 2000 m. A proportion of the currents, increasing with height, was colder than the environment, Grant (1965) has shown that such currents have a high humidity, which gives them buoyancy.

The number of pulses decreased with height, corresponding at 500 m to 40 plumes km^{-2}, or 620 μ bubbles km^{-3}, where μ is the ratio of the horizontal and vertical radii. This is considerably more than the numbers given by glider pilots, who also state average dimensions greater than those above, as already noted. The relative area of rising air also decreased with height.

The pulses were found to be slightly smaller and warmer in high atmospheric instability, i.e. during fast cloud development, than in clear weather. However, the number and relative area of thermals, and the depth of the convective layer were all greater in unstable conditions. These changes were reflected in variations with time of day, latitude, and underlying surface. In the middle of the day, thermals were more numerous, smaller, and warmer than in the morning and evening. The

greater instability at low latitudes, and over land as opposed to water surfaces, produced similar changes. (The presence of more thermals colder than their surroundings over water was presumably due to the buoyancy gained from higher humidity.)

As would be expected from gliding observations, thermals over mountains were larger, warmer, but still as numerous, as over plains. Under these conditions, permanent plumes were found attached to hotspots, mainly south-facing slopes. Hotspots on level ground, such as asphalt roads and ploughed soil, were found to be effective to only 50 - 100 m.

1.6 Summary and Conclusion

It is clear that the form of convection in the atmosphere varies considerably from time to time and from place to place. There is strong evidence that over some parts of the ocean, for example in the trade-wind zones, some form of cellular convection takes place, although the exact mechanism is not yet clear. Over land, there is no evidence of Bénard cellular convection below cloud-base, and the roughness of the surface, and, more especially, its wide variation in specific heat and conductivity, and the variations with height found for the numbers and dimensions of thermals, make the

presence of this type of convection most unlikely.

Near the ground, the evidence strongly suggests that plume convection is the most common form between the forced convection region and a few tens of metres at least, although the work of Bunker (1953) may show that bubble convection sometimes occurs. The exact form of the plumes remains in doubt. Vul'fson's (1964) discovery that the mean radius varies as $z^{1/3}$ and not as z, and that the temperature profile is not Gaussian, makes Priestley's (1956) model in need of revision, although these data still require confirmation for the first ten metres. An attempt to relate Vul'fson's measurements to the heat-flux measurements of Swinbank (Priestley, 1955) would be valuable.

At higher levels, Vul'fson points out that his success in explaining his results theoretically on a plume model indicates that such plumes probably exist, although some other explanation is not excluded, and the length of time (about half an hour) required for a plume to propagate to the top of the convective layer would seem to exceed the likely lifetime. His results, especially on the variation of radius with height, make some transition at about 300 m possible, and this would agree with observations by glider pilots and other

workers from aircraft that thermals often seem to fade out at a few hundred metres and then reform. Whether this is a transition to bubbles, or to some other form of plume, is unknown. The success of Angell (1964) in correlating vertical currents at different levels suggests plumes as the more likely model. On the other hand, despite the reservations expressed about gliding evidence, the general support of the gliding fraternity for the bubble theory cannot be lightly set aside.

There now seem to be sufficient data to justify a theoretical investigation of the possible decay of the Vul'fson plume at about 300 m.

Experimentally, the situation is unlikely to be resolved except by the aircraft surveys of the vertical velocity fine structure of thermals, to prove or disprove the entraining bubble theory, and by simultaneous flights at different altitudes, to do the same for the plume model. Another promising line of investigation is the extension to his work suggested by Angell, using at least one more barrage balloon downwind from the first, and obtaining many more results than he was able to. Until these experiments are carried out, it seems unwise to draw any firmer conclusion.

CHAPTER 2

THE PRODUCTION AND TRANSPORT OF SPACE CHARGE

2.1 Scope of the Chapter

The purpose of this chapter is to survey the influence of electric fields, and, more fully, the wind-structure on the distribution of charge near the ground. It is not intended as a complete account of atmospheric space charge, such as that given by Chalmers (1967, Chapter 6).

2.2. Production of Space Charge

Space charge is a function of different concentrations of positive and negative ions. If there are n_1 positive and n_2 negative ions, each of charge e, per unit volume, the space-charge density σ is given by

$$\sigma = e(n_1 - n_2) \qquad (2.1)$$

Ionization of a neutral medium always produces equal numbers of positive and negative ions, of course, and therefore no net space charge. However, local space charge may arise if the ions are separated by an imposed electric field. This takes place in the atmosphere, but a more important source in heavily polluted regions is the injection into the air of ions of one sign in preference to the other, the ions of the other sign

flowing to earth, e.g. via the walls of the furnace.

2.2.1 Charge Injected into the Air

Various natural processes produce charge of one sign preferentially in the air. Several workers have shown that snow can cause separation of charge, either by friction in dry snow, or by melting and sublimation. Splashing water-drops, particularly in high potential gradients, can give charge to the air, the sign depending on that of the potential gradient. Point discharge at elevated points also produces charge, whose sign again depends on the sign of the potential gradient, but is more often positive. Bursting of air bubbles at the sea surface is a source of positive charge. Other natural sources are dust-storms, and volcanoes.

All these effects are local, however, and, for almost all the time in heavily-populated areas, the artificial sources produce more charge. Charge from industrial and traffic pollution is more fully dealt with in Chapter 9. This includes the positive charge from steam locomotives, which has long been recognized, but with the passing of the steam train from regular service, has ceased to be an important source in this country, compared with road traffic. Most charge from this source

seems to come from diesel engines, and is positive. According to Mühleisen (1953), chemical laboratories and gas-works emit negative charge.

Some other artificial structures produce charge separation. In high humidity, corona effects on insulators of high-tension power-lines give negative charge to the air (Chapter 8). Moore, Vonnegut, Semonin, Bullock, and Bradley (1962) observed positive charge downwind of a television tower, where it had presumably been concentrated by the electrode effect, and then blown away. Accidental or deliberate corona discharge at high-voltage lines will also produce charge, as will, of course, sparking in electrical machinery.

Mechanical effects can also sometimes separate positive and negative ions, because of their different mobilities. For this reason, fans produce positive charge, and there is an excess of positive ions in air diffusing from the ground.

2.2.2 Electrostatic Charge Separation

(a) Variation of conductivity with height

Ionization of the lower atmosphere is due to radioactivity in the ground and air, and, to a lesser extent, to cosmic rays. The first two influences vary

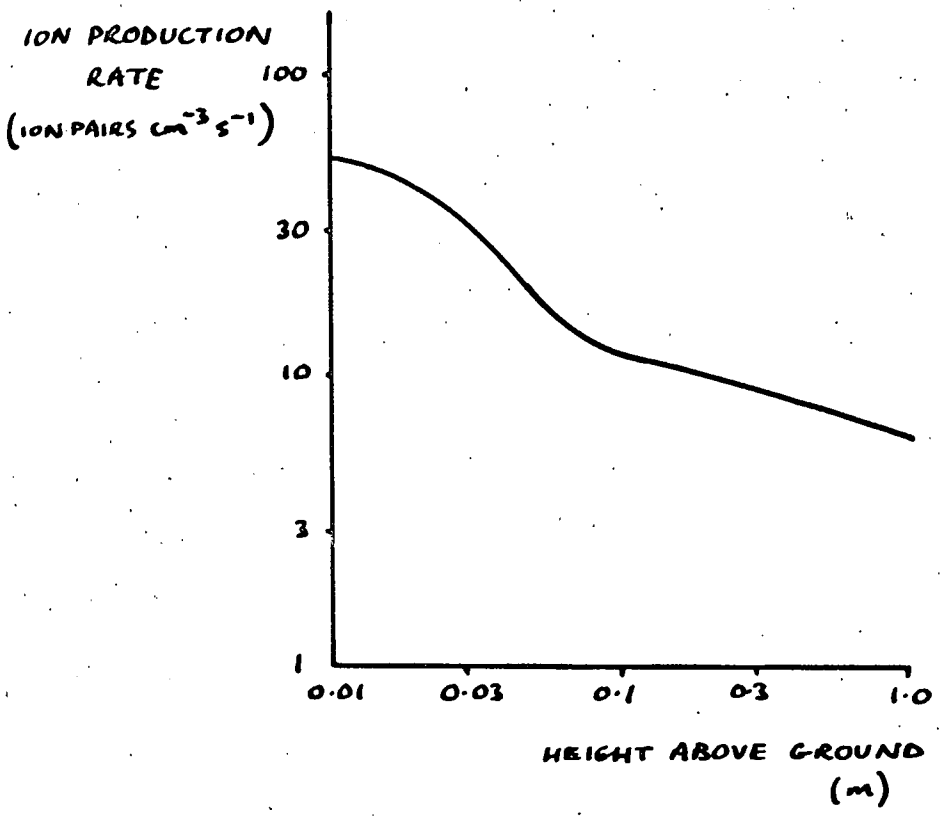

FIG. 2·1 IONIZATION-RATE IN THE FIRST METRE

with height near the ground, and the average resultant variation in total ionization-rate in the first metre over land, as estimated by Pierce (1959), is shown in fig. 2.1. This ionization is not in itself space charge, of course, but it produces charge by one of the two electrostatic processes of possible importance near the ground - the variation of conductivity with height.

From the relationships of potential gradient F, conduction current i_1, conductivity λ, space-charge density σ, and the constancy of conduction current with height,

$$\frac{dF}{dz} = -\frac{\sigma}{\varepsilon_0} \qquad (2.2)$$

$$i_1 = F\lambda \qquad (2.3)$$

$$\frac{di_1}{dz} = 0 \qquad (2.4)$$

it follows directly that

$$\sigma = \frac{\varepsilon_0 i_1}{\lambda^2}\frac{d\lambda}{dz} \qquad (2.5)$$

λ is related to the total ionization and mobility w:

$$\lambda = e(n_{s1}w_1 + n_{s2}w_2) \qquad (2.6)$$

where the suffix s refers to small ions, and so (2.5) implies that a decrease of conductivity with height will be accompanied by negative space charge. The decreasing ionization-rate shown in fig. 2.1 is likely to be accompanied by falling conductivity, but the space charge in the first metre is usually positive. This is because

the assumption (2.4) that the conduction current is constant with height is very questionable in conditions of wind (section 2.4), and other sources of charge usually mask the effect. (These two factors are, of course, linked.) Charge might be produced by this process at the edges of a layer of high concentration of pollution, if the pollution were sufficient to affect the conductivity, and steady enough for the quasi-static state equations to be applicable. The effect is, however, important higher in the atmosphere, at sharp discontinuities of conductivity, such as the top of the exchange layer (Sagalyn, 1960), and the edges of clouds. A picture of the physical process by which this production of space charge comes about has been given by Chalmers (1967, section 2.25).

(b) The electrode effect

The other electrostatic source of charge possibly of importance in the first few metres is the electrode effect. This is taken to mean here the concentration of positive charge at a negative electrode, in this case the earth, because the potential gradient tends to remove negative ions from the vicinity of the cathode. Since the concentration of ions itself effects the potential gradient critically, and the relative concentrations of

large and small ions, the variation of ionization with height, and the convection current all appear to be important, the theoretical analysis is difficult, and has not yet been successfully completed. The fullest attempt is that of Chalmers (1966 - 1967, I-IV). (This was an attempt by series solution which was incomplete at the time of the author's death. He thought that adaptation of his method with the further condition of the effect of the convection current, not so far dealt with, might yield a complete solution with the aid of a computer. (Chalmers, personal communication, 1967)).

Not many measurements have been made of the height variation of space-charge concentration in the first metre. The only clear evidence for space charge produced by the electrode effect has been obtained by Pluvinage and Stahl (1953), and Ruhnke (1962), working over the Greenland ice-cap, where the stratification is always very stable, the ionization does not vary with height, and the nucleus concentration is very small. Under the often polluted conditions of the temperate zone, however, the effect seems to be usually undetectable.

We may conclude that although the two electrostatic effects may be detectable under the right conditions, they are unlikely to be significant sources of charge

under the conditions of the measurements described in this thesis. Where they did occur they would produce concentrations of opposite sign.

2.3 Interactions of Atmospheric Electric Parameters

Potential gradient, space charge, conductivity, and the conduction current are linked by the equations

$$\frac{dF}{dz} = \frac{\sigma}{\varepsilon_0} \qquad (2.2)$$

$$i_1 = F\lambda \qquad (2.3)$$

$$F = V/\lambda P \qquad (2.7)$$

V is the potential of the electrosphere, and P the columnar resistance of the atmosphere. Also, from 2.1 and 2.6, a change in conductivity with time may be accompanied by a change of space charge; and, from 2.5, a change of conductivity from place to place always involves space charge. The effect of changes with time in any of these quantities on the others will now be considered, to clarify the various effects likely to accompany space charge.

The immediate effects of changes with time in any of the quantities for the region under consideration may be represented by a diagram (fig. 2.2), the arrows pointing from cause to effect. Ionic concentration changes may produce changes in either space charge or conductivity, depending on how the relative concentrations

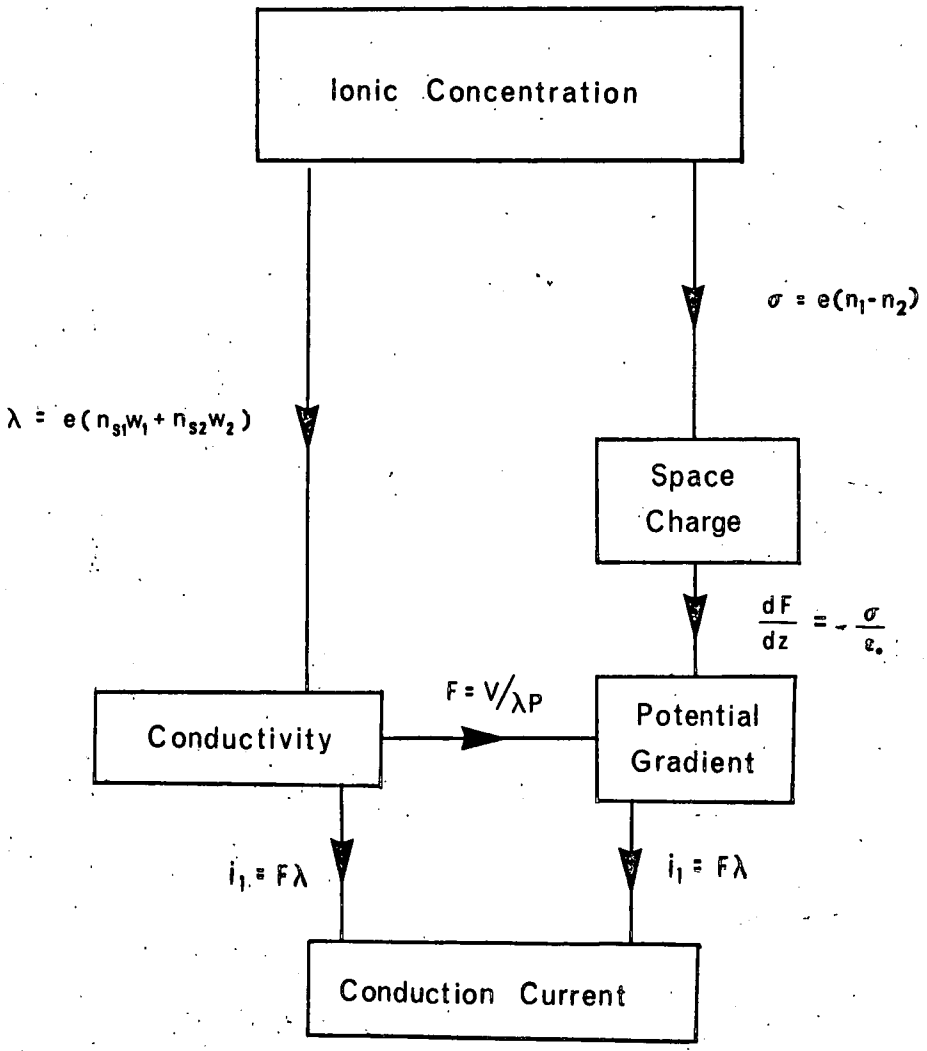

Fig. 2.2 Interaction of Atmospheric Electric Parameters

of large and small, positive and negative, ions change. For example, an influx of predominantly positive or negative large ions from a pollution source will change the potential gradient and the conduction current immediately, but not the conductivity. A sudden uniform change in small ion concentration, producing equal numbers of positive and negative ions, such as might be produced by a burst of ionizing radiation, will not affect space charge, but will increase conductivity locally. The effects here are more complicated: the potential gradient is decreased, according to (2.7), but the conduction current is not affected, because potential gradient and conductivity in (2.3) have changed in inverse proportion.

From this it can be seen that short-term changes of potential gradient can be caused by changes in space charge or conductivity near the ground. The exact space-scale on which the above arguments apply depends on the assumption, in applying (2.7), that the columnar resistance is unchanged. This is obviously true for changes in conductivity over a few tens of metres, but a very large-scale change of conductivity, for example the column of ionization produced by a cosmic ray extensive air shower, will affect P as well, and this must

be taken into account. The above arguments also neglect possible changes in mobility of the small ions.

There is also a time-scale limitation. The sudden injection of space charge into a system in a quasi-static equilibrium (Chalmers 1967, section 2.23) will immediately change potential gradient and conduction current as shown above. However, all the space charges present will begin to move in the conduction current, affecting the field distribution, until a new equilibrium is set up. This means that after the initial instantaneous change, there is a slow change to a new equilibrium, with a time constant equal to ε_0/λ (the "relaxation time" of the atmosphere), the potential gradient and conduction current changing together (Kasemir, 1950). This implies that the arguments from fig. 2.2 only apply for changes short compared with the relaxation time (about 16 min). However, Collin, Groom and Higazi (1966) have shown that the changing of the air at the experimental site by wind is much more important than electrical relaxation in changes of conductivity, implying that, at Durham in daytime at least, the quasi-static equilibrium is never attained, and the time limitation is therefore not serious. For a site with horizontal uniformity of electrical

conditions over several miles, this conclusion would presumably not apply, because the "new" air brought by the wind would not differ from the "old" blown away. In long-term changes, the effects of changes in the equilibrium of large and small ions, due, for example, to the introduction of more large ions, must be taken into account.

As illustrations of magnitude of the effect of space charge on potential gradient, a horizontal layer of space charge of density + 20 pC m^{-3} (125 e cm^{-3}), one metre thick, would produce a potential gradient underneath of about 2.26 V m^{-1}. The potential gradient is inversely proportional to the conductivity of the air in which it is measured.

The other questionable assumption in the above arguments, that only the conduction current is responsible for the transport of charge, does not affect short-term changes, but will now be dealt with more fully.

2.4 The Convection Current

2.4.1 Importance

Discrepancies in conduction current values obtained by the direct and indirect methods, i.e. by measuring the current to an exposed plate, and by calculating the current from the conductivity and potential gradient,

have long suggested that the transport of charge by convective movement, the convection current, may be important in the first few metres. Chalmers (1957) doubted its importance on the grounds of the small space-charge densities found, but Law (1963) considered his results required a convection current, and the same conclusion seems to be required by the results of Higazi and Chalmers (1966), which will be taken as an illustration.

Measuring conductivity at three heights, Higazi and Chalmers found the following average values (in Ω^{-1} m^{-1}): at the ground, 1.09 x 10^{-14}; at 0.2 m, 0.93 x 10^{-14}; at 1 m, 0.84 x 10^{-14}: Measurements of space charge at the same site during the same period gave values of about + 10 pC m^{-3} at 1 m (Bent and Hutchinson 1966), corresponding to a change in potential gradient in the first metre of about 1 V m^{-1}. It can be seen (equation 2.3) that these values therefore lead to a decrease in conduction current with height in the first metre of about 30% and any positive space charge will make the discrepancy bigger. The values are 1.31 x 10^{-12}, 1.12 x 10^{-12}, and 1.01 x 10^{-12} A m^{-2}.

The obvious conclusion is that there is a convection current which combines with the conduction current to

give a total charge transport independent of height. It is important to realise that, since the conduction current transfers positive charge downwards, these figures imply that a convection current transferring positive charge upwards decreases with height. The sign conventions for currents and space-charge density gradients were given in the Foreword.

The purpose of this section is not to attempt a complete theoretical solution of the complex problem of charge transport, but to show how measurements of space-charge density gradients, such as are easy to make with filtration apparatus, might enable the practical calculation of convection currents. The cases of forced and free convection will be dealt with separately.

It is easy to justify the treatment of space charge as carried entirely by the wind. Small ions have mobilities of about 10^{-4} m s^{-1} per V m^{-1}, and large ions about one-twohundredth of that. The average fair-weather potential gradient should therefore give small ions a velocity of about 1 cm s^{-1}, which is usually small compared with the velocity given to it by wind-generated turbulence. An illustration of the truth of this is the success of Maund and Chalmers (1960) in

confirming experimentally the applicability of diffusion theory to space charge in much higher potential gradients. For the same reason, the use of an earthed support for, say, space-charge measurement apparatus, does not electrically affect the space-charge stratification, provided the support is not too high. The conduction current involves a net movement through the turbulent layer, of course, but this is an overall movement occurring in a generally almost-random motion.

2.4.2 Forced convection

Over any vegetated surface at appreciable wind-speed, "aerodynamically rough" flow occurs, in which the wind-speed profile is influenced only by turbulence, and not by molecular viscosity. This is the case that will be considered.

By the usual arguments, a turbulent transfer coefficient K_q can be defined for space charge, so that the convection current

$$i_z = K_q \frac{\partial \sigma}{\partial z} \qquad (2.8)$$

This is analogous to the momentum flux equation, for example:

$$\tau = -\rho K_m \frac{\partial u}{\partial z} \qquad (2.9)$$

where ρ is the density of air. K_q and K_m are equal under the same conditions, being properties of the field

of air motion. A difference between these equations is that τ is constant with height, whereas it is the total current ($i = i_1 + i_2$) that is constant. Because of this, we can make no deductions from (2.8) about the shape of the space-charge density gradient. The difference of sign between (2.8) and (2.9) is a consequence of the sign conventions explained in the Foreword.

Because of the dependence of K_q on u and z, it is more convenient to express results in terms of a reference velocity, the "friction velocity" u_*, defined by

$$u_*^2 = \left| \frac{\tau}{\rho} \right| \qquad (2.10)$$

(The basis of this definition is that experimentally τ is proportional to u^2.) From (2.10), it is clear that u_* is a quantity independent of height, but proportional to wind-speed at a particular height.

Experimentally, for aerodynamically rough flow in neutral stability,

$$\frac{\partial u}{\partial z} \propto \frac{1}{z}$$

Hence we can put

$$\frac{\partial u}{\partial z} = u_* / kz \qquad (2.11)$$

where k is a constant independent of surface, u, and z, known as Von Karman's constant. The wind profile is obtained by integration:

$$\frac{u}{u_*} = \frac{1}{k} \log_e \frac{z}{z_0} \qquad (2.12)$$

where z_o is another constant, the "roughness length". The magnitude of this depends on the surface, and is usually an order of magnitude less than the size of the roughness elements. Sutton (1953) gives typical experimental values of u_* and z_o for natural surfaces, the u_* values being for a wind of 5 m s^{-1} at 2 m, in neutral stability.

Table 2.1

Surface	u_* (m s^{-1})	z_o (cm)
Very smooth (mud flats, ice)	0.16	0.001
Grass up to 1 cm high (lawn)	0.26	0.1
Thin grass up to 10 cm high (downland)	0.36	0.7
Thick grass up to 10 cm	0.45	2.3
Thin grass up to 50 cm	0.55	5
Thick grass up to 50 cm	0.63	9

From (2.9), (2.10), and (2.11),

$$K_q = K_m = -\tau/\rho \frac{\partial u}{\partial z}$$

$$= kzu_* \qquad (2.13)$$

$$= k^2 z^2 \frac{\partial u}{\partial z} \qquad (2.14)$$

Hence, from (2.8),

$$\frac{\partial \sigma}{\partial z} = i_z / kzu_* \qquad (2.15)$$

and

$$i_z = kzu_* \frac{\partial \sigma}{\partial z}$$

We are now in a position to consider again the

results of Higazi and Chalmers. These require a positive convection current increasing with height, or a negative current decreasing with height. The results of Bent and Hutchinson, and other workers, lead one to expect a positive space charge whose density decreases with height, and this will fulfill the above conditions provided that $\frac{d\sigma}{dz} \propto \frac{1}{z^n}$, where $n>1$, giving a negative current whose magnitude decreases with height.

Bent and Hutchinson (1966) found that the space-charge densities at 1 m and 2 m, on the site where Higazi and Chalmers worked, did not usually differ by more than 1.6 pC m^{-3} (the limit of accuracy of measurement). Taking $k = 0.4$, and $U_* = 0.5$ m s^{-1}, (2.15) gives for the density difference between 1 and 2 m

$$\Delta\sigma = 5 \int_{1m}^{2m} \frac{i_2}{z} dz \qquad \text{(MKSA units)}$$

Assuming i_2 constant with height ~~1 m~~ over this region i_2 is less than 5.10^{-13}A m^{-2}, which is about half the value for the conduction current at 1 m obtained from the results of Hagazi and Chalmers. The calculations of Law (1963) show that $\frac{d\sigma}{dz}$ decreases rapidly with z, and so realistic attempts to calculate convection currents from space-charge density gradients would seem to be limited, by the sensitivity of the apparatus, to the first metre, and can only give a mean value of i_2 over the height

range measured. Simultaneous measurements of $\frac{du}{dz}$ are required to calculate u_*.

2.4.3 Free Convection

For the free convection zone (section 1.3.3), Priestley (1954a) obtained, by dimensional analysis, an expression for the heat flux

$$H = h\rho C_p \left(\frac{g}{T}\right)^{1/2} z^2 \left(\frac{\partial\theta}{\partial z}\right)^{3/2} \qquad (2.16)$$

where h is a dimensionless constant. By similar arguments, we can derive an expression for the convection current. It is reasonable to assume that the current i_2 through a level z depends on z, the space-charge density gradient $\frac{d\sigma}{dz}$, the potential temperature gradient $\frac{\partial\theta}{\partial z}$, and a factor including g which represents the expansion of the air as it rises, and, for a perfect gas, should appear as g/T. Putting, then

$$i_2 \propto z^\alpha \left(\frac{\partial\theta}{\partial z}\right)^\beta \left(\frac{g}{T}\right)^\gamma \left(\frac{\partial\sigma}{\partial z}\right)^\delta$$

and equating dimensions in the usual way, we obtain

$$i_2 \propto z^2 \left(\frac{\partial\theta}{\partial z}\right)^{1/2} \left(\frac{g}{T}\right)^{1/2} \left(\frac{\partial\sigma}{\partial z}\right) \qquad (2.17)$$

This is analogous to (2.16), with i_2 replacing H, and $\frac{\partial\sigma}{\partial z}$ replacing the "potential heat gradient" $C_p\rho \frac{\partial\theta}{\partial z}$. This is what would be expected, since the same field of motion is responsible for the transport of space charge as for the heat transport. The same dimensionless constant should

occur in both equations.

Rewriting (2.16),

$$\frac{\partial \theta}{\partial z} = \left(\frac{T}{g}\right)^{\frac{1}{3}} \left(\frac{H}{h \rho C_p z^2}\right)^{2/3} \qquad (2.18)$$

Substituting in (2.17),

$$i_z = h z^2 \left(\frac{g}{T}\right)^{\frac{1}{3}} \left(\frac{H}{h \rho C_p z^2}\right)^{\frac{1}{3}} \frac{\partial \sigma}{\partial z}$$

$$= \left(\frac{h^2 H g}{T \rho C_p}\right)^{\frac{1}{3}} z^{4/3} \frac{\partial \sigma}{\partial z}$$

$$\therefore \quad \frac{\partial \sigma}{\partial z} = i_z \left(\frac{\rho C_p T}{g h^2 H}\right)^{\frac{1}{3}} z^{-4/3} \qquad (2.19)$$

Priestley (1959, P.44) gives h = 0.9 as the best experimental value. Putting ρ = 1.20 kgm m^{-3}, Cp = 1.01 x 10^3 J kgm $^{-1}$, degC $^{-1}$, T = 293 ^{o}A, g = 9.81 m s^{-2}, $\frac{\partial \theta}{\partial z}$ = -1 degC m^{-1} at 1 m, we get H = 200 watts m^{-2} from (2.16). Substituting these figures in (2.19) gives (MKSA units)

$$i_z = 0.16\, z^{4/3} \frac{\partial \sigma}{\partial z} \qquad (2.20)$$

For a difference of 1.6 pC m^{-3} between 1 and 2 m as before, $i_2 = 4.2 \times 10^{-13}$A m^{-2}, which is slightly less than was obtained for the forced convection case. For experimental determination of i_2 in this case, knowledge of $\frac{du}{dz}$ is not necessary, of course; T, $\frac{\partial \theta}{\partial z}$, and $\frac{\partial \sigma}{\partial z}$ must be known, however, $\frac{\partial \theta}{\partial z} = \frac{\partial T}{\partial z} + \Gamma$ where Γ is the dry adiabatic lapse-rate. The accuracy of the determination

is likely to be limited by the uncertainty in h, which is perhaps known to ± 0.05 (see Priestley, 1959, chapter 4).

Of more immediate interest is the size of the peaks in space-charge density that might be expected to coincide with Priestley's plumes. The treatment of Priestley and Ball (1955), summarized in section 1.3.3, can be adapted to derive the space-charge transfer, instead of heat transfer. Referring to that section, the equations of mass continuity (1.4) and vertical motion (1.5) are clearly unchanged. Rewriting (1.6),

$$\frac{\partial}{\partial z}\left(C_p r w \theta \rho\right) + \frac{\partial}{\partial r}\left(C_p r u_r \theta \rho\right) = -\frac{\partial}{\partial r}\left(rF\right) \qquad (1.6)$$

(F is here the radial turbulent potential heat flux)
As above, since the same pattern of motion is responsible for space-charge transport as for heat transport, it seems reasonable to follow the mathematical argument of Priestley and Ball, substituting the space-charge density for "potential heat" density (i.e. $C_p \rho \theta$) throughout. Only the parts of the treatment that require this substitution are given here.

(1.6) becomes

$$\frac{\partial}{\partial z}\left(\sigma r w\right) + \frac{\partial}{\partial r}\left(r u_r \sigma\right) = -\frac{\partial}{\partial r}\left(rQ\right) \qquad (2.21)$$

where Q is the radial space-charge flux. Priestley and Ball give (1.6) in terms of the excess of quantities in the plume (denoted by $'$) over the environment (denoted by

$_e$), which, in adapted form, gives

$$\frac{\partial}{\partial z}\left(r w \sigma'\right) + \frac{\partial}{\partial r}\left(r u \sigma'\right) = -\frac{\partial}{\partial r}\left(rQ\right) - r w \frac{\partial \sigma_e}{\partial z} \qquad (2.22)$$

This can now be integrated in the same way as equation (5) of Priestley and Ball. The different condition is that as $r \to \infty$, rQ, w and $\sigma' \to 0$. The integration becomes

$$\frac{d}{dz}\int_0^\infty r w \sigma' \, dr = -\int_0^\infty r w \frac{\partial \sigma_e}{\partial z} \, dr \qquad (2.23)$$

We need to make an assumption about the form of the radial space-charge density profile in the plume. We assume $\frac{\sigma'}{\sigma'_m}$ to be a function of r/R, where R is some linear characteristic of lateral extend, and m denoted the axial (maximum) value, i.e.

$$\frac{\sigma'}{\sigma'_m} = h\left(\frac{r}{R}\right) \qquad (2.24)$$

and the velocity profile by another function

$$\frac{w}{w_m} = f\left(\frac{r}{R}\right) \qquad (2.25)$$

This gives from (2.23)

$$\frac{d}{dz}\int_0^\infty r w_m f\left(\frac{r}{R}\right) \sigma'_m \, h\left(\frac{r}{R}\right) dr = -\int_0^\infty r w_m f\left(\frac{r}{R}\right) \frac{\partial \sigma_e}{\partial z} \, dr \qquad (2.26)$$

which, according to Priestley and Ball again, gives

$$\frac{d}{dz} R^2 w_m \sigma'_m = -d R^2 w_m \frac{\partial \sigma_e}{\partial z} \qquad (2.27)$$

where d is a profile constant, which is determined by f and h. They then assumed that the profiles of

temperature and vertical velocity had the same form (i.e., were "similar"), and this form was Gaussian. It is reasonable to assume that the space-charge density profile is similar to the vertical velocity profile, but Vul'fson (1964) has shown $(1 - r^2/R^2)^{\frac{1}{2}}$ to be a much more likely form than $\exp(-r^2/2R^2)$. The difference this makes is considered below, but, for the moment, we follow the solution of Priestley (1956), and assume

$$f = h = \exp\left(-r^2/2R^2\right) \qquad (2.28)$$

This gives the profile constant $d = 2$.

For free convection, from (2.19),

$$\frac{\partial \sigma_z}{\partial z} = \frac{\partial \sigma}{\partial z} = i_2 \left(\frac{\rho C_p T}{g h^2 I}\right)^{\frac{1}{3}} z^{-4/3} = 0.61\, i_2 z^{-4/3} \qquad \text{(MKSA units)}$$

Hence, from (2.27)

$$\frac{d}{dz} R^2 w_m \sigma'_m = -d R^2 w_m\, 0.61\, i_2 z^{-4/3} \qquad (2.29)$$

From (2.29) can be obtained the expression for the maximum space-charge excess in the plume:

$$\sigma'_m = \left(\tfrac{1}{2} d\right) 0.61\, i_2 z^{-1/3} \qquad (2.30)$$

This is analogous to the temperature excess equation:

$$\vartheta'_m = \left(\tfrac{1}{2} d\right) C z^{-1/3} \qquad (2.31)$$

where $C = \left(\frac{T}{g}\right)^{\frac{1}{3}} \left(\frac{H}{h \rho C_p}\right)^{2/3}$.

We decided earlier that the maximum probable value of i_2 between 1 and 2 m, on the basis of the results of Bent and Hutchinson (1966), was 4.2×10^{-13} A m^{-2}. Substituting

$i_2 = 4 \times 10^{-13}$ A m^{-2}, d = 2, z = 1 m in (2.30), we obtain

$$\sigma_m' = 0{\cdot}24 \text{ pC m}^{-3} \quad (1{\cdot}5 \text{ e cm}^{-3}) \qquad (2.32)$$

The corresponding value of θ_m' is 1°C, which is of the right order of magnitude.

Vul'fson's results on the radial profile can be taken into account by substituting in (2.26)

$$f = h = \left(1 - \frac{r^2}{R^2}\right)^{\frac{1}{2}}$$

Since this form of plume has a boundary at r = R, instead of r = ∞, the limits of integration become o and R, giving

$$\frac{d}{dz}\int_0^R r\, w_m \sigma_m' \left(1 - \frac{r^2}{R^2}\right) dr = -\int_0^R r\left(1 - \frac{r^2}{R^2}\right)^{\frac{1}{2}} w_m \frac{\partial \sigma_e}{\partial z}\, dr \qquad (2.33)$$

The left-hand side of this can be integrated directly, and the right-hand side by means of the substitution $r = R\cos\phi$. The result is

$$\frac{d}{dz}\,\frac{1}{4} w_m \sigma_m' R^2 = -\frac{1}{3} w_m R^2 \frac{\partial \sigma_e}{\partial z} \qquad (2.34),$$

and so, by comparison with (2.27),

$$d = \frac{4}{3}$$

Hence, from (2.30), at 1 m,

$$\sigma_m' = 0{\cdot}16 \text{ pC m}^{-3} \quad (1 \text{ e cm}^{-3})$$

As was noted in section 1.3.3, this model gives considerably worse agreement with observation than the Gaussian cross-section, as far as heat-flux measurements are concerned. In any case, since Vul'fson found $R \propto z^{\frac{1}{3}}$, and Priestley's

equations give $R \propto z$, the validity of the whole treatment is suspect. However, the treatment does give answers correct to within an order of magnitude for the temperature and heat-flux values, and the same measure of agreement can be expected for the space-charge density values.

2.4.4 Summary

Applying well-known turbulence theory, the convection current in the forced turbulence regime is shown to be proportional to $u_* z \frac{\partial \sigma}{\partial z}$ (from 2.15); and, by dimensional analysis, in the free convection regime, to $(\frac{H}{\rho})^{1/3} z^{4/3} \frac{\partial \sigma}{\partial z}$ which is itself proportional to $z^2 T^{-1/2} \left(\frac{\partial T}{\partial z} + \Gamma\right)^{1/2} \frac{\partial \sigma}{\partial z}$ (from 2.16 and 2.19). In both these cases, a convection current comparable with the conduction current is necessary before the space-charge density gradient is detectable with apparatus available at present.

The convection plumes postulated by Priestley will produce a peak in space-charge density, but one whose magnitude at 1 m is well below the random "noise" of space-charge density variations usually measured in any weather. Previous space-charge measurements in convective weather are discussed in the light of these conclusions in the next chapter.

CHAPTER 3

PREVIOUS MEASUREMENTS, AND THE GENERAL PLAN OF THE EXPERIMENT

3.1 Previous Space-Charge Measurements in Convective Weather

This section reviews, as far as is relevant, the measurements of Law (1963), Bent and Hutchinson (1966), and Whitlock and Chalmers (1956).

3.1.1 The Measurements of Law (1963)

Law's measurements are relevant to the theory in the previous chapter, but only incidentally to the rest of the thesis, and so they will be dealt with briefly.

Law measured the positive and negative small-ion concentrations, and the nucleus concentration, at various heights; the space-charge density at 0.5 m, the conductivity below 0.5 m and at 1 m, and the potential gradient at 1 m. He found that the space charge was generally positive during the day, but negative at night, and that the variation of the parameters with height required an appreciable convection current. By assuming constancy of the total current with height, Law worked out variations of space-charge density with height in the first two metres consistent with his results, and with the small variation of potential gradient with height commonly

found. The turbulent transfer coefficient K was not measured, and Law's assumption of one value for daytime and another for night amounts to assumed, fixed values for the wind-speed. This is, however, a relatively minor criticism. In view of the low values of z, the implicit assumption of forced convection is probably justified. The calculations are effectively based on theory similar to that of section 2.4.2, and cannot of course be taken as confirmation of the theory, except in a broad sense.

Law also calculated, with some success, the likely distributions of small ions with height under various conditions, making assumptions about the variation of ionization with height. He does not seem to have explained fully the sign difference between day and night, however.

3.1.2 The Measurements of Bent and Hutchinson (1966)

This experiment was originally designed to detect space-charge density gradients associated with a convection current. As already noted, it did not generally detect any. On some occasions, however, they seem to have detected free-convective buoyant elements. During the periods in question, measurements were made of space-charge density at 1 and 19 m, wind-speed at 17 m,

humidity at 1, 2 and 19 m, and temperature at 0.5, 1, 2 and 19 m. On days when free convection might be expected, they found positive peaks of space-charge density at both heights, frequently 25 pC m^{-3} in amplitude, coinciding with rises in temperature and humidity at all heights, and less marked falls in wind-speed. The temperature rises were often about 1°C. The vertical continuity and sharp-edged nature of these disturbances makes it very probable that they were due to some kind of plume of air rising from the ground. However, interpretation of the peaks in terms of plumes like those postulated by Priestley faces one major difficulty: the magnitude of the space-charge pulses. It was shown in the last chapter that the plumes might be expected to give peaks of perhaps 1.0 0.1 or 1.0 0.2 pC m^{-3}. This is only a rough estimate, but is unlikely to be in error by more than an order of magnitude. The size of the pulses in the theory is governed by the size of the space-charge density gradient, which, of course, was measured. It might be argued that we do not know how this gradient varies with height, and that it might increase sharply below 1 m. Law's (1963) calculations show this to be so - he obtained a gradient at 0.1 m of about 24 pC m^{-4}.

However, even with this gradient, equations (2.20) and (2.30) only give a peak of 16 (1.6) pC m^{-3}. In view of the uncertainties in both theory and measurement, it would be unwise to say that these space-charge peaks do not arise simply from transfer of charge from close to the ground - it is difficult to see where else the charge could come from - but the theory and experiment must be said to disagree seriously.

The average separation of the peaks was about 9 min, and the spatial separation, obtained by multiplying this by the wind-speed, averaged 2.1 km. These figures will be discussed further in chapter 6. Unfortunately, details of the average magnitudes and durations of the peaks were not given.

3.1.3 The Measurements of Whitlock and Chalmers (1956)

Working at Durham University Observatory, the site used later by Bent and Hutchinson, Whitlock and Chalmers found in fair weather with some cumulus cloud, but not in completely cloudless weather, positive peaks of potential gradient of amplitude about 100 V m^{-1}. By correlating the records from two field-mills separated in the direction of the wind, and comparing the delay with the surface wind-speed, Whitlock (1955) concluded

that the peaks were due to packets of space charge moving with the wind at a height of a few tens of metres. The average separation in time was about 6.2 min, and the average spatial separation 3.4 km.

Whitlock and Chalmers attributed these peaks to vertical columns of positive charge carried up in the updraught of a convective process, and the magnitude and shape of the peaks is approximately what would be expected from a vertical semi-infinite line of charge, of density similar to that measured by Bent and Hutchinson in their plumes.

We may conclude that these results are consistent with those of Bent and Hutchinson (1966).

3.2 The General Plan of the Experiment

3.2.1 Inspiration and Objects

The experiment was originally conceived to investigate the convective phenomena described by Whitlock and Chalmers (1956), to see over what distances the potential gradient pulses persisted, as the space charge was moved by the wind, and to relate the changes to measurements of vertical air velocity. During the early stages of preparation, the results of Bent and Hutchinson (1966) came to hand, and these changed the emphasis of the experiment slightly. It was decided to try to confirm

experimentally that the space-charge pulses were a convective phenomenon, and to relate them more definitely to one or other of the theories of convection, to define more closely the conditions under which they occurred, and, by simultaneous measurements at separated points, to determine the lateral extent and speed of movement of the pulses. It was also planned to repeat the observations at a site other than Durham University Observatory, to confirm that the phenomenon was not just a consequence of the local topography.

3.2.2 Sites and Transport

The Observatory (National Grid Reference NZ 267415) stands on a small hill about 1 km south-west of the centre of Durham City, with the land sloping gently away to the north and west, and more quickly to the south and east. The building is immediately surrounded by fields, but, except to the south and south-east, there is some built-up area beyond these fields in every direction. The local details especially relevant to the convection study are described in Chapter 6. At 1 km to the north of the Observatory passes the main London-Edinburgh east-coast railway line, and the main London-Edinburgh trunk road (the A1) passes ½ km to the west. In every direction,

there are villages or small towns within a few kilometers. The North Sea lies 18 km to the east, and in on-shore winds the low cloud and mist it produces frequently reach as far as Durham.

The site clearly differs from the type usually selected for convection studies, but this is not altogether a disadvantage: it would be useful if the measurements made near the ground on very flat sites could be confirmed here.

Permission was also obtained to make measurements at Mordon Carrs (NZ 3226), which is probably the flattest ground in County Durham not dominated by industry, and, apart from occasional small trees and low fences, is very flat, and rural. The main railway line runs through the area, but the open pastureland gives a good view of the line, and would allow any pollution effects from trains to be quickly identified. The region is not as heavily populated as the coalfield immediately around Durham, and the nearest town is Newton Aycliffe, about 4½ km west-south-west.

A long-wheelbase, hardtop Land-Rover, equipped as a mobile laboratory, was used as a base and for transport.

3.2.3 Principles of Design of Equipment

It was decided that the advantage of having fully-

mobile equipment, and being able to select and change experimental sites at will, outweighed the advantages of a fixed site, especially as part of the object of the experiment was to confirm that the phenomenon investigated was not a purely local effect. This imposed severe limitations on the equipment: firstly, on its physical size and amount, both because of the limited carrying capacity of the Land-Rover, and the need to be able to set up or stow away the equipment in a reasonable time; and secondly because of the need to work from mobile power supplies of limited capacity.

Measurements made at the Observatory could be supplemented by the Observatory Meteorological Station's instruments. At the other site, it was intended that temperature, wind, and possibly humidity gradients should be measured. Space-charge density measurements were to be made at 1 m, which, in view of the results of Bent and Hutchinson (1966), was thought to be a sufficient height to detect the convection effects. Besides the temperature gradients, it was thought useful to measure rapid changes of temperature, to relate these to the space-charge pulses. Provision was also made to measure the general ambient brightness, to see if changes in the strength of sunlight had anything to do with the triggering of the

pulses, and the brightness of the sky overhead, to detect any relation between clouds overhead and updraughts on the ground, as suggested by Durst (1932). Potential gradient was also measured.

One parameter obviously relevant was vertical air velocity, and some time was spent designing and partly constructing apparatus to measure this. Before the apparatus was complete, however, the author had the opportunity of a conversation with J.W. Telford, of C.S.I.R.O. Radiophysics Division, who advised him that variations in vertical velocity were so changeable, especially near the ground, that the difficulty of measurement was barely justified. For this reason, greater priority was given to other equipment, and this apparatus was never finished, although measurements of this quantity were made later, by a more primitive method described in Chapter 6.

So that the same pulses could be identified at different places, three field-mills and quick-response thermometers were made. Ideally, space-charge density would have been the quantity measured in this way, but this was prevented mainly by the cost of the equipment, especially the electrometer needed with each collector, and also the size and power consumption of the apparatus, and the difficulty of moving it about in the field.

When the experiment was originally planned, it was hoped to use an automatic recording system under development by K.N. Groom (Groom 1966, Chapter 10), in which a voltage signal between 1 and 10 V from each instrument would be converted to a frequency and recorded in turn on a tape-recorder, to be played back later, and automatically converted to punched-tape form, suitable for use as a computer data tape. For this reason much of the equipment was designed to give a voltage output between 1 and 10 V, with an output impedance small compared with the 56 KΩ input impedance of the voltage-to-frequency converter. Also, with this system it would have been easy to handle a large number of parameters, and it was originally planned to use 27 recording channels.

However, due to shortage of time, this system was unfortunately not completed, and so recording was carried out on a 4-channel 0 - 1 mA galvanometer pen recorder, of coil resistance 1.3 KΩ . A "telephone-exchange" switching system enabled any four of the parameters to be measured simultaneously, and in the circumstances this was found satisfactory.

The time constant of each piece of apparatus was originally designed to be about equal to the cycling time

of the proposed automatic recording system, viz.10 s. This seemed a suitable interval for the study - short enough to bring out any large-scale structural detail in the convection pulses, but long enough to smooth out many of the higher-frequency changes - and so this was the requirement generally observed even after the automatic system had been abandoned.

The apparatus is described in detail in Chapters 4 and 5.

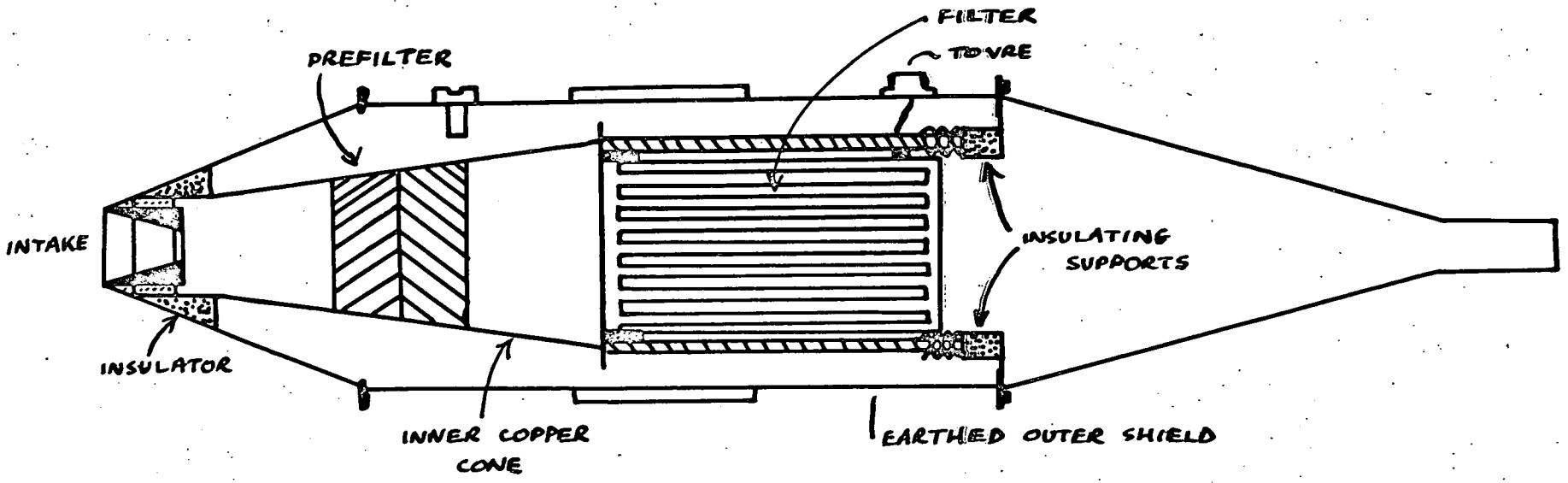

FIG. 4-1 THE SPACE-CHARGE COLLECTOR

CHAPTER 4

THE SPACE-CHARGE COLLECTOR

4.1 Scope of the Chapter

It is not the intention to review here the various methods of measuring space-charge density, for which the reader is referred to Vonnegut and Moore (1958). In this work, a filtration apparatus, similar to that described by Bent (1964, and 1965 chapter 3) was used, and this chapter is an account of its construction, testing, and use, with the difficulties encountered in using the apparatus, and improvements suggested for the design of future instruments.

4.2 Construction and Use

The detailed structure has been described by Bent (1964, and 1965, chapter 3). The collector is shown in figs. 4.1 and 4.2. Basically, it consists of a glass-asbestos filter, which captures the ions as the air passes through. The ions induce an equal and opposite charge on the enclosing frame of the filter, and a charge of the same sign and magnitude as the captured charge is repelled to earth through the measuring apparatus, to which the filter frame is connected. Both the glass-

FIG. 4·2 THE SPACE-CHARGE COLLECTOR

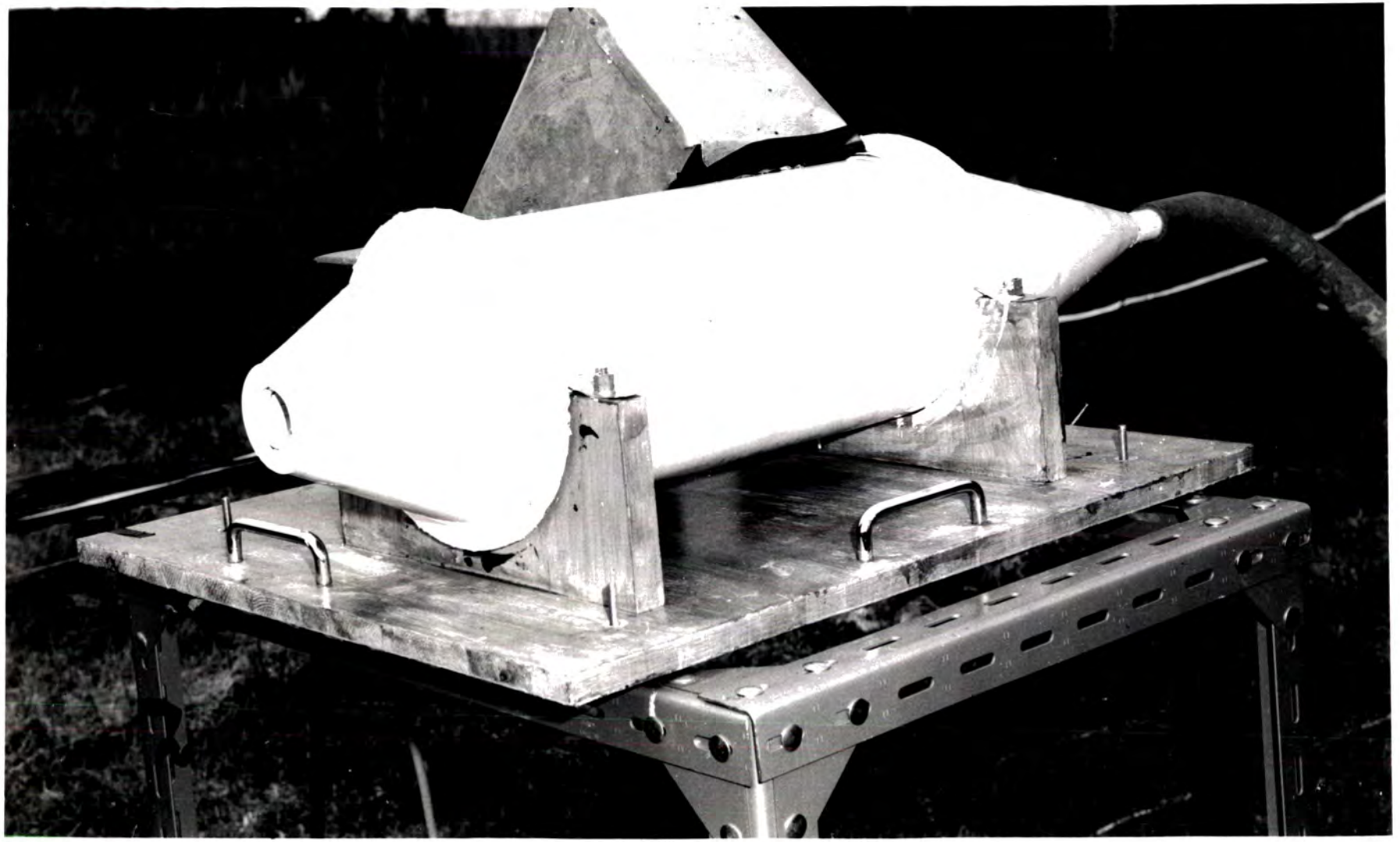

asbestos filter and a stainless-steel-wool prefilter are enclosed in an earthed copper shield, which protects them from the Earth's electric field (therefore preventing displacement currents), but from which they are highly insulated.

Two minor modifications were made to Bent's design. On his advice, the nose-cone was redesigned so that the intake tube was tapered to slope outwards, instead of inwards. This meant that any condensation in the intake tube tended to roll out of, rather than into, the collector. The other modification was made to the back support of the inner cone (which held the filter). The support here was by four brass rods attached to the front support of the filter, which mated with holes in four insulators attached to the back bulkhead of the outer, earthed shield. When the back cone of the collector was removed, the bulkhead came with it, and it was very difficult to replace it so that the four rods, which were quite springy, because of their length, matched the holes in the insulators. A brass mask was made, with four holes to match the holes in the insulators, and this was slipped over the top of the rods to hold them the correct distance apart to match the insulators. This simple improvement made the overhauling of the collector a much easier task.

The meter used was an "Ekco" Vibrating Reed Electrometer (V.R.E.), type N616B - the same sort as was used by Bent. This consisted of a head unit, which had to be mounted with less than two feet of cable between the filter and the unit input, and an indicator unit, which was mounted in a rack in the Land-Rover, and connected to the head unit by two twelve-way cables, each 100 feet long. The applied signal flowed to earth through a $10^{12}\Omega$ resistor, and the instrument measured the voltage across the resistor. The output from the V.R.E. was displayed on a panel meter, and as a 0 - 1 mA recorder output. The most sensitive full-scale deflection of both outputs corresponded to an input of 3 mV, i.e. 3.10^{-15} A through the input resistor.

It was easy to adjust the time constant of the V.R.E., simply by putting a capacitor in parallel with the $10^{12}\Omega$ resistor, each pF corresponding to 1 s. The minimum allowable capacitance was 1 pF. For almost all the work, a time constant of 5 s was used. It is important to realise that, because the signal was applied to the grid of a valve, and then leaked away through the $10^{12}\Omega$ resistor and the capacitor, the time constant applied to the decay of signals, and not to their increase. A sudden increase in charge density would be registered

immediately, but a fall to zero would show as a decay with the time constant.

To minimize the movement of the cable between the collector and head unit, which caused piezoelectric effects in the cable insulator, the two were mounted together on a thick piece of blockboard (fig. 4.2), and the connection made using anti-microphonic cable in a copper tube, which was rigidly fixed at each end, and covered with a sunshade. These precautions against noise are described more fully in section 4.6.

During transport, the collector was mounted on the inside wall of the Land-Rover, and the cables left connected. Because the V.R.E. is supposed to take 24 hours after switching-on to settle down, it was left on almost permanently. In fact, it was found that the device was quite usable half an hour after switching-on from cold: presumably the instability shows itself mainly in slow zero drift, which was not a source of concern, since short-period space-charge pulses were being studied. If the V.R.E. were just switched off for a few minutes, ten minutes warm-up was found to be ample, and, in fact, it was found convenient to switch off and disconnect the cables while the collector was being put out.

In use, the collector was set up, and, after the warm-up period, the V.R.E. was zeroed. A record was then taken for a few minutes with everything switched on, except the fans to suck air through the filter. This determined the noise level before the space-charge was measured. This noise determination was occasionally carried out at the end of a record as well, and it was generally found that the noise had decreased considerably, presumably because both the V.R.E. and the power supply were more stable.

In the field, the collector was mounted on a cuboid adjustable-angle frame (fig. 4.2) which supported it fairly rigidly 1 m above the ground.

It was sometimes necessary to check that the collector and V.R.E. were working properly. The connection to the V.R.E. could be checked by charging the barrel of a fountain-pen by rubbing it on woolen cloth, and inserting it in the inlet orifice of the collector. The displacement current caused a big deflection on the V.R.E., and the decay of this deflection could also be used to check the time constant of the instrument. To check that the collector was actually measuring space charge, a smoking cigarette was held in front of the inlet, and the charged smoke caused a big negative deflection.

4.3 Air flow-rate

A reasonably fast air flow is desirable for two reasons: because the sensitivity of the collector is proportional to the flow-rate, and because, according to Bent, the air-speed into the collector inlet must be greater than the fastest wind-speed likely to be encountered. Bent was able to have a flow-rate of 3 l s^{-1}, but in the present work shortage of power for the fans limited the flow to 2.25 l s^{-1}. This was obtained by having two 12-volt, 20 watt D.C. fans in series. Both were of the centrifugal type, driven by motor-car heater-fan motors, which were powered by a 12 - volt storage battery. Fans are supposed to produce copious positive charge, but a test in the laboratory with the fan exhaust nozzle about 2½ cm from the front of the collector yielded a measurement of about - 10 pC m^{-3}. As a precaution, however, in measurement the fans were separated from the collector by about 2.5 m of 1" diameter rubber tubing, and placed downwind from it.

The collector was generally mounted with its axis perpendicular to the wind direction, to minimize any effect of the wind on the flow-rate.

It was not possible to moniter the flow-rate continuously with a gas meter, as Bent did, partly

because of the room this would have taken up in the Land-Rover, but mainly because a considerable pressure drop is required to operate such a meter, and its inclusion would have very much reduced the flow. The flow-rate was therefore measured in the laboratory in the following way, and assumed constant. By measuring the pressure-drop across the collector with a water manometer, and simultaneously measuring the flow-rate with a gas meter, a calibration curve was obtained of flow-rate against pressure-drop. Because it was possible to use powerful A.C. fans in the laboratory, this calibration could be extended as far as was desired, despite the large pressure-drop needed to drive the meter. The gas meter was then removed, and the pressure-drop measured across the collector with the two fans used in the field supplying the power. From the calibration, the flow-rate could be determined. The calibration was found to be almost linear, and the pressure-drop produced by the fans was 6 cm of water, corresponding to a flow-rate of 2.25 l s^{-1}. Similar measurements showed that the two fans produced a much greater flow when operated in series than in parallel, and that the performance of the fans did not change appreciably with their position, i.e., they could be operated vertically or horizontally. The

length of rubber tubing used was also found to be unimportant.

It was thought that the gradual accumulation of dust in the filter and pre-filter might reduce the flow-rate as time went by. For this reason, the calibration was repeated after the readings of summer 1966 had been completed. It was found that in the five months that had elapsed since the initial calibration, the flow-rate/pressure-drop curve had not moved significantly, indicating that the filter characteristics had not changed, and the flow-rate was not altered by this factor.

A more serious fault, which only came home to the author towards the end of the experiment, was that the speed of a D.C. fan, when running near the rated voltage, is approximately proportional to the voltage. This presumably meant that as the battery ran down, the flow-rate decreased, and, for this reason, the absolute values of space-charge density obtained during the experiment are not known more accurately than $\pm$ 5%. However, in practice, the absolute values obtained were not very important, and, since changes from this cause would be slow, the swift changes were being studied, the fault was not thought a very important one.

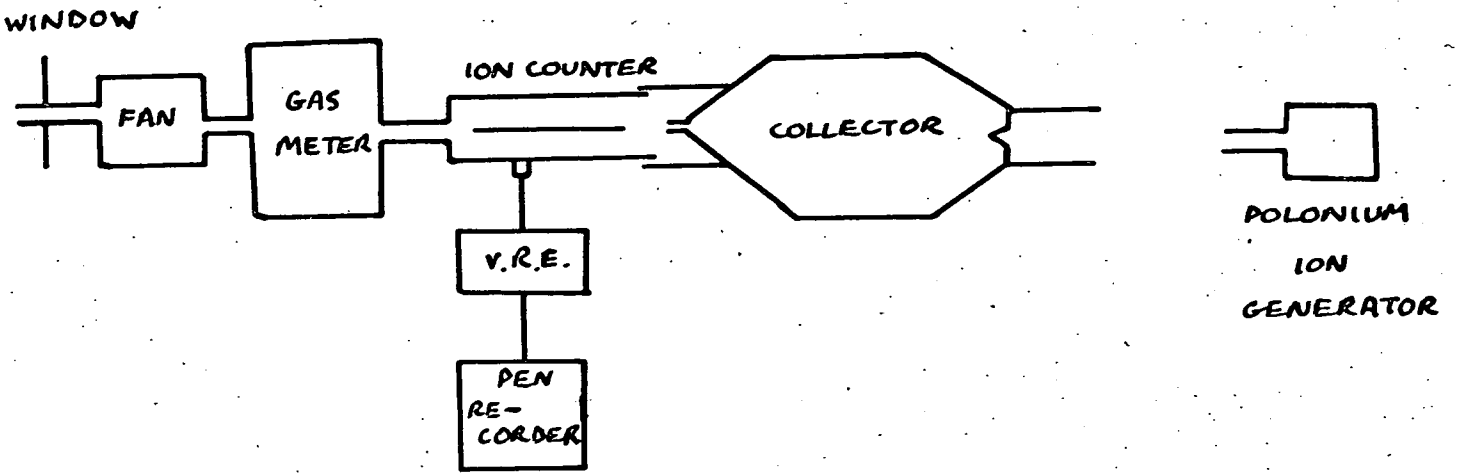

FIG. 4·3 COLLECTOR EFFICIENCY TEST

With a flow-rate of 2.25 l s^{-1}, a reading of 1 mV on the V.R.E. corresponded to a space-charge density of 0.44 pC m^{-3} (2.8 e cm^{-3}).

4.4 Test of Collector Efficiency

This experiment, designed to test the efficiency of the filter at catching small ions, was similar to that described by Bent (1964). Basically, it consisted of measuring the small ion concentration in a room with an Ebert ion counter (Chalmers 1967, section 2.54), and then repeating the measurement with air sucked through the space-charge collector. Measurements of the current flow from the filter were not made.

The schematic layout of the apparatus is shown in fig. 4.3. The ion generator and counter were those described by Bent (1964). Cardboard tubes were attached to the fronts of the space-charge collector and the ion counter, so that each presented the same "catching area" to the ion generator. When the collector was removed, the generator was moved to be the same distance (25 cm) from the front of the counter as it was from the front of the collector. The pen-recorder was used to measure the output from the counter when the collector was removed, and to detect the variability of the output. It was found, in fact, to be quite steady. With the air

passing through the collector, the reading was taken from the panel meter on the V.R.E., as this was more sensitive than the recorder.

With the collector in position, readings were taken for flow-rates between 1.1 and 5.3 l s^{-1}, and, with the collector removed, between 2.9 and 6.0 l s^{-1}. It was found that with the collector in position no detectable output from the counter was obtained for any flow-rate, and so the minimum efficiency must be determined from the minimum deflection that would be detected on the panel meter. This was taken as 0.3 mV on the 30 mV range. The deflection without the collector at 4 l s^{-1} was about 280 mV, and so the collection efficiency of the filter for small ions is greater than 99.9%.

The efficiency of the electrostatic shielding was also tested by recording displacement currents measured by the probe described by Groom (1966), alongside the output of the collector. There was no noticeable relationship. When a charged fountain-pen was used to get a deflection on the V.R.E., as described in the previous section, it was found necessary to put the barrel right inside the inlet orifice of the collector to cause a deflection, which confirms this result.

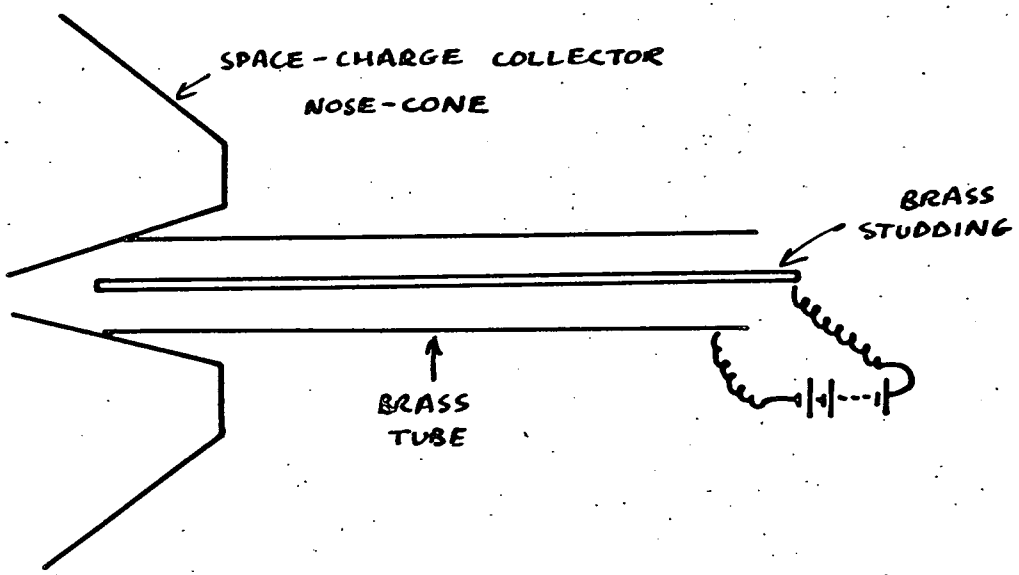

FIG. 4-4 CROSS-SECTION OF SMALL-ION FILTER

4.5 Attachments for the Collector

Two devices were designed to improve the usefulness of the collector, one of which was used, and the other rejected as impractical.

4.5.1 The Small-Ion Filter

This was developed in conjunction with K.N. Groom, to enable measurements to be made of how the proportions of small and large ions in fog varied with distance downwind from power-line support towers. It was, in effect, a miniature Ebert ion counter put on the front of the collector, and consisted of a piece of brass tubing about 15 cm long and 3 cm in diameter (fig. 4.4). Down the centre of this was a piece of brass studding, which acted as the centre electrode, and which was suspended from the outer tube by lacing-cord passing through holes in the tube. Because of the big difference in mobility between small and large ions, it was possible to apply sufficient voltage difference between the tube and studding to remove all the small ions electrostatically, without affecting the large ions significantly. Thus, measurements of the space-charge density with the voltage switched on gave the large-ion component separately. It was unnecessary to take the precaution usual with an ion counter to ensure that the

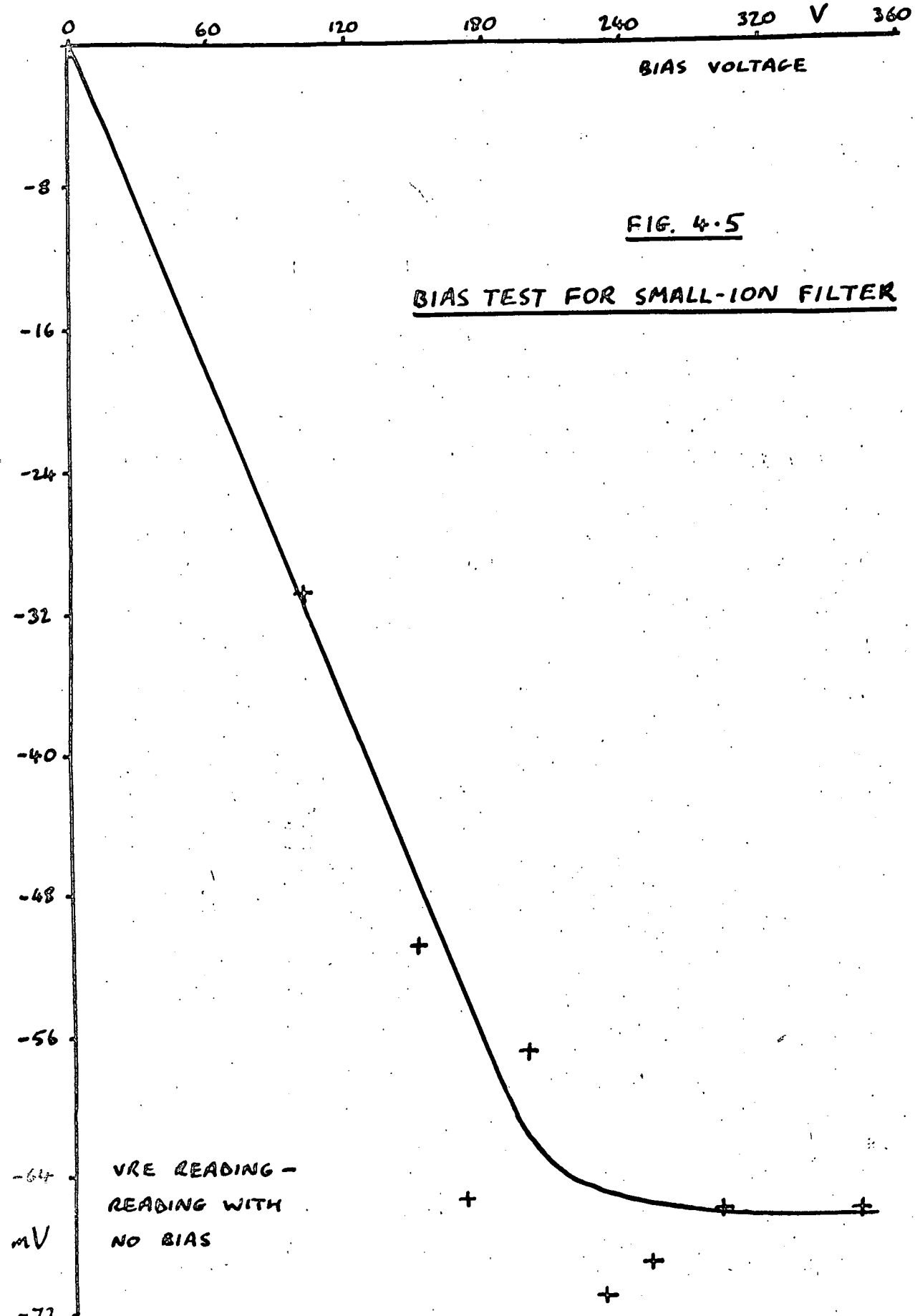

FIG. 4·5

BIAS TEST FOR SMALL-ION FILTER

entrance of the counter was at the potential of the surroundings, because it was not intended to count the small ions - only remove or repel them.

When the filter was required, it was attached to the collector with plasticine and sticky tape, a satisfactory but clumsy procedure that will be further remarked on in section 4.7.

To determine the voltage necessary to remove all the small ions, the collector, with the small-ion filter attached, was shut in a room with the polonium ion generator referred to in section 4.4, until the space-charge reading was steady. Various voltages were then applied to the central rod. As the bias voltage was increased, a greater proportion of the small ions was removed, but when all the small ions had been removed, an increase in bias voltage had no further effect on the space-charge density measured. It was found that the critical voltage was about 200V. A potential difference of 240 V was employed when the device was used.

4.5.2 The Front Tube

The investigation of the space charge produced by melting snow (chapter 7) required measurements to be

made of space-charge density at various heights. In trying to avoid moving the collector bodily up and down between measurements, a rubber tube was fixed to the front of the collector. It was felt that the tests conducted by Bent (1964) with his two collectors in series, using rubber tube to connect them (K.N. Groom, personal communication), showed that the tube did not generate charge. However, it soon became apparent that the space-charge density readings were not what would be expected, and direct comparison of measurements by the collector and rubber tube with measurements by one of Bent's collectors, when the two were side-by-side, showed that the rubber tube made the readings about 50 pC m^{-3} more positive than they should have been. This was provisionally attributed to charges resident in the rubber. Later, the author noticed the report by Nolan and Kenny (1953) of a similar observation, which they explained in terms of charges produced in the rubber by bending, which removed many of the ions.

Later, the possibility of using a brass tube attached to the front of the collector by a short length of flexible tubing was investigated. This time, due attention was given to the danger of ion loss to the walls of the tube, which in this case would be by simple

mechanical and perhaps electrical diffusion. As far as mechanical diffusion is concerned, Nolan and Kenny (1953) give values for the proportion of ions surviving a journey along a tube in terms of h, where

$$h = \frac{\pi l D}{2Q}$$

(l is the length of tube, Q the volume flow-rate of the gas down the tube, and D the diffusion coefficient of the ions.)

Einstein (1905) gives

$$D = \frac{kTw}{e}$$

(k is Boltzmann's constant, T the absolute temperature, w the mobility of the ions, and e the electronic charge.)

Taking $k = 1.38 \times 10^{-23}$ J degC^{-1}, T = 273°A, $e = 1.6 \times 10^{-19}$C, for small ions of mobility 2×10^{-4} m s^{-1} per V m^{-1}.

$$D = 4.7 \times 10^{-6} \text{ m}^2 \text{ s}^{-1}$$

and for large ions of mobility 5×10^{-7} m s^{-1} per V m^{-1},

$$D = 1.75 \times 10^{-8} \text{ m}^2 \text{ s}^{-1}$$

Hence, for a 2 m tube with a flow-rate of 2×10^{-3} m^3 s^{-1}, $h = 7.4 \times 10^{-3}$ s^{-1} for small ions, and 2.7×10^{-5} s^{-1} for large ions. Nolan and Kenny's table shows that small ions should therefore suffer a loss of about 13%, and large ions a loss very much less than 1%. It is interesting to note that these losses are independent of the diameter of the tube, because although an ion does

not have as far to travel to the walls of a narrower tube, it spends less time in the tube for the same flow-rate. The diffusion loss is related to l in a complicated way.

These calculations neglect the electrostatic attraction of the tube walls for the ion due to the image effect, which may increase the diffusion rate, but is probably negligible.

Assuming positive and negative ions to have the same mobilities, the space-charge density values will be affected by the same percentages as the total ionic concentrations. We can therefore conclude that the small-ion space-charge density would be reduced by more than 13%, and the large-ion density would not be appreciably affected. The small-ion filter could have been used to determine the two space-charge densities separately, and the above calculation, and another for the electrostatic effect, used to make allowance for the loss of small ions; but in view of the uncertainties involved, and the extra time the procedure would take during measurements in the field, it was not felt worthwhile to use the tube. The idea was therefore abandoned, and gradients were measured by moving the collector bodily up and down.

4.6 Fault-Finding on the Collector

Although the space-charge collector is fundamentally a very simple device, the very small currents that must be measured mean that noise is very hard to eliminate. Indeed, much of the time that might have been used to take measurements in the early months of the experiment seemed to be spent in tracing spurious signals or faults on the collector or V.R.E. This section is included to help future workers to identify and correct faults more quickly, although, if the recommendations for improvements in the design made in section 4.7 are adopted, many of the spurious signals should be eliminated.

4.6.1 Effect of Wind

Bent (1965, chapter 3) reported that wind interfered with the collector by causing vibration in the cable connecting the collector to the V.R.E. head unit, producing piezoelectric effect in the insulator between the outer conductor and the core. This was found to be an important source of noise in the present case also. Co-axial cable with a rigid outer conductor was tried, but was found not to be very satisfactory, presumably because the rigid connection between the outer conductor and the insulator meant that every vibration was

transmitted to the insulation. Another method tried and rejected was anti-microphonic cable stapled to the wooden base of the collector. The best solution was found to be that of Bent: antimicrophonic cable inside a copper tube soldered at both ends to plugs connecting rigidly with the sockets on the collector and head unit. Soldering the tube to the plug was found to be a problem, because an iron hot enough to melt solder on the copper tube melted the insulation on the cable inside. However, since an electrical connection between the tube and plug was not important, it was found satisfactory to use a commercial "cold solder", which appeared to be some sort of metallic suspension in an organic solvent which evaporated when the solder had been applied.

Even with this arrangement, it was found that the cable was still disturbed, presumably by minute wind-induced vibrations. Bent was apparently able to overcome this fault, but he had the advantage of being able to mount his collector on a mast considerably more rigid than the portable support used here. The signal from this source varied with mean wind-speed, of course, but was sometimes more than 2 0 mV, varying with a time constant of the order of half a minute. The time constant was

presumably a function of the time taken for the charge produced in the insulator to leak to the conductor. If flexing the cable one way produced a positive signal, flexing it the other way produced a negative one, but in the field the noise signal might stay of one sign for minutes at a time.

Fortunately, the effect of this noise on the convection measurements was not as serious as might be expected, because, although it made accurate measurements of space-charge density impossible in high winds, the space-charge pulses measured in convective weather had very sharp leading edges, and could easily and unmistakably be picked out from a wind-noise background.

4.6.2 Effect of Sunshine

Bent (1965) found that signals from his collector as clouds passed in front of the sun could be attributed to the expansion and contraction of the copper tube holding the cable from the collector to the head unit, causing flexing, and therefore piezoelectric effect, in the cable insulator. He succeeded in preventing this by shading the cable, but in the present work it was found that, although this improved the situation, it was by no means a complete solution. It was found that the sun shining on the collector itself gave a large signal.

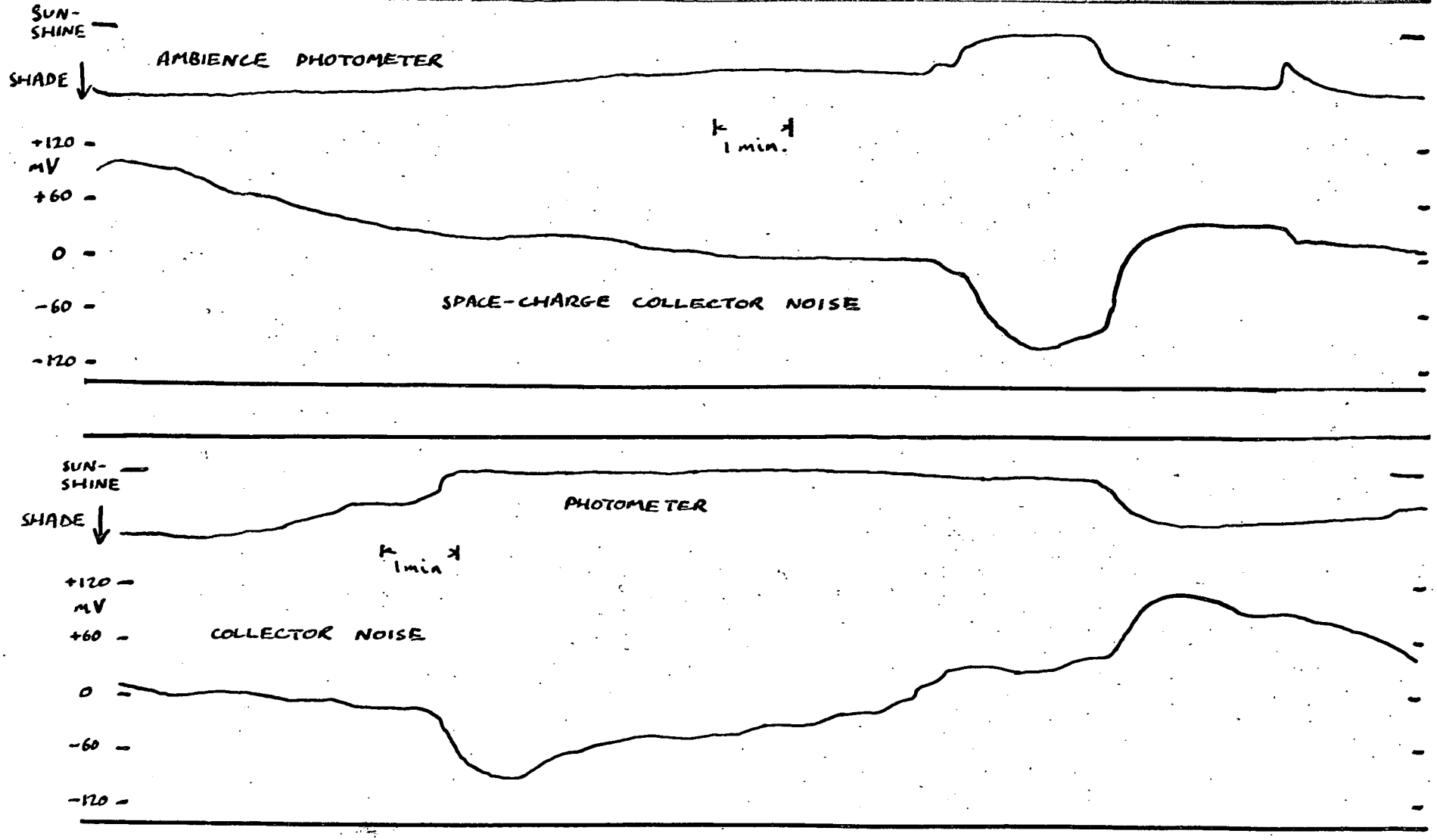

FIG. 4·6 COLLECTOR NOISE DUE TO SUNSHINE

By shading different parts of the collector, the sun was found to have most affect on the front cone, although the disturbance was by no means confined to this region. On some days, the apparatus could be set up so that the front cone was shaded by the rest of the collector, and as the sun moved round in the sky and began to shine on the front cone, the noise increased considerably.

It was only changes of light intensity that gave the signal: steady, unclouded sunlight gave none. Fig. 4.6 illustrates the effect. Channel 1 is the record of the ambience photometer, designed to detect sunlight shining on the site, and described in chapter 5. Channel 2 is the space-charge collector noise record. From this and other records it can be seen that when a cloud passed in front of the sun, the collector signal showed a positive kick of about 100 mV, which then decayed towards zero with a time constant of a minute or two. When the cloud moved away, the effect was exactly similar, but of opposite sign. The effect was quite sensitive to changes of light intensity, and, although continuous sunlight gave no effect, it was noticeable on a reduced scale in "cloudy-bright" conditions.

The effect would seem to be best explained as expansion and contraction of the copper case of the

collector causing flexing of the connecting cable. The sensitivity of the nose is hard to explain on this basis: there may be some affect on the insulator in the nose, although the form of P.T.F.E. used is said not to show piezoelectric effects; it is more likely that, for some reason connected with the way the collector was attached to its blockboard base, expansion of the nose was particularly easily transmitted to the cable. Photo-electric or thermo-electric effects, the other possible explanations, give even less satisfactory accounts. They are unlikely to occur because all the surface exposed to the light is earthed copper or brass, and, in any case, do not explain, as the expansion and piezoelectric effect theory does, why going into shadow produces a mirror image of the signal obtained when the sun first shines, and why, in constant conditions, the noise decays slowly to zero.

The collector was painted white as a simple, but rather optimistic attempt at a cure. This had little affect, but it was later found that an even simpler expedient was much more effective. Aluminium foil was loosely taped all over the outside of the collector, leaving an air-gap between the two, and this very much reduced the noise.

Although the noise signals caused by sunlight were fairly sudden, they were not nearly as sharp-edged as the space-charge pulses attributed to convection, and these could easily be distinguished. In any case, once the cause of the noise had been identified, it was easy to monitor sunlight changes by taking notes, or by running the ambience photometer on a spare channel, and the sunlight effect was more a nuisance than anything else.

4.6.3 Insects in the Collector

This effect was also obtained by Bent (1964), but was only observed once during the present experiment. According to Bent, small flies are sucked straight onto the prefilter and cause no interference beyond a small contribution to the space charge registered. Large flies, however, have sufficient strength to fly against the air flow, and may fly many times between the prefilter and the outer earthed shield.

Only one record was obtained which showed this. The effect lasted for about fifteen minutes, and showed as rapid fluctuations, of amplitude about 10 mV, consisting of a sudden fall in signal towards zero, followed by a return with the time constant of the V.R.E. Towards the end of the period, the frequency of the oscillations

decreased, perhaps as the fly weakened.

4.6.4 Insulation Breakdown

Because of negative feedback in the amplifier, the effective input impedance of the V.R.E. is about $10^{10}\Omega$, and insulation resistance in the collector must therefore exceed $10^{12}\Omega$. In dry weather, this presented little problem. P.T.F.E. is water-repellent, and the insulators were well protected from the outside air, and only got dirty very slowly. They were periodically cleaned with trichloroethylene followed by absolute alcohol. In high humidity, however, and especially, in the present study, in fog, a film of water formed over the surface of the nose insulator, and shorted the inner cone, holding the filter, to earth. This process generally took about half-an-hour's running. It showed itself not, as might be thought, in zero deflection on the V.R.E., but, because of the feedback characteristics of the amplifier, as a fairly sudden rise to a high steady deflection, usually of several hundred millivolts. It could easily be identified because stopping the collector fans would not affect the deflection.

A heating tape, sold to protect domestic water-pipes from frost, was kept wrapped round the collector, and used to warm it. This was switched on when the

collector was housed in the Land-Rover to dry it out after insulation break-down, and during the winter was kept switched on all the time.

4.6.5 Broken Filter Connection

Its inaccessibility made the connection between the filter and the plug on the collector outer shield rather difficult to solder, and, under the strains experienced by the instrument in being moved about, from time to time the connection broke. This fault, although usually easily recognized, is mentioned here because it did not necessarily mean no response to signal at all on the V.R.E. If the two broken pieces of wire were still close together, a large charge on the filter would register by electrostatic induction between the two pieces. For this reason, the "pen test" (section 4.2) would give a positive response, although reduced in magnitude, but the "cigarette test" generally would not.

4.6.6 Faults on the Vibrating Reed Electrometer (V.R.E.)

The V.R.E. indicator unit was fixed to the rack in the land-rover by anti-vibration mounts, but, even so, did not react very well to the continual vibration it sustained, and faults on it were fairly frequent. The head unit also reacted badly to being continuously moved

about. Another source of trouble was the 48 soldered connections at the ends of the two 12-way cables, which were also subjected to frequent strain. However, the main source of trouble with the V.R.E. was the power it consumed from the inadequate supplies. The voltage from the transverter (described in the next chapter) fell gradually as the batteries ran down, giving symptoms of "power failure" on the V.R.E. This showed itself first as a fast flicker on the meter needle, followed, within a few minutes, by violent irregular fluctuations, or sometimes a high fairly steady reading, and total lack of response to input. A temporary cure could be effected by switching off and reducing the mains voltage tapping on the instrument.

4.7 Recommendations for Future Designs

The greatest sources of spurious signals were the wind and sun effects, both of which are thought to have acted through piezoelectric effect in the insulator in the cable connecting the collector to the V.R.E. head unit. When measurements were made at night in low winds, as during the fog measurements, the noise level was often only two or three millivolts. Clearly, it would be a great advantage if this insulator could be removed, and this could quite easily be done by connecting the

filter to the head unit by a single uninsulated wire. It would be necessary to enclose the wire in an earthed shield to protect it from displacement currents, but this could be done by extending the outer cone - the electrostatic shield - of the collector to enclose the wire and at least part of the head unit, or whatever replaced it. This would make the collector more difficult and expensive to construct, but the saving in time in the field and the great increase in sensitivity would well justify it.

If space-charge measurements with mobile apparatus are intended, the V.R.E. of the type used, although very sensitive, is clearly not very suitable, because of its relatively high power requirements, and its bad response to movement. A solid-state circuitry electrometer would probably not be quite as sensitive, but would be adequate, lighter to move, would travel much better, and would probably be cheaper.

A small but useful improvement would be a short threaded length on the inside of the inlet orifice of the collector. This would facilitate the attachment of such devices as the small-ion filter.

FIG. 5-1 THE LAND-ROVER INTERIOR.

CHAPTER 5

OTHER APPARATUS

5.1 The Land-Rover Installation

5.1.1 Power Supplies

The Land-Rover power-supplies were originally installed by the previous user of the vehicle (Groom 1966), and were modified for the present use by the author. The source of power in the field was four 12V lead-acid storage batteries, of 60 AH capacity each. These supplied a "Valradio" transverter, type 24/120T, which converted a 24V input to 230 V, 50 c/s, to drive the V.R.E. and pen-recorder motor. When the Land-Rover was not being used, the apparatus was connected to the mains supply, which then ran the V.R.E., and charged the batteries by means of a battery charger in the vehicle. By use of switches, the batteries were all connected in parallel for re-charging, and in two parallel sets of two in series, giving 24V, for supplying the transverter, and also the electronics, via a 12V stabiliser described in section 5.1.2. The transverter itself required about 55 W to drive it, and the V.R.E. about 65 W, giving a total current drain of about 2½ A from each battery. The recorder took negligible current.

FIG. 5-2 THE INSTRUMENT RACK

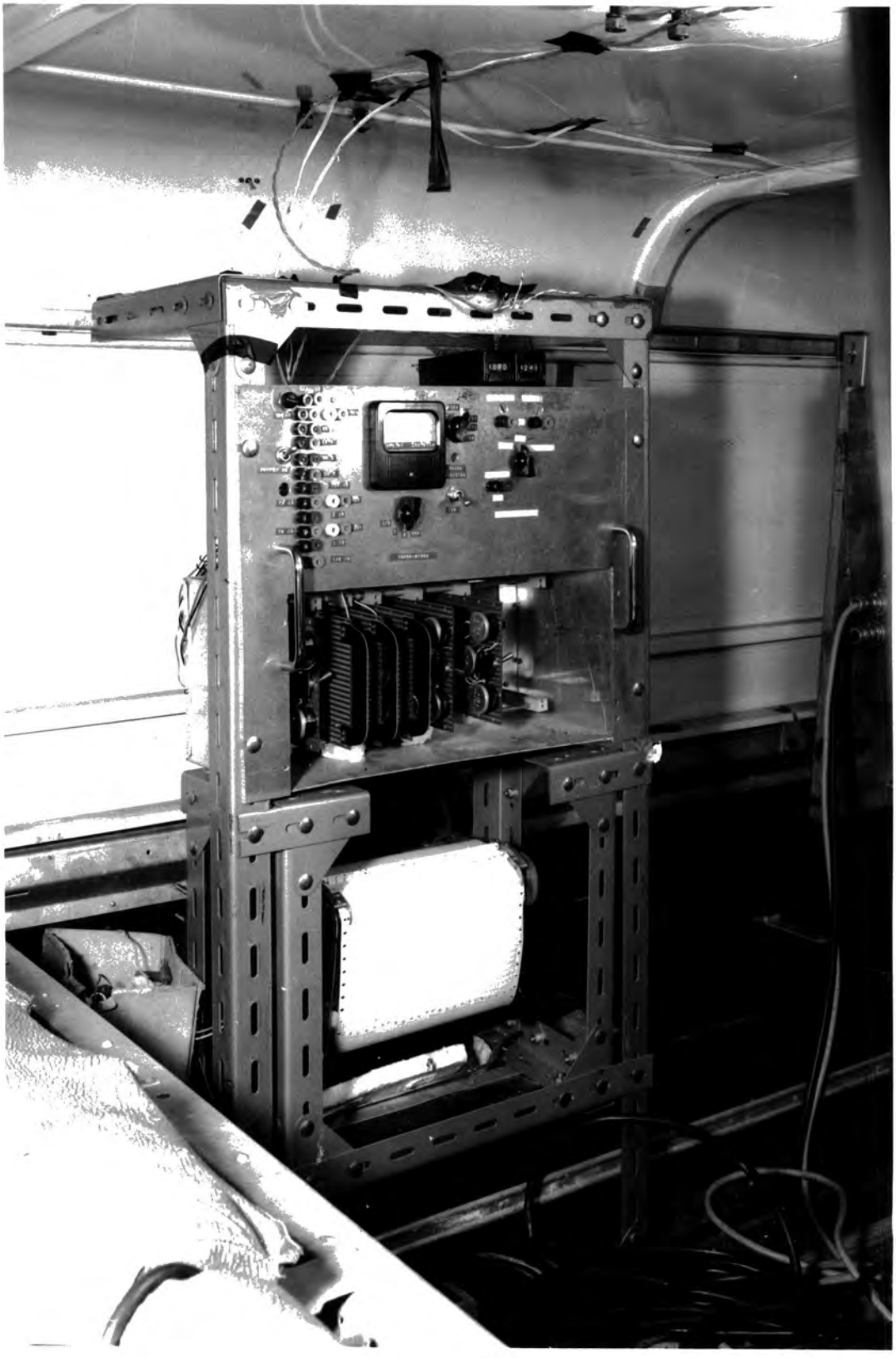

The readings at the Observatory were made within reach of a mains supply, and so the transverter was needed only for the Mordon readings, and for the minor measurements, such as the fog experiment. When the Land-Rover supply was used, it was found to be much less satisfactory and have a much shorter lifetime (about four hours) than might have been expected. This may have been due to the age of the batteries rather than to an inherent shortcoming of the transverter.

5.1.2 Installation of Circuitry and its Power Supply

Fig. 5.2 shows the layout of the rack in the Land-Rover. The panel at the top carried the controls, the anemometer counters, and the meter for the thermistors, and, below these, the electronic circuitry, built on "Veroboard" panels and readily accessible from the front.

Most of the electronics used a -12V, zener-diode stabilized power supply, which was also installed in the "Veroboard" rack.

The input to all the recorder channels was through single sockets on the panel, and the 0 - 1 mA outputs from the circuits in the rack were also carried to sockets on the panel. This meant that, by means of connecting plugs and wire, any of the outputs could be displayed on any of the recorder channels, giving the system maximum flexibility.

5.2 The Field Mills

Three mills were built, in case potential gradient changes proved distinct enough to enable tracking of the convective plumes by this measurement.

5.2.1 Frequency Independence

The theory of the field mill has been studied by several workers, most recently by Groom (1966), who concluded that if R and C are the resistance and capacitance respectively of the rotor-stator assembly (including the input to the amplifier), for practical purposes their values must be

$$R \ll 10^{10}\,\Omega$$

$$C < 350\,pF$$

One interesting aspect is the condition which makes the mill output independent of the frequency f of the signal. The condition is usually stated to be

$$\frac{1}{f} \ll 2RC$$

Groom showed that this corresponds mathematically in the theory to the approximation,

$$\frac{1-e^{-x}}{1+e^{-x}} = \frac{x}{2}$$

and that this condition is fulfilled even if $\frac{1}{f} = RC$. Mr. D.R. Lane-Smith, of Fourah Bay College, University of Sierra Leone (Personal communication, 1966), questioned the validity of this conclusion, and suggested the following

approach. If V is the measured voltage from the stator (the detecting plate), I the current to earth, and ω the angular frequency of the signal, then

$$V = I/\left(\frac{1}{R} + j\omega C\right)$$

$$= I\left(\frac{1}{R} - j\omega C\right)/\left(\frac{1}{R^2} + \omega^2 C^2\right)$$

$$= IR\left(1 - j\omega CR\right)/\left(1 + \omega^2 C^2 R^2\right)$$

Hence, the modulus of V

$$|V| = IR/\sqrt{1+\omega^2 C^2 R^2}$$

If V_∞ is the voltage output for $\omega = \infty$,

$$|V_\infty| = 1/\omega C$$

$$\frac{|V|}{|V_\infty|} = \omega CR/\sqrt{1+\omega^2 C^2 R^2}$$

As $w \to \infty$, $V \to V_\infty$, and clearly becomes less and less frequency dependent. This is shown by the plot of this function (fig. 5.3).

A rough experimental check of the validity of this treatment was made, using a field mill and simple cathode-follower circuit, putting the output from the follower onto an oscilloscope, which was used to measure the voltage and frequency. The resistance and capacitance in the input of the cathode follower were 100 MΩ and 100 pF respectively, and so, allowing 35 pF for the capacitance of the rotor-stator assembly and cable, we have

$$R = 100\ M\Omega\ ;\quad C = 135\ pF$$

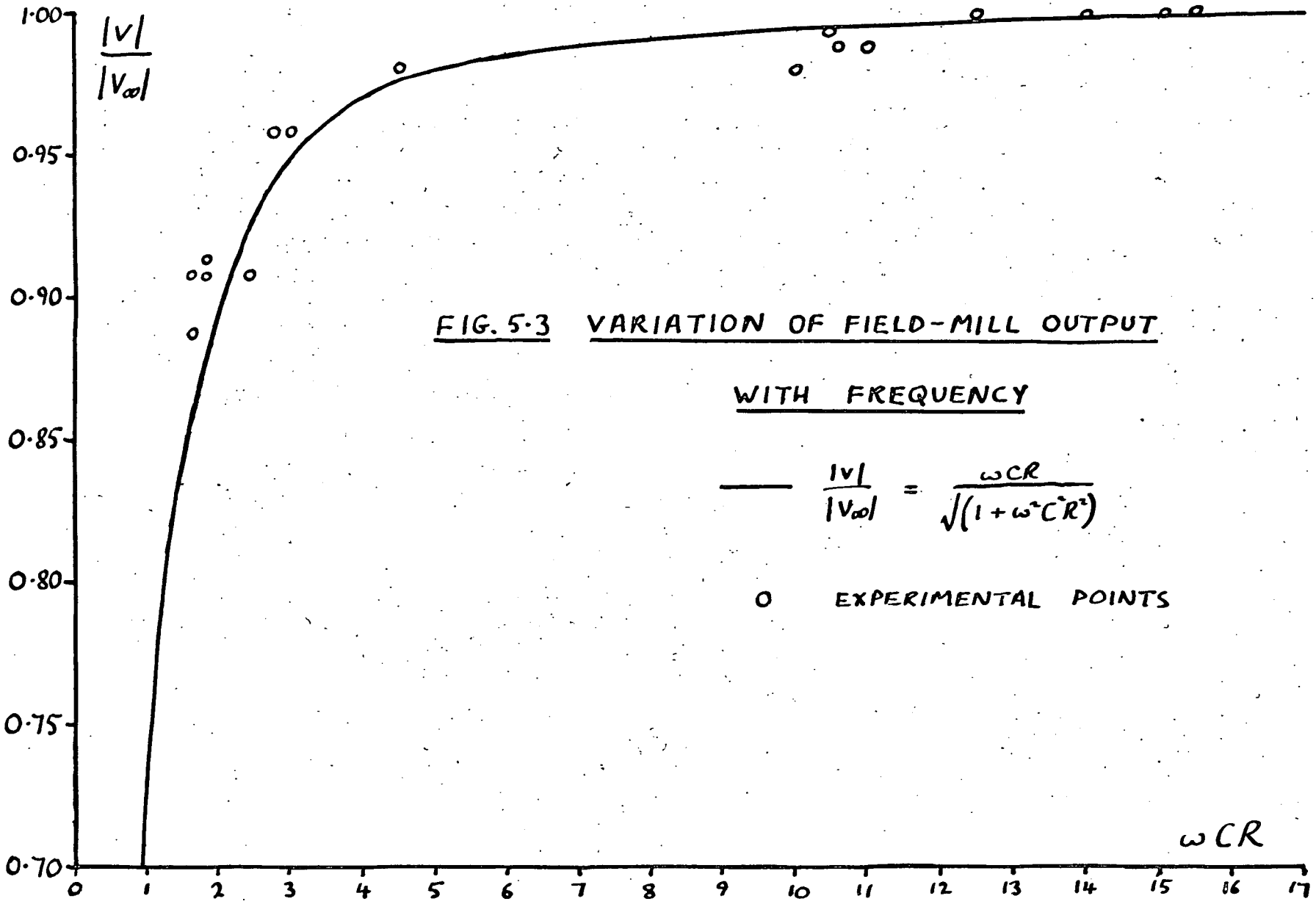

FIG. 5·3 VARIATION OF FIELD-MILL OUTPUT WITH FREQUENCY

$$\frac{|V|}{|V_\infty|} = \frac{\omega CR}{\sqrt{(1+\omega^2 C^2 R^2)}}$$

O EXPERIMENTAL POINTS

The frequency was varied by changing the voltage to the A.C. motor of the mill, and the resultant outputs plotted on fig. 5.3. It was necessary to assume a value for $|V_\infty|$, and this was done to give the best fit to the curve. Taking into account the uncertainty in C, and the crude method used to measure w and $|V|$, the way in which the output declined with falling frequency agreed well with the theoretical curve.

From the curve, we can obtain reasonable working limits for frequency independence. Assuming a change in output of 1% for a change in frequency of 10% can be tolerated, it can be seen from the curve that this is equivalent to the condition

$$\omega CR \geq 3$$

For R = 100 Mα, and C = 135 pF, this corresponds to a signal frequency of 28 c/s. For a four-vaned mill, the signal frequency is four times the mill frequency, and so this means the mill motor must have a speed greater than 420 r.p.m. This agrees quite well with Groom's more stringent condition, which gave f > 40 c.p.s.

It will be noticed that at WCR = 3, $|V|$ is only 95% of $|V_\infty|$. Provided the mill is calibrated at its working frequency, however, this does not matter.

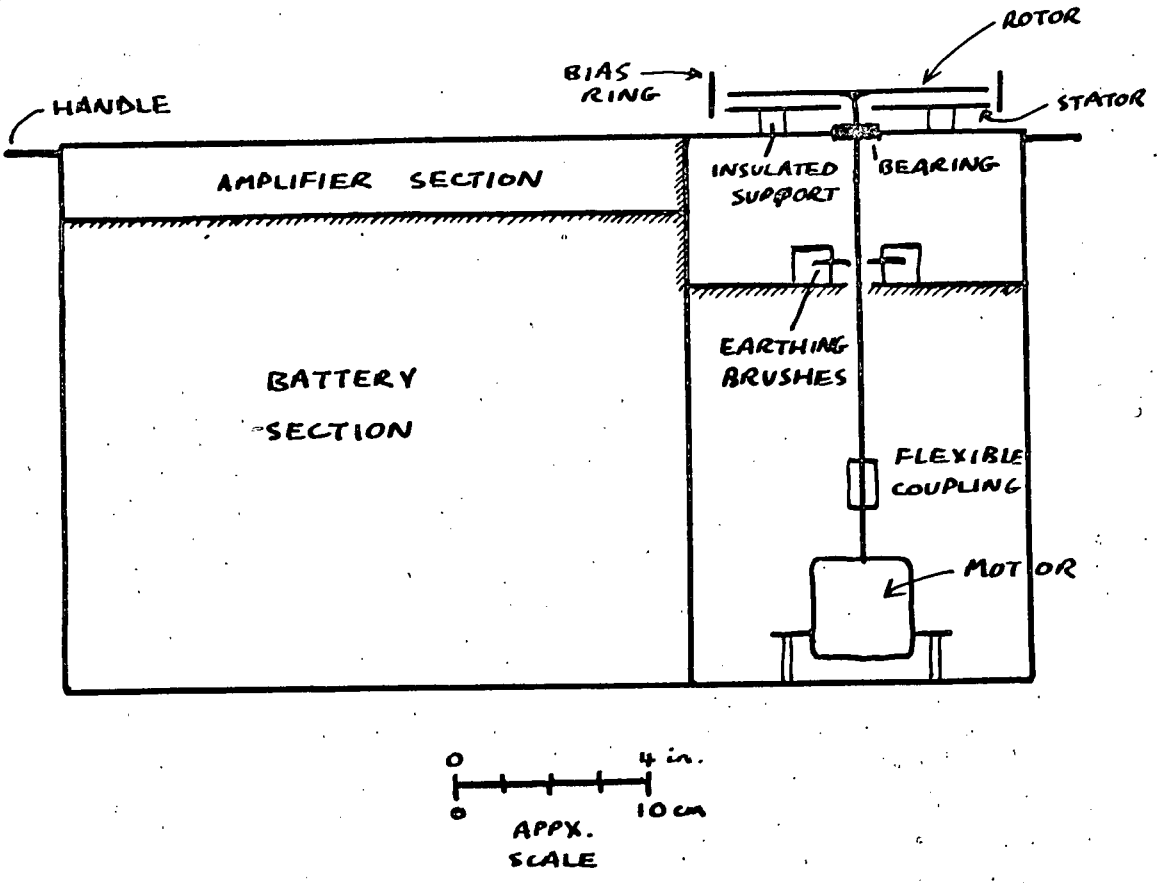

FIG. 5·4 SIMPLIFIED LONGITUDINAL CROSS-SECTION OF FIELD MILL.

PERMALLOY SHIELDING

THE MILL IS SEVEN INCHES DEEP

For practical calculation of the necessary input resistance of the amplifier, the condition $WCR \geq 3$ can be written, for a four-vane mill, as

$$R \geq 7{\cdot}16/nC$$

where n is the speed of the motor in r.p.m., and C the capacitance between the stator and earth, usually taken as the input capacitance of the amplifier plus 35 pF. In this formula, R is in ohms and C in farads. It will be seen that in most cases a very high input impedance is unnecessary for frequency independence: for a 3000 r.p.m. motor and an amplifier input capacitance of 200 pF, R needs only to be about 12 MΩ.

5.2.2 The Field Mill Design

For this experiment it was clearly necessary to have a portable, self-contained mill, and it was decided to use a D.C. motor driven by a storage battery, all enclosed with the amplifier in one case. D.C. motors are liable to sparking at the brushes, and the high input impedance amplifier makes it important to avoid any pickup on the stator, or the wires from there to the amplifier. For this reason, the mill was designed to get the maximum separation between the motor and the stator and amplifier, and had permalloy C sheets as shielding where necessary.

The mill (fig. 5.4) was built on a frame ½in. by ½in.

FIG. 5-5 A FIELD MILL

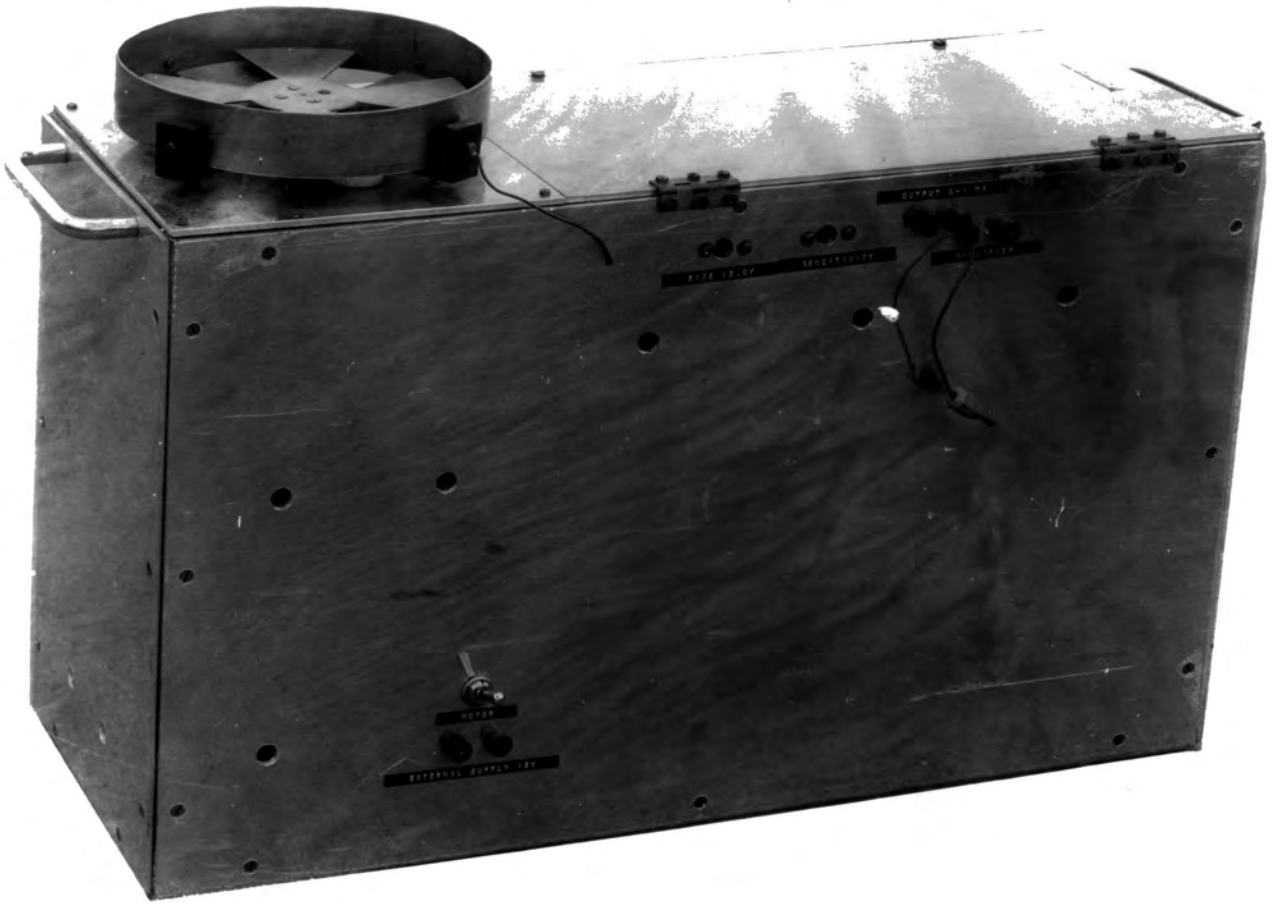

by ⅛in. brass angle, clad in ⅛in. duralumin sheets on the outside, with $\frac{1}{16}$in. duralumin forming the internal divisions, with permalloy sheets attached where appropriate. One large side was hinged, at the bottom, and so was the roof of the amplifier section, so that removal of four screws gave complete access. The flexible coupling on the mill shaft allowed for any asymmetry of mounting of the motor, and electrically insulated the shaft from it, preventing any sparking pickup reaching the vanes that way. The leads from the battery were shielded, again to reduce risk of pickup.

Fig. 5.5 is a photograph, from the side without hinges, showing the controls. The switch in the bottom left-hand corner controlled the motor, and the two single sockets immediately beneath it were connected direct to the battery, so that this could be used as a power source, or recharged, without opening the mill. From left to right along the top are the bias and sensitivity controls (pre-set potentiometers reached from the outside by screwdriver), and the two sockets for the amplifier output. The other socket and plug acted as a switch for the amplifier power supply, and enabled this to be checked with a meter. Single sockets were used to carry the outputs from all the apparatus, except the anemometers, and this

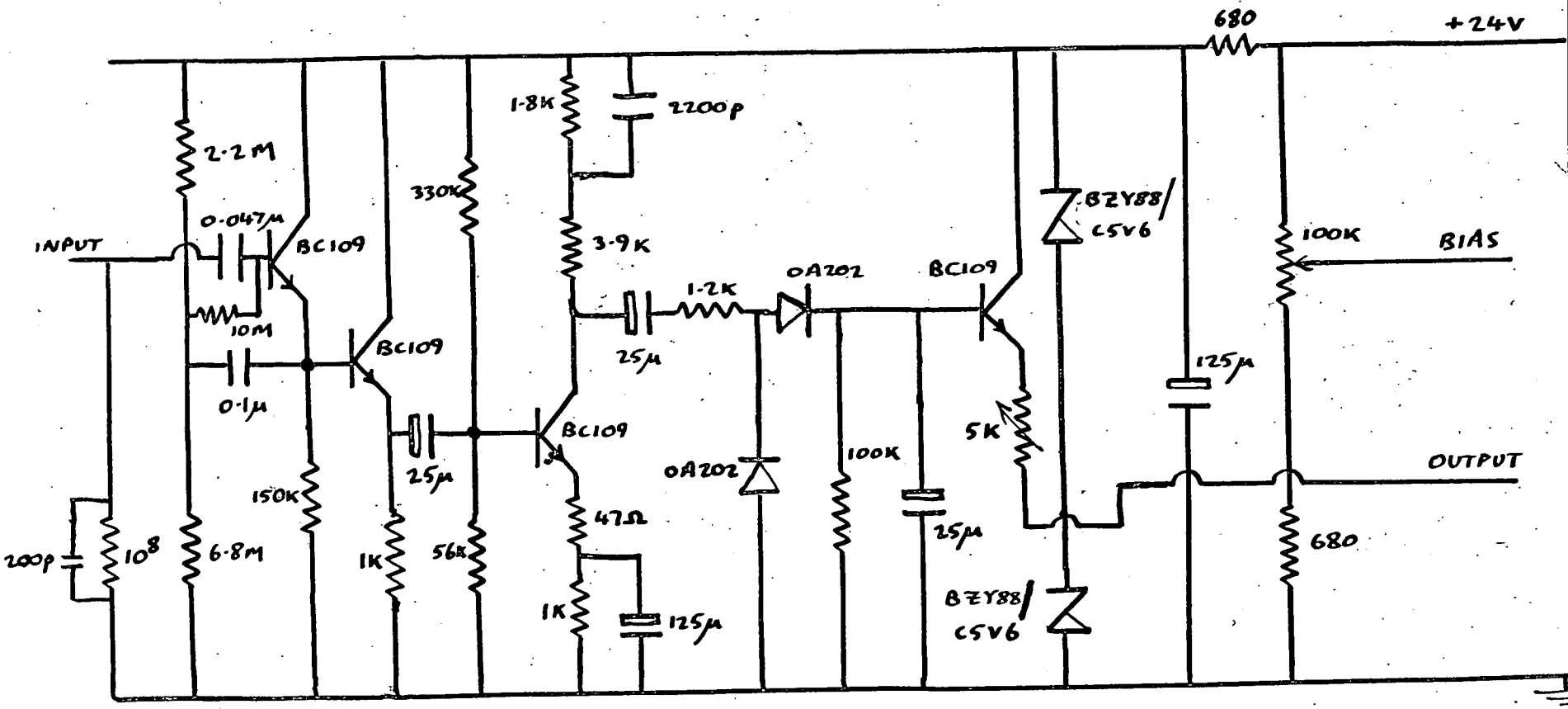

FIG. 5·6 THE FIELD-MILL AMPLIFIER

RESISTANCES IN Ω (½W, 10%); CAPACITANCES IN F

allowed the use of similar drums of twin flex, with wander plugs on each end, to connect the apparatus to the recorder, or rack electronics. The holes in the sides of the case of the mill were for ventilating the motor and battery.

Sign discrimination was made by having an offset zero, produced by a potential applied to the ring round the rotor and stator. This and the amplifier were supplied by three Ever-Ready PP9 batteries in series, making a nominal 27V, stored in the battery compartment.

The amplifier (fig. 5.6) was a very slight modification of a design by Mr. I.M. Stromberg, using four silicon planar-epitaxial transistors. As already mentioned, the very high input impedance requiring the use of an electrometer valve is unnecessary, and the use of a bootstrap input circuit gave the first stage here an input impedance of 32 MΩ, which, in parallel with the 100 MΩ resistor, gave a net input impedance R of 25 MΩ. For a stator-earth capacitance C=235 pF, and a 3000 r.p.m. motor, WCR = 7.4. Two 5.6 V zener diodes in series stabilized the amplifier supply, these being chosen in preference to one 12 V diode, because of the much better temperature stability of the 5.6 V. It was found that about 20 mA was drawn from the 27 V supply. According to

Mr. Stromberg, a change of 1% in output was brought about by a 10% change in the unstabilized supply voltage, or a 50% change in the signal frequency, and a temperature rise of 20°C changed the output by 2%.

5.2.3 Calibration and Use

The method of calibration used was to stand the mill on a large horizontal metal plate on the ground, to suspend another horizontally above it, and apply voltages to the upper plate. The calculation of the potential gradient simply as the voltage difference between the upper plate and the lower divided by their separation h assumed that the plates were very wide compared with the distance between them, and that the separation was very much greater than the height of the mill. This second condition arises because, in the atmospheric field, the presence of the mill distorts the field, so that the equipotentials above it are not horizontal. In the calibration, however, we impose a horizontal equipotential in the form of the upper plate, with the result that the shape of the field between the plates is slightly different from the field surrounding the mill in the open, unless the upper plate is effectively at infinity. It was decided that a reasonable way of assessing the error involved from this cause was to calculate the difference

at the height h in the Earth's field between the potential directly above the mill, and the potential in its absence. The separation required was the value of h for which the difference became negligible. To simplify matters, the mill was assumed equivalent to a hemispherical boss of the same height on an infinite plane, to which a standard result could be applied. In this case, at a distance r from the centre of the boss radius a, and at an angle θ to the perpendicular to the plane through the boss centre, the potential V in a potential gradient whose magnitude at infinity is Eo, is given by

$$V = \left(1 - \frac{a^3}{r^3}\right) E_o r \cos\theta$$

(Page and Adams, 1958, p.78)

For r = 3.5a, the potential immediately above the boss is numerically 3.43 Eo, the error then being 2%. It was felt that this was satisfactory.

Another possible source of error was the field due to the electrical image of the bias ring in the upper plate. This, however, would probably be very small.

This method of calibration involved a number of assumptions, of course, but the important thing was that the mills should be able to measure fairly short-period changes of about 100 V m^{-1}, and that they should all read the same. It was relatively unimportant if the measurement they gave was absolutely in error by 5% or so, as long as

they all gave the same reading. For this reason, the procedure outlined was regarded as satisfactory, and an absolute accuracy of 5% was aimed for overall.

The plates used were about 2.3 m by 2.8 m. Since the total height of the mill was about 33 cm, the plate separation was made 120 cm, with a maximum variation from place to place of 3 cm. The mill was placed in the centre of the bottom plate, and it was found that moving it 20 cm in any direction changed the output by less than 1%, indicating that the plates were sufficiently large in comparison with their separation.

Various voltages were applied to the top plate, and the mills calibrated one at a time. The current output was measured with an Avometer, with a series resistor to make its resistance equal to that of the recorder galvanometer coil (1.3 Ka). By adjustment of the bias and sensitivity controls, it was possible to give the three mills virtually identical and linear calibrations within the range required, viz. - 175 to + 350 V m^{-1}, giving a 0 - 1 mA output. For convenience, this linear calibration was assumed for all the mills during the experiment, the maximum divergence of any of the mills from it being about 5 V m^{-1}.

From the decay of the output when the upper plate was earthed, the time constant of each mill was estimated as

five seconds.

The relatively small range and offset-zero sign discrimination were satisfactory for the fair-weather use that was envisaged. However, in May 1967 an unusually long spell of thundery weather occurred, during which the point-discharge experiment described in chapter 8 was carried out. This made it desirable to extend the range of the mill. The usual way of doing this would have been to reduce the gain of the amplifier, but this would have meant recalibration of the mills, and, for the limited use thought probable, it was felt it was better not to change the amplifier proper, but merely to put a resistor in series with the output so that the full-scale deflection of 1 mA would be achieved for the maximum signal the amplifier was capable of handling as it stood. This limit was set by the input for which the amplifier "bottomed", beyond which an increased input produced no increase in output.

A full re-calibration was not necessary; the following procedure was adopted. A sine-wave signal was applied to the stator end of the stator-amplifier lead, using a signal generator with a meter reading in mV peak-to-peak. First, this was done using the mill without any extra resistor in the output, i.e. in the state in which it was calibrated in the field, and, by comparing the out-

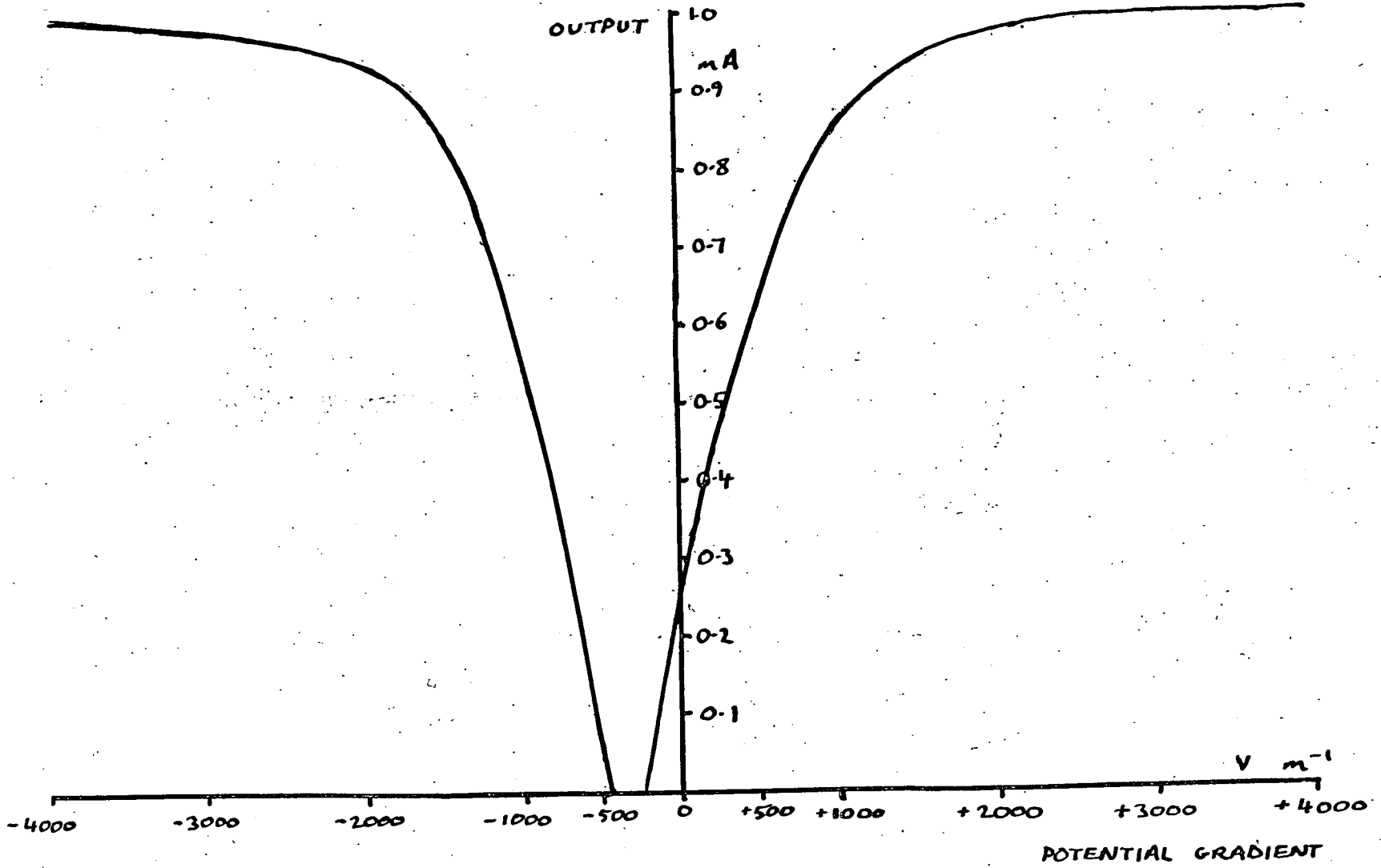

FIG. 5·7 TYPICAL FIELD-MILL HIGH-RANGE CALIBRATION

puts in the two cases, the mV input which corresponded to 1 V m^{-1} was determined. This depended on the geometry of the mills, and was typically about 0.2 mV. It was then possible to put a suitable resistor in the output, calibrate the mill in terms of mV from the signal generator, and convert this to a V m^{-1} calibration. A typical result is shown in fig. 5.7. The offset-zero sign discrimation gave an ambiguity in sign for fields greater than about 200 V m^{-1}, but in the only record put to any practical use, it was possible to follow through the record from the fair-weather potential gradient, taken as positive, and the places where a change of sign occurred were obvious enough from the trend of the record to overcome this difficulty. A small region occurred about zero input, in which there was no output. This was because a small signal was necessary to switch on the rectifying diodes in the amplifier. It can be seen that the output is useful for potential gradients between plus and minus 3000 V m^{-1}.

This high-range calibration was not, in fact, carried out until after the useful series of measurements described in chapter 8. The rapidly-changing weather made it necessary to guess the values of the resistors to put in the outputs of the mills, carry out the experiment,

and calibrate, in the way described above, afterwards. The resistance values selected were too high, and the amplifiers bottomed for outputs of 0.7 mA. More carefully calculated resistances were then selected, and the above calibrations carried out to be ready for subsequent use. The resistance values then averaged about 4 KΩ.

The mills worked well, although the storage batteries made them rather heavy. Originally, it had been intended to take the bias potential from the stabilised supply, using a potential divider. Unfortunately, it turned out that the potential required was about 15 V, and so had to be obtained by dropping from the unstabilised battery supply. This voltage dropped slowly during operation (about 1 V for six hours recording), and the bias voltage, measured by connecting a voltmeter between the ring and the mill case, had therefore to be adjusted from time to time, although the effect of such changes on the output was barely detectable. This fault could have been overcome by using a separate zener-stabilized voltage (say 20 V), and taking the bias voltage from this through a potential divider.

5.3 The Aspirated Thermistors

FIG. 5·8 A THERMISTOR AT 1 m.

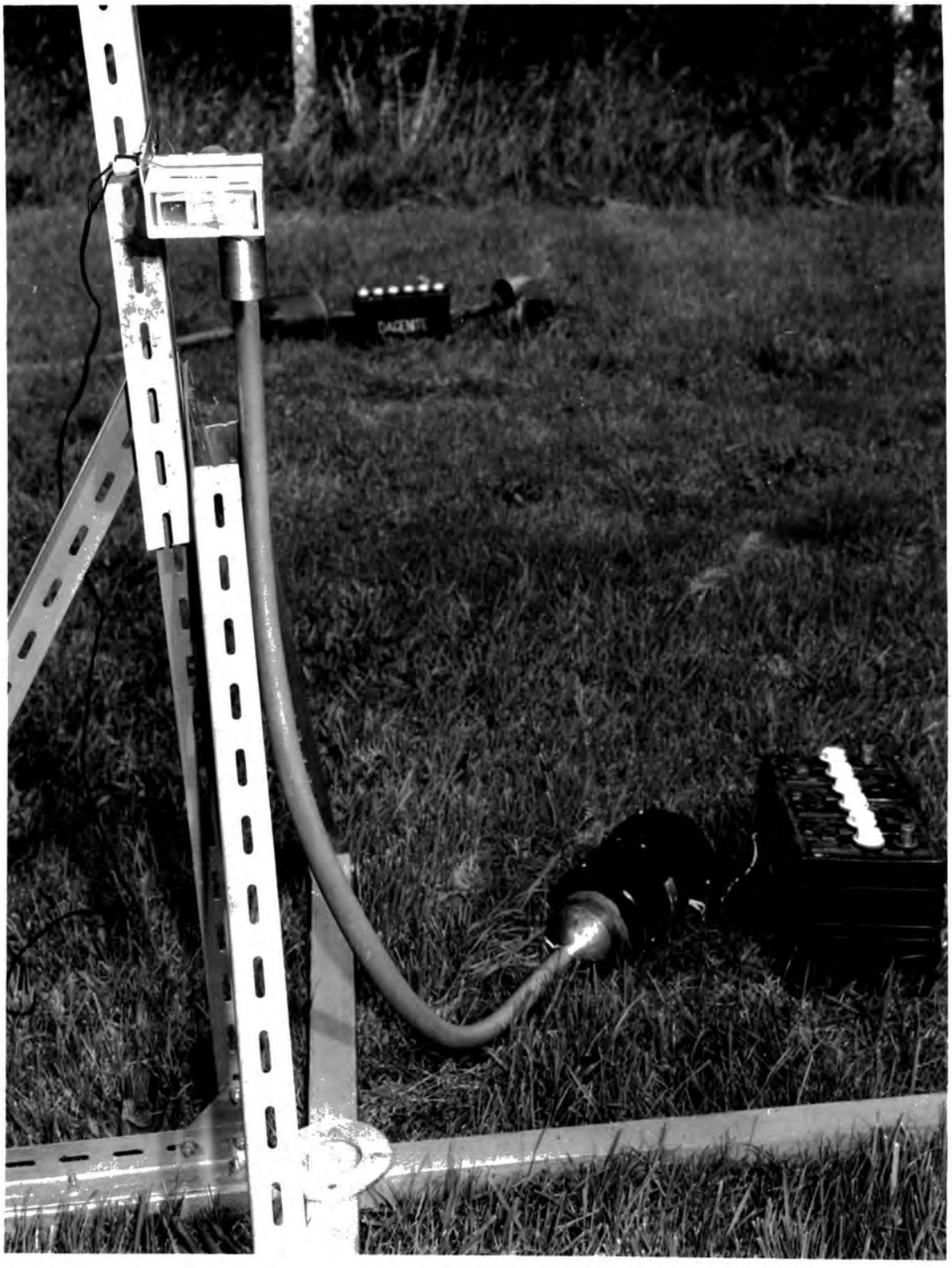

5.3.1 Basic Design

The thermistors for measuring temperature gradients and small short-period changes of temperature were mounted in cases identical to those of the psychrometers of Bent (1965) (fig. 5.8). Each of these was a double-walled plastic case, 5 in. by 3 in. by 1½ in., open at one end, and with a tube at the other to connect to a fan, for aspiration. The double-walled structure meant that the thermistors were protected from the effects of direct sunlight. Each psychrometer was designed to hold two thermistors, one "dry-bulb" and the other "wet-bulb", although they were never used to measure humidity in this experiment. Sufficient psychrometers were constructed to enable temperature measurements to be made at ½, 1, 2, and 10 m at one place, and at 1 m at two other places, in case the small changes were sufficiently distinctive to enable the same plume to be picked out at different places in this way. 12 V car heater fan units were used for aspiration.

The thermistors used were manufactured by "YSI - Components", and were supplied with a resistance-temperature calibration curve to which all thermistors of the same type complied within 0.2°C. The type selected had a resistance of 3 KΩ at 25°C, increasing to about 10 KΩ at

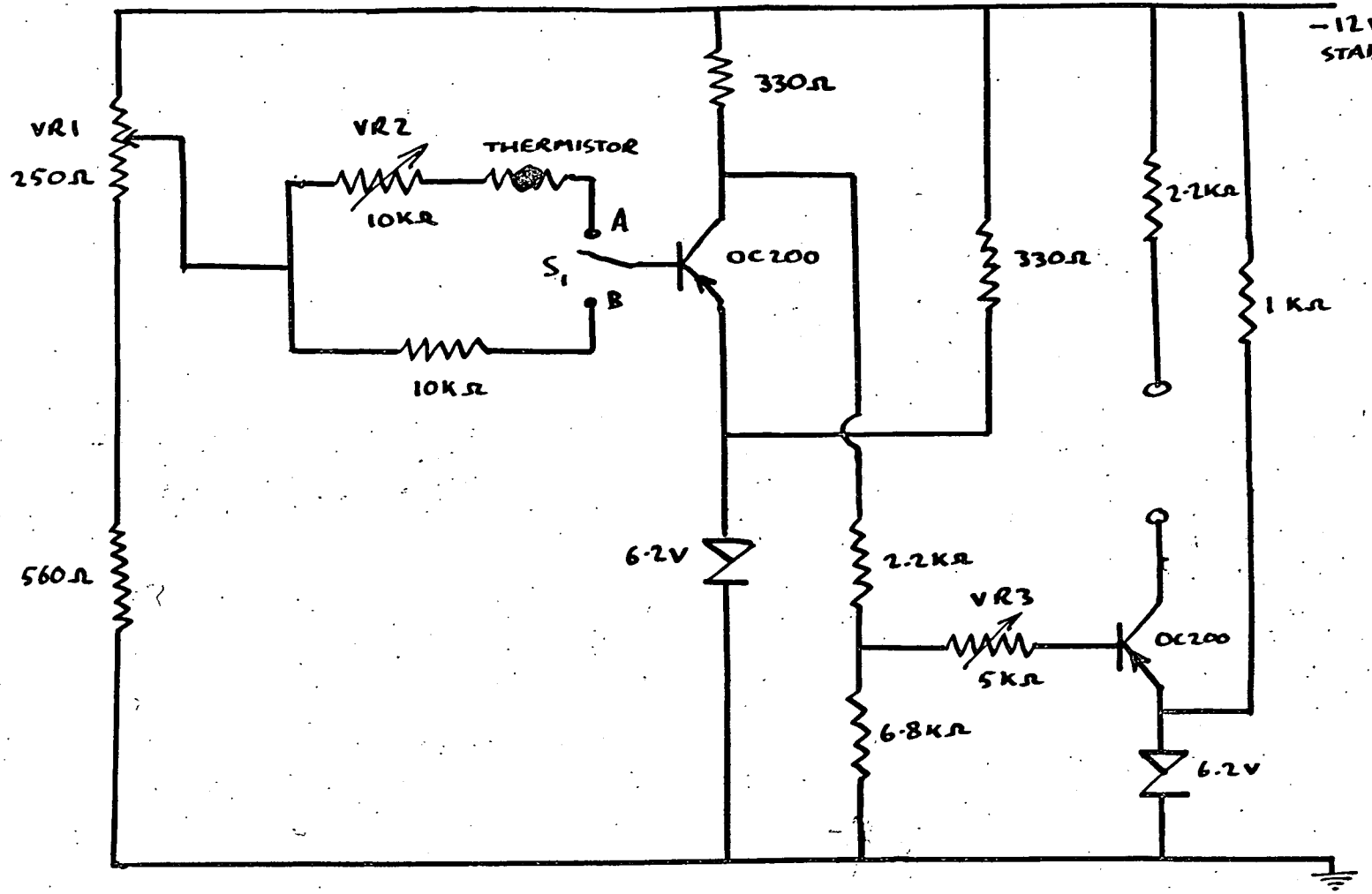

FIG. 5·9 THERMISTOR CIRCUIT FOR SMALL TEMPERATURE CHANGES

0°C, and decreasing to about 2 KΩ at 35°C.

5.3.2 Measurement of Small-Scale Changes of Temperature

The measurement of temperature gradients, and of small-scale variations at one height due to passing plumes, presented two different problems. The first involved accurate temperature measurement over a range of 30 degC, but the second required measurement of small changes, without knowledge of the actual temperature being necessary. For the second task, a detection circuit was required which would give a 0 - 1 mA current output for a range of temperature of 10 degC anywhere between, say, 5°C and 25°C. In both cases, it was important to keep the current through the thermistor as low as possible to avoid warming it. The manufacturer's specification stated that a dissipation of 1 mW in still air would cause a temperature rise of 0.1 degC, this dissipation corresponding at 25°C to a current of 170 μA.

The circuit used was designed by Mr. I.M. Stromberg, and is shown in fig. 5.9. By connecting the thermistor in the base of a transistor, the current through it was kept below 200 μA. A variable resistor in series with the thermistor allowed the value of the base current to be adjusted to a fixed value, giving a fixed output,

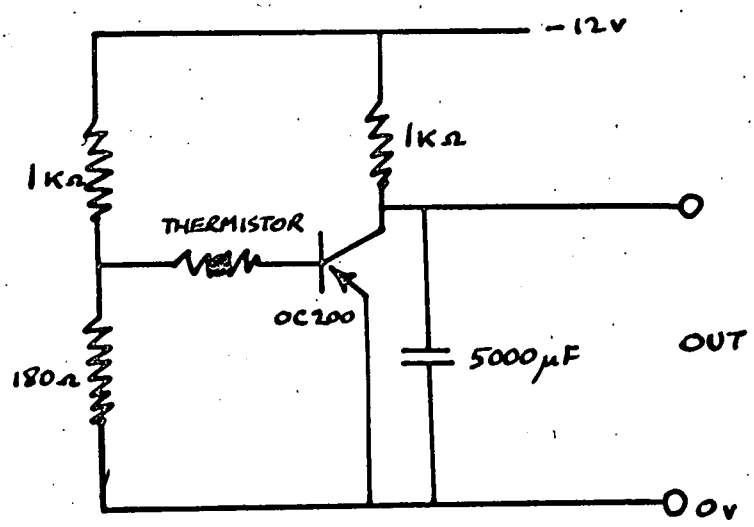

FIG. 5·10 TEMPERATURE MEASUREMENT CIRCUIT

whatever the temperature. Variations in thermistor resistance then caused variations in base current which underwent amplification. In practice, S1 was put in position B and VR1 adjusted to give an output at the centre of the meter scale, i.e. at 0.5 mA. The setting position of VR1 changed from day to day because of the influence of temperature on the transistor characteristics. With the switch at A, VR2 was then adjusted to make the output 0.5 mA, making the total resistance of VR2 and the thermistor 10KΩ. VR3 controlled the sensitivity, and its optimum position did not in practice vary. The sensitivity of the equipment near the centre of the scale was about 0.1 mA per degree centigrade, and its time constant was a few seconds.

This arrangement worked well. Examples of its records accompany the next chapter. Three such circuits were built, to be ready to correlate temperature variations at different places.

5.3.3 Measurement of Temperature Gradients

Once again, the author is indebted to Mr. I.M. Stromberg for a circuit design (fig. 5.10). Like the last, this limited the current in the thermistor by connecting it in the base of the transistor. The output was taken between collector and emitter. The circuit had

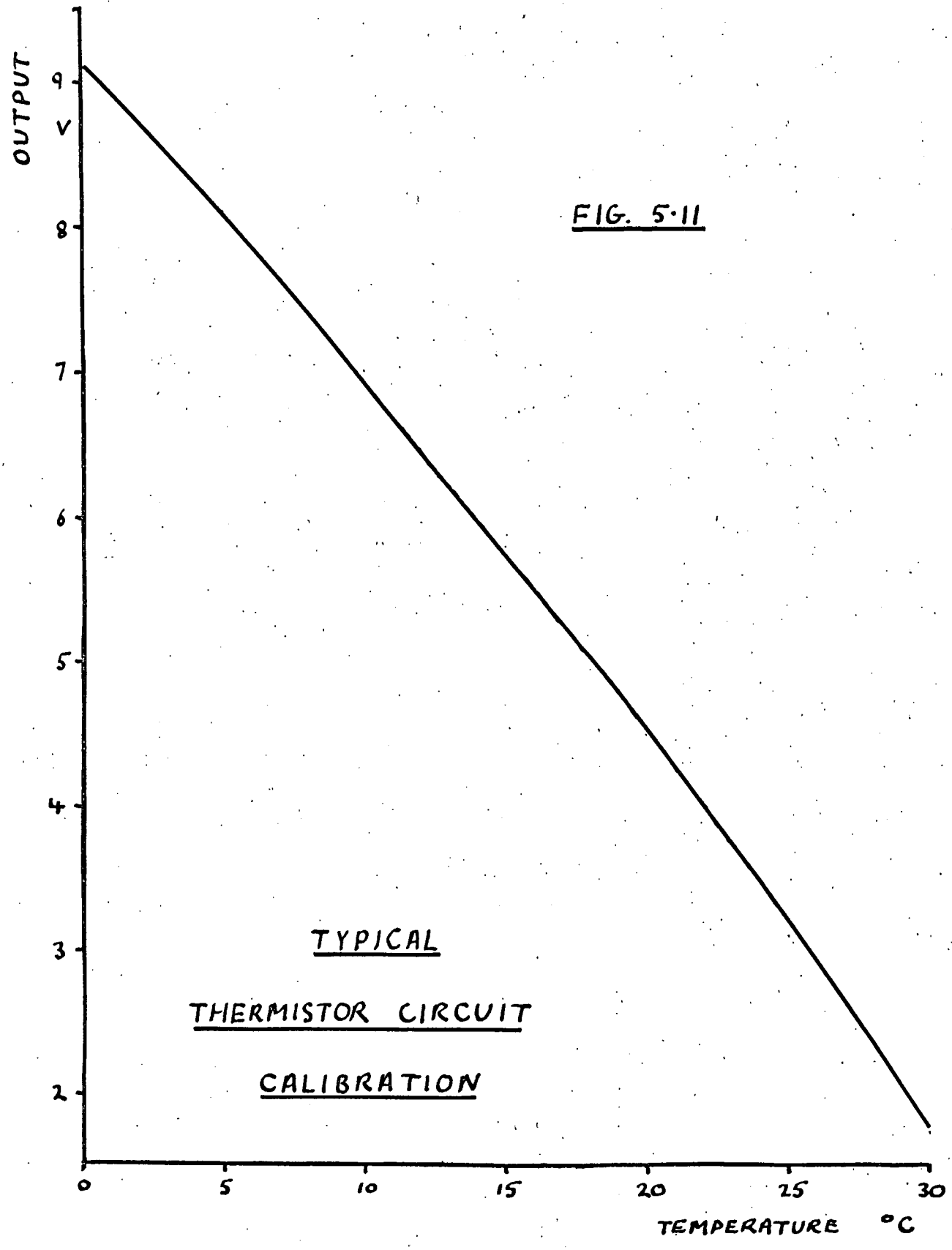
OUTPUT
9
V
8
7
6
5
4
3
2
0
5
10
15
20
25
30
TEMPERATURE °C
FIG. 5·11
TYPICAL
THERMISTOR CIRCUIT
CALIBRATION

the fortunate property of turning the non-linear temperature/resistance calibration into an almost linear temperature/voltage output. A large capacitor was necessary to lengthen the time constant, to about nine seconds (with some slight temperature variation). This circuit was designed when it was still hoped to use automatic recording, and so gave a 1-10V output (fig. 5.11), but when this scheme was abandoned, the output was put onto a 0 - 25 μA panel meter, with 100 KΩ in series to make the full-scale deflection equal to 2.5 V. A bias switch connected one end of the meter to various points on a resistance chain from the -12 V stabilised supply to earth, so that the meter read 0 - 2.5 V, 2.5 - 5.0 V, 5.0 - 7.5 V, or 7.5 - 10.0 V. The thermistor circuits were connected to the meter via another switch, which enabled any of them to be selected. In practice, temperature gradients were read by measuring temperatures at all the heights in turn several times, and finding the average for each height.

The calibrations were obtained using a resistance box in place of the thermistor, and using the thermistor manufacturer's resistance-temperature calibration. Unfortunately, the author did not at that time sufficiently appreciate the influence of temperature on the output of a zener-controlled stabilizing circuit, and during the

measurements over melting snow it soon became apparent that the calibration obtained in this way gave results near freezing point inaccurate by a degree or more, probably because the resistance of the zener diode had changed with temperature, although the performance of the OC 200 in the thermistor circuit was presumably also influenced. The only valid method of calibration would have been to put the thermistor, its circuit and stabilizer in a controlled temperature enclosure. Instead, immediately after each gradient measurement, a resistance box was substituted for the thermistors, and the resistances required to give the meter readings just obtained was found. These could be equated to temperatures using the manufacturer's calibration. This method, although cumbersome, was accurate.

Each thermistor was used at a particular height during the experiment, so that individual variations could be allowed for. Comparison of the thermistors in the laboratory with an accurate mercury-in-glass thermometer at 20°C indicated that the thermistors (identified by the heights at which they were used) required the following corrections: ½ m, + 0.13 degC; 1 m, - 0.11 degC; 2 m, - 0.33 degC.

5.4 The Cup Anemometers

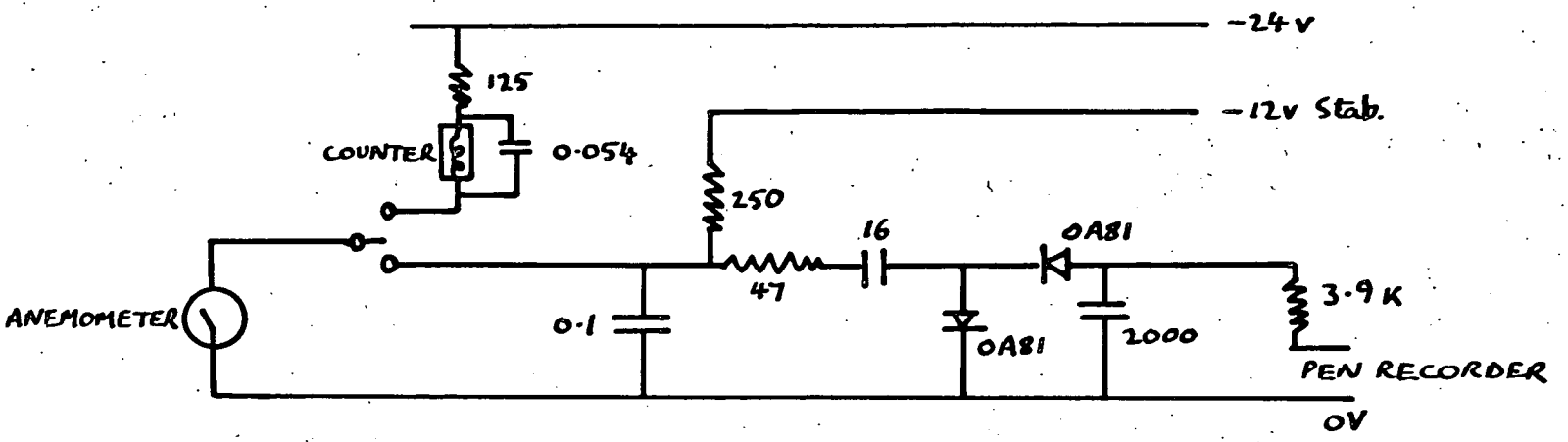

FIG. 5·12 ANEMOMETER COUNTER & RECORDER CIRCUITS

RESISTANCES IN Ω ; CAPACITANCES IN μF

To facilitate measurements of wind speeds and gradients, two sensitive, three-cup anemometers manufactured by C.F. Casella and Co. Ltd. (London) were borrowed from the Meteorological Office, whose help is gratefully acknowledged. Each anemometer operated a contact breaker, which closed twice every three revolutions of the cups. The Meteorological Office supplied calibrations giving the wind-speed in terms of contacts per minute. The wind-speed required to start the anemometers turning was about 0.25 m s^{-1}, and the maximum recommended speed of operation was about 12 m s^{-1}, which corresponded to 350 contacts per minute.

For the gradient measurements, two electromagnetic counters were used, one for each anemometer. In operation, the counters could be switched on for as long a period as the average gradient was required, and from the readings, the wind-speeds found by means of the calibrations. In view of the observation of Bent and Hutchinson (1966) that the space-charge peaks were accompanied by falls in wind-speed, it was thought desirable to be able also to record the speed continuously, and a diode pump circuit was built to convert the voltage pulses from one anemometer into a 0 - 1 mA signal for the recorder. There were two sets of input single sockets on the panel, one for each

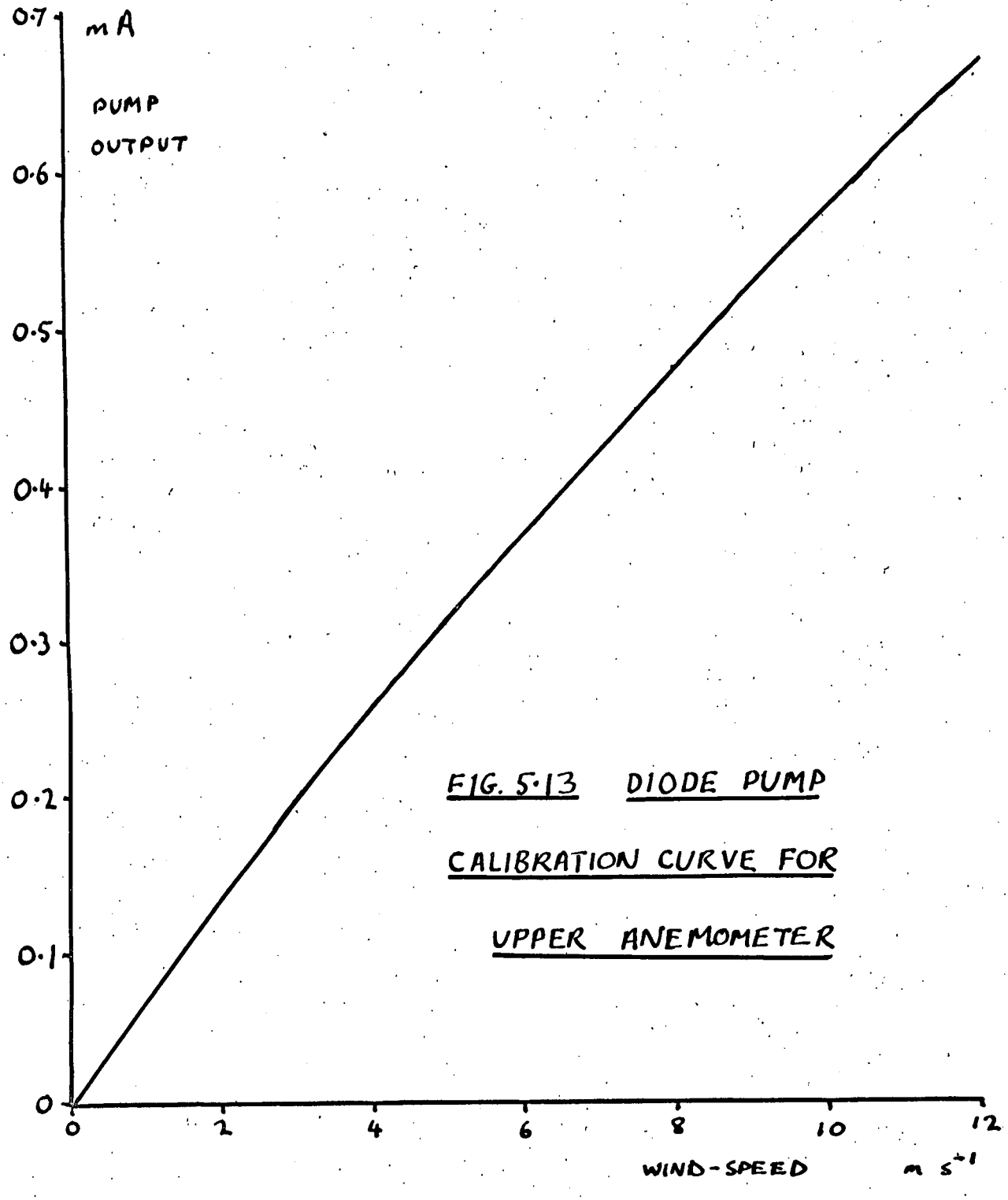

FIG. 5·13 DIODE PUMP CALIBRATION CURVE FOR UPPER ANEMOMETER

anemometer, and a switch enabled the input from one of these to be changed from the counter to the recorder at will. The circuits are shown in fig. 5.12. They are quite standard, and the only features worthy of note are the 0.1 and 0.054 μF capacitors, included to prevent sparking at the anemometer contact-breaker. The 2000 μF capacitor gives the output a time constant of about ten seconds.

The circuit for the recorder was calibrated in the laboratory by attaching the apparatus to an anemometer, as in the field, and using a fan to provide wind. The speed derived from the counter was compared with the recorder output, and the result for the upper anemometer, the one generally used with this system, is shown in fig. 5.13.

During the course of the work, one of the anemometers was broken, and was recalibrated after repair against the other using a wind tunnel in the University Engineering Science Department. The two anemometers were put in the tunnel, and their outputs compared using the counters. Their positions were interchanged and the process repeated. The mean of the two straight lines obtained gave the new calibration.

These arrangements worked satisfactorily, except that

FIG. 5-14 A TOTAL-VECTOR ANEMOMETER

it proved impossible to record wind-speed and temperature continuously and at the same time, because the current pulses caused in the making and breaking of the anemometer contact affected the output of the zener-stabilized 12 V supply causing pulses on the temperature output. The counter was run off the unstabilized 24V supply, and so this effect did not occur when the counter was used.

5.5 The Total-Vector Anemometers

As explained in section 3.2.3, three of these were designed and partly built, but were not completed. Basically, each consisted of a wind-vane with its axis of rotation horizontal, mounted on the front of a conventional vane (fig. 5.14). On the front of the smaller vane it was intended to mount a thermistor to measure the wind-speed, and with the two directional measurements this would have allowed the calculation of the horizontal and vertical components of speed, and the horizontal direction. With this, it was hoped to detect changes of vertical velocity and horizontal direction accompanying plumes.

The usual way of detecting direction in wind-vanes is to use a rotary potentiometer with its sliding contact attached to the spindle of the vane. Unless special expensive low-torque potentiometers are used, however, the friction at the sliding contact means the minimum

(a) VARIABLE COLLIMATOR

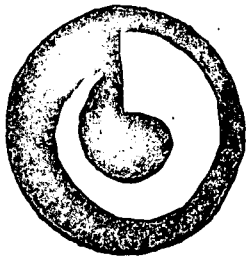

(b) DIAGRAMMATIC SECTION OF BOX

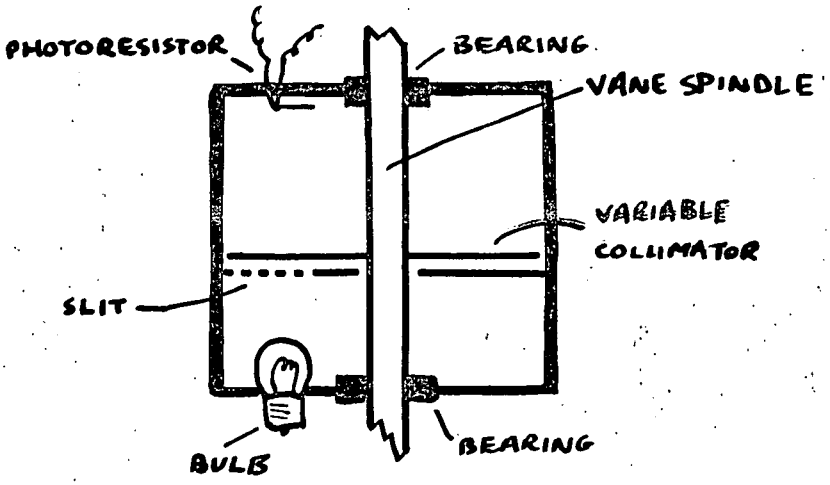

FIG. 5·15 DIRECTION SENSING UNIT

speed detectable is higher than could be tolerated in this case. Experiments were therefore carried out to see if a photoelectric system could be devised, which might keep the sensitivity limit of the instrument to a fraction of a metre per second. The system devised is shown in fig. 5.15. A small torch-bulb was used as a source, and a Mullard ORP 16 photoresistor as detector. Between these was a slit in a mask attached to the box, and a variable collimator, a thin disc of perspex blacked as shown in fig. 5.15(a), attached to the spindle of the wind-vane. As the collimator turned with the vane, the effective length of the slit varied, giving a varying output from the photoresistor. Each anemometer had two of these units, one for the horizontal and one for the vertical vane.

Mechanically, the system was satisfactory. A laboratory measurement of the torque required to move the large vane indicatedthat a wind of 0.3 m s^{-1} would turn it, and the small vane was even more sensitive. The vane was put outside in a moderate breeze for a few hours, and found to operate satisfactorily.

Electrically, the system was never fully tested. Preliminary measurements showed that a satisfactory output variation could be obtained, but there was a region of ambiguity about 40 wide where the collimator moved

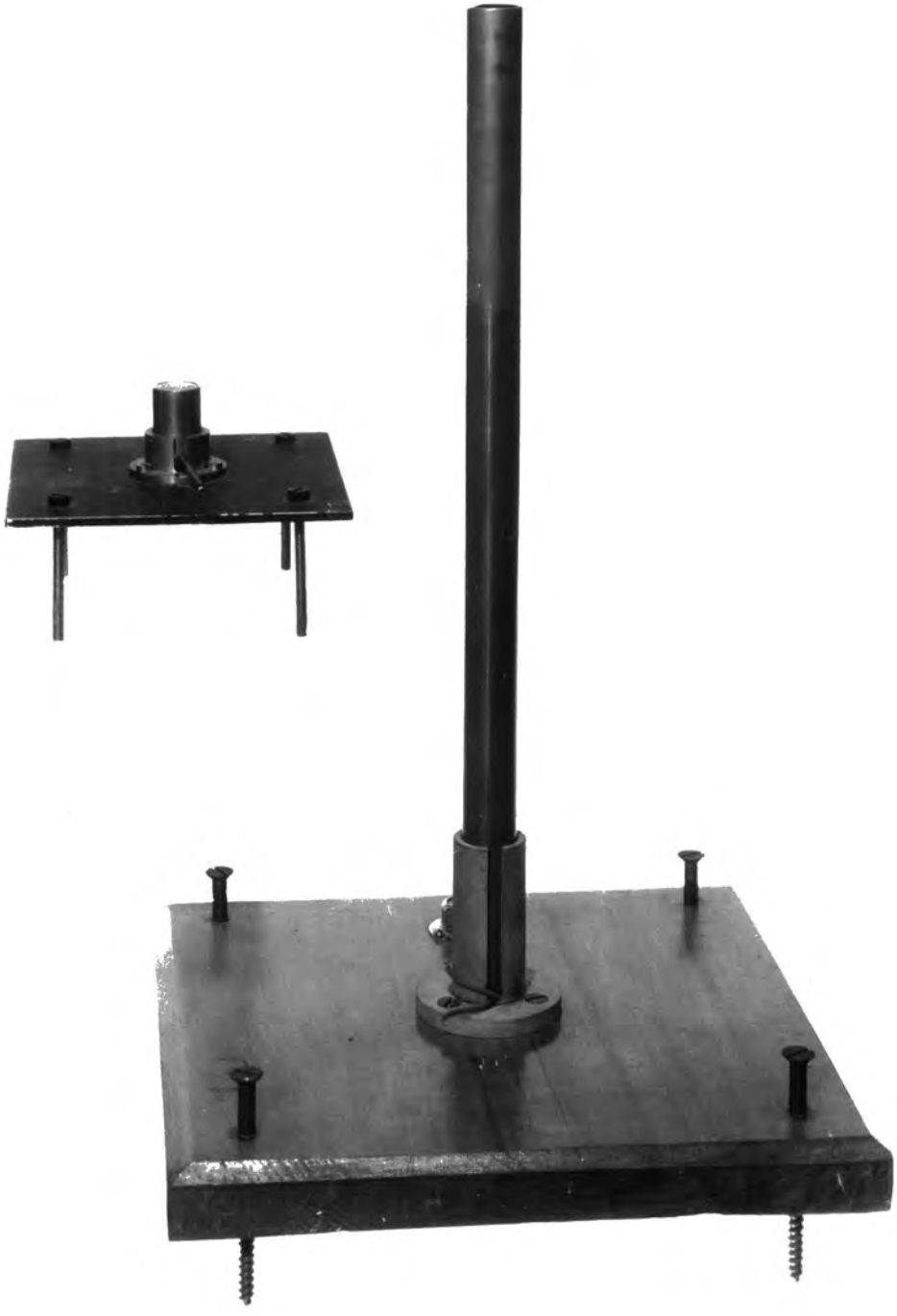

FIG. 5.16 THE PHOTOMETERS

suddenly from its narrowest to its widest, and there seemed to be some variation with time, perhaps due to blackening of the bulb. It seems likely that the system would not have worked well in the field, and the expense of low-torque, 360° potentiometers is justified.

Three thirty-foot, hydraulic telescopic masts (by A.N. Clark, Binstead, Isle of Wight) were obtained to carry these anemometers, and were later used for the cup anemometers.

5.6 The Propeller Anemometer

As described in chapter six, rough measurements of vertical velocity were made using a sensitive propeller anemometer (manufactured by Davis and Son, London), which was mounted horizontally and levelled. The scale registered the run of wind in feet, with a minimum division of one foot (0.30 m). The starting speed was not measured, but was estimated to be about 0.2 m s^{-1}.

5.7 The Overhead-Sky Photometer

It is well known that potential gradient changes at the ground are often associated with clouds overhead, and Durst (1932) suggested that the positions of clouds might be related to convection currents at the ground. The sky photometers were built to monitor the cloud cover to aid interpretation of the potential gradient record, to test

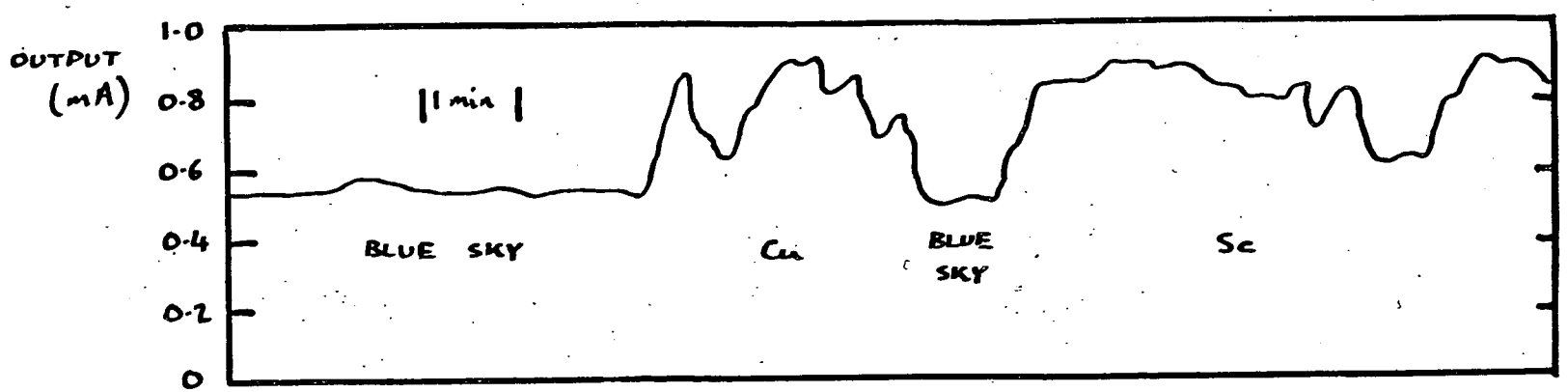

FIG. 5·17 TYPICAL OVERHEAD-SKY PHOTOMETER RECORD

Durst's theory if possible, and to determine cloud height and speed.

5.7.1 Design

The design was based on that of Whitlock (1955) and consisted essentially of an ORP 16 photoresistor at the bottom of a brass tube about 33 cm long, blackened on the inside (fig. 5.16). The tube was mounted vertically on a wooden base, which also carried a circular spirit level to ensure the tube pointed vertically. Small white clouds gave a brightness reading greater than blue sky, and the dark centres of larger clouds gave brightness readings below the blue sky level. Tests were made with colour filters to see if blue sky could be made the brightest condition or the darkest, but without success. In practice, however, it was easy to pick out the blue sky on the records. A typical record is shown in fig. 5.17, registering blue sky at first, and then a small cumulus cloud, followed almost immediately by a more extensive sheet of stratocumulus. The resistance of the ORP 16 varied from about 6 KΩ to about 50 KΩ, so it was quite satisfactory just to put a 6 V dry battery in series with the photoresistor and the pen recorder.

5.7.2 Measurement of Cloud Speed and Height

In the early stages of the experiment, when the

measurements of Whitlock and Chalmers (1956) were still the chief guide in planning, consideration was given to methods of determining the change of wind speed with height. It was felt that knowledge of cloud height and speed would give one height at which the wind-speed was known, and possible simple methods of determining these quantities were considered. The results are given here, although any such method is more likely to be of value in work on rain under layer clouds than in this type of work.

In principle, the system devised was to determine cloud direction and angular velocity using a form of nephoscope (see "Meteorological Office Observer's Handbook" (H.M.S.O.), 2nd Edn. 1956, pp30-34), and to measure the cloud's ground-speed using overhead-sky photometers. This second measurement could easily be made using two photometers in the line of cloud movement, separated by two or three hundred metres, and correlating their outputs, (or else by using three photometers forming a right-angled triangle, and calculating the components of cloud velocity). A pilot experiment with two photometers showed this to work well. As a nephoscope, two 2 m ranging poles and one of the thirty-foot masts could be used as follows: (1) one of the ranging poles could be stuck in the ground a few metres from the foot of the mast, and a feature on

the cloud sighted past the tops of the pole and mast;
(2) after a short delay the other pole could be stuck in so that the tops of the mast and second pole lined up with the same feature. The direction of the line joining the two poles would give cloud direction.
(3) The time taken for further cloud features to pass the two sighting ~~points~~ lines would give angular velocity, knowing the dimensions of the arrangement. From angular velocity and ground velocity, the height of the clouds could be calculated. In practice,it would probably be easier in the long run to construct a portable form of comb nephoscope.

If automatic recording were more convenient, it would be easy to mount two sky photometers together so that their tubes were in the same plane, and pointed at, say, 15° to the vertical on opposite sides of the vertical, giving an angular separation of 30°. If the instrument were then lined up with cloud direction, the delay between the records would give angular velocity. Cloud at 500 m moving at 15 m s^{-1} would give a delay between the records of about 15 s.

5.8 The Ambient-Brightness Photometer

This instrument is also illustrated in fig. 5.16, where it is only slightly further from the camera than the sky photometer, but supported at a higher level - its

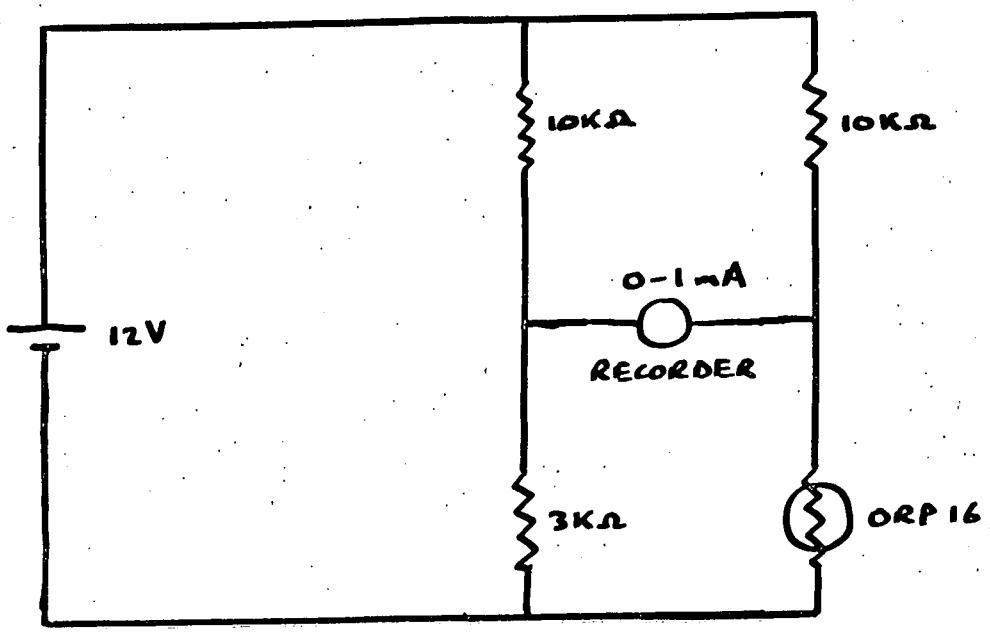

FIG. 5·18 AMBIENT BRIGHTNESS PHOTOMETER CIRCUIT

apparently much greater distance is an unfortunate optical illusion.

The sensing element here was also an ORP 16, this time at the bottom of a brass tube just long enough to prevent direct sunlight falling on the resistor. At the top of the tube was a disc of perspex "frosted" by rubbing on sandpaper, and designed to diffuse the light falling onto it. The whole was mounted on a blackened brass base.

The chief object of the photometer was to detect sunlight falling on the site, at which it was highly successful, to see if the space-charge peaks were connected with direct sunlight initiating a very local convective plume. A typical record was given on fig. 4.6. The resistance of the ORP 16 varied from about 250Ω in bright sunlight to about 3KΩ in deep shade. Fig. 5.18 shows the circuit used with the recorder.

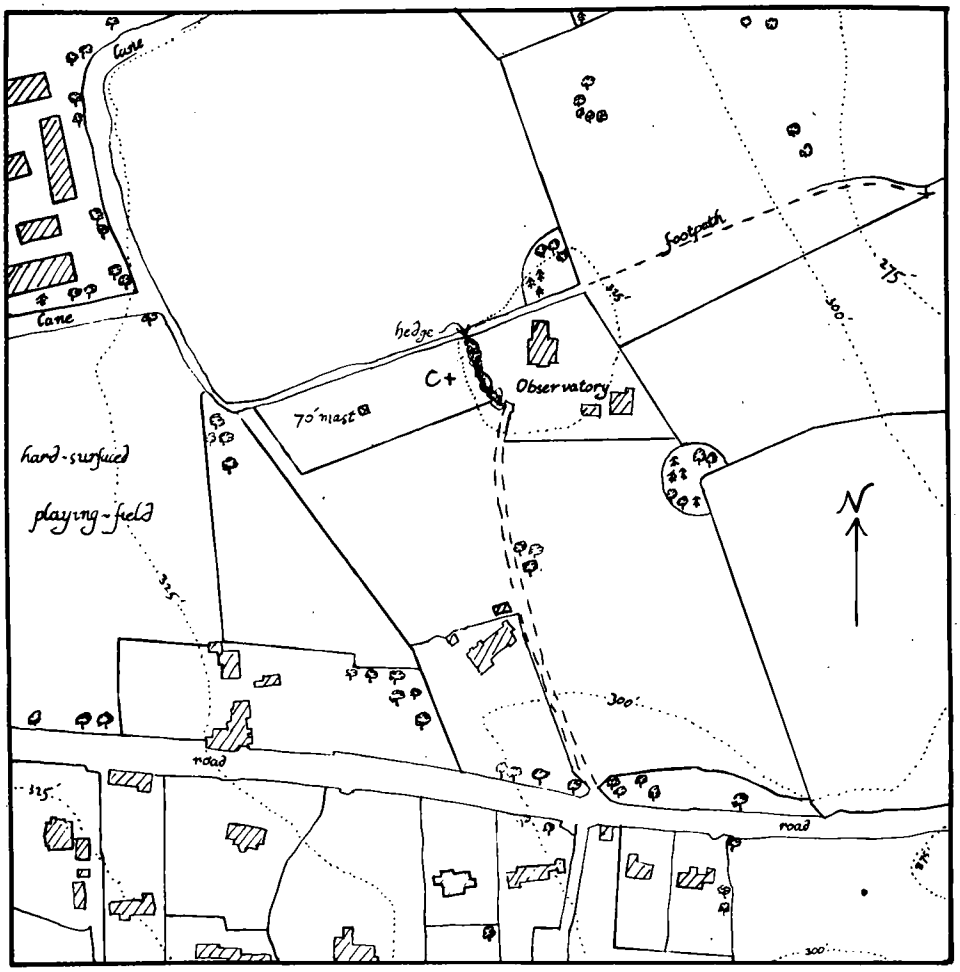

Scale

The cross at C shows the position of the space-charge collector

The Observatory Site

FIG. 6·1

CHAPTER 6

MEASUREMENTS IN CONVECTIVE WEATHER

6.1 Introduction

Measurements were made at Durham University Observatory through the summer of 1966, and at Mordon in the early summer of 1967. As already mentioned, although the rainfall at Durham is only 25.6 inches per annum, the proximity of the North Sea depresses sunshine totals, and both 1966 and early 1967 were unfortunately particularly badly affected from this point of view. Although such figures are only a rough guide, the seven months from March to September 1966 had 87% of the average sunshine, and the mean wind-speed, on which, of course, depends the depth of the forced convection layer, was 4.2 m s^{-1}, 124% of the average. The sunniest month of the year was May, with 180 hours sunshine (113% of average), during much of which the V.R.E. was out of commission. However, it was in the early summer months of 1966 that the majority of the Durham results were obtained.

The first few months of 1967 were also poor. Although March had 154 hours of sunshine (145% of average), the mean wind-speed in that month was 9.6 m s^{-1}, over twice the average. The majority of the results at Mordon were

FIG. 6·2 THE OBSERVATORY SITE, LOOKING SOUTH-WEST

obtained in a very fine spell in the otherwise poor month of June, when the daily sunshine total exceeded 10 hours for seven days.

6.2 Measurements at the Observatory

6.2.1 The Site and Apparatus

As the results of both Bent and Hutchinson (1966) and Whitlock and Chalmers (1956) had been obtained at this site, measurements were made there first, to make sure the apparatus would detect the phenomena they had described. This site, and also the one at Mordon, have already been described generally in Chapter 3, and fig. 6.1 shows the immediate environment of the Observatory in more detail. The Land-Rover was positioned in the Observatory garden, against the hedge labelled on the map, and the leads to the apparatus were carried through the hedge. Figs. 6.1 and 6.2 show the relative positions of the collector and the mast used by Bent and Hutchinson. The grass in the area immediately surrounding the collector was kept below 5 cm long.

Fig. 6.2 shows the south-westerly aspect of the site. It can be seen that there are rather more trees than are shown on the map, especially in the line bounding on the east the hard-surface playing-field. These trees form the horizon in the photograph. Fig. 6.3 again shows the

FIG. 6·3 THE OBSERVATORY SITE, LOOKING NORTH - EAST

apparatus, but this time the camera faces north-east, and the 5 m hedge bounding the field on the east can be seen. Throughout the experiment, the apparatus was about 9 m west of this, and in any wind between N and SSE the air reaching the collector would have blown over it.

In this situation, there was clearly no point in measuring wind and temperature gradients near the collector and applying them in the equations of chapter 2, which require horizontal uniformity. Some measure of the turbulence could be obtained, however, from the wind-speed measured by the Observatory Meteorological Station anemometer, a Dynes pressure tube device mounted above the roof of the building at a height above the ground of 18.5 m, with an exposure reckoned by the Meteorological Office to make its effective height 10 m. It was also desirable to have some measure of the temperature gradient in the first metre, and this was obtained by comparing the reading from a continuous-recording thermometer mounted at 1.2 m in the Observatory Stevenson screen with the temperature at the ground. This was measured with a mercury-in-glass thermometer supported about 1 cm from the ground on a lawn in the Observatory garden. The grass here was kept very short, and readings taken by placing the thermometer on its

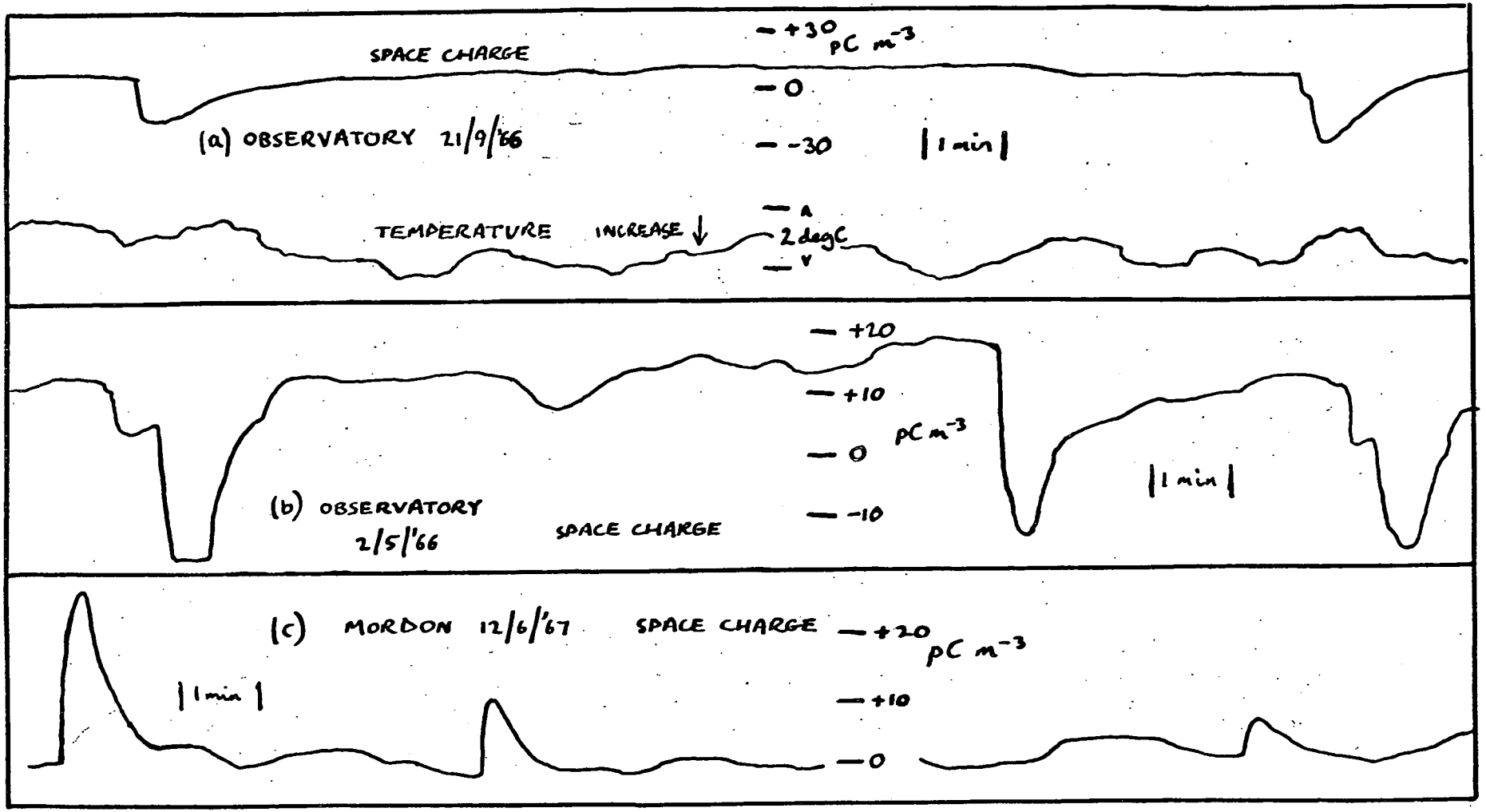

FIG. 6·4 TYPICAL SPACE-CHARGE PULSES

support on a sunlit patch of grass, shading it for a minute, and then reading the temperature. Such measurements, of course, had little absolute meaning, but provided a rough and ready indicator of the magnitude of the mean temperature gradient over the general area of the experiment.

Early in the summer the thermistor circuit for measuring small temperature changes was not ready, but it was available in time for use later on.

6.2.2 The Space-Charge Pulses

Soon after measurements in convective weather had begun, the space-charge pulses which are the main concern of this thesis were observed. Typical examples are shown in fig. 6.4, (a) and (b) being copies of records at the Observatory, and (c) at Mordon. The most striking characteristic of the pulses is their shape: a very sharp leading edge, with the recorder pen often moving almost to the peak in two or three seconds, and a slower decay. Usually, the peaks were 30 to 40 pC m^{-3} high, but were sometimes as much as 100 pC m^{-3} in amplitude. Between 80 and 90 such pulses were recorded at the Observatory, on nine different days. On seven of these days, the pulses were negative, and on the other two positive. At the Observatory, although not at Mordon, the positive pulses

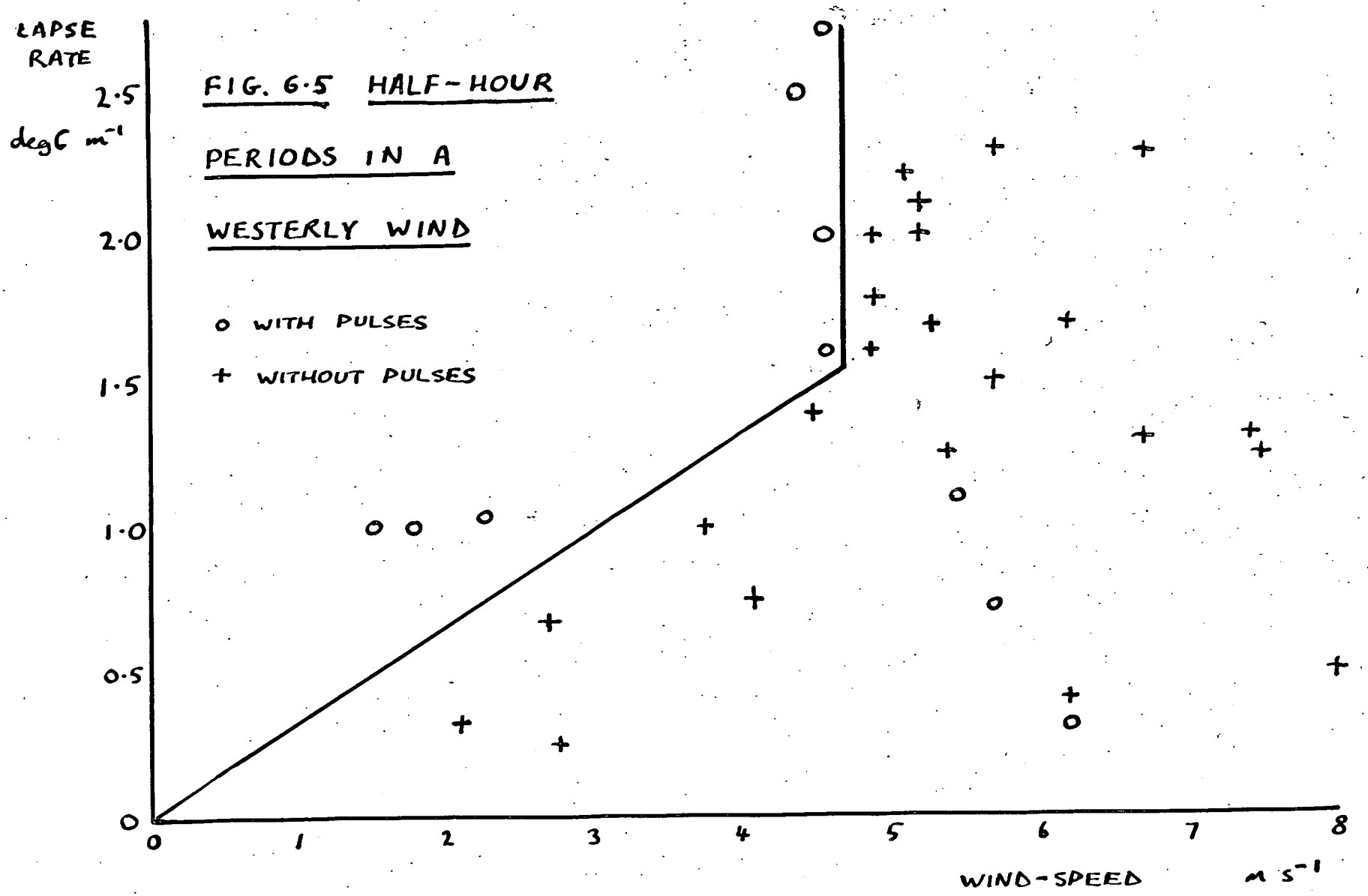

FIG. 6·5 HALF-HOUR PERIODS IN A WESTERLY WIND

were perhaps a little less sharp-edged than the negative, although this may have been chance. Otherwise, the positive and negative pulses were exactly similar. At the Observatory, there was no day with both positive and negative pulses.

It was apparent that the pulses were associated with convective weather. They only occurred on sunny days, and there was only one half-hour period during which they occurred when the average low-cloud cover exceeded $\frac{2}{8}$, and that was with $\frac{3}{8}$ cover. In order to investigate the relation of the pulses with lapse-rate and wind-speed conditions, these two parameters were measured as described above every half-hour, and the records divided into corresponding half-hour periods, with the average of the lapse-rate and wind-speed measurements at the beginning and end of the half hour taken as the average conditions for that period. The half-hour periods were plotted on distribution diagrams of wind-speed and lapse-rate. It was soon noticed that the pulses occurred in different conditions in an easterly wind from those in a westerly wind. The presence of the hedge was an obvious explanation, and so one diagram was plotted for periods when the wind was blowing from the hedge to the collector (i.e. in all winds with an easterly component) and

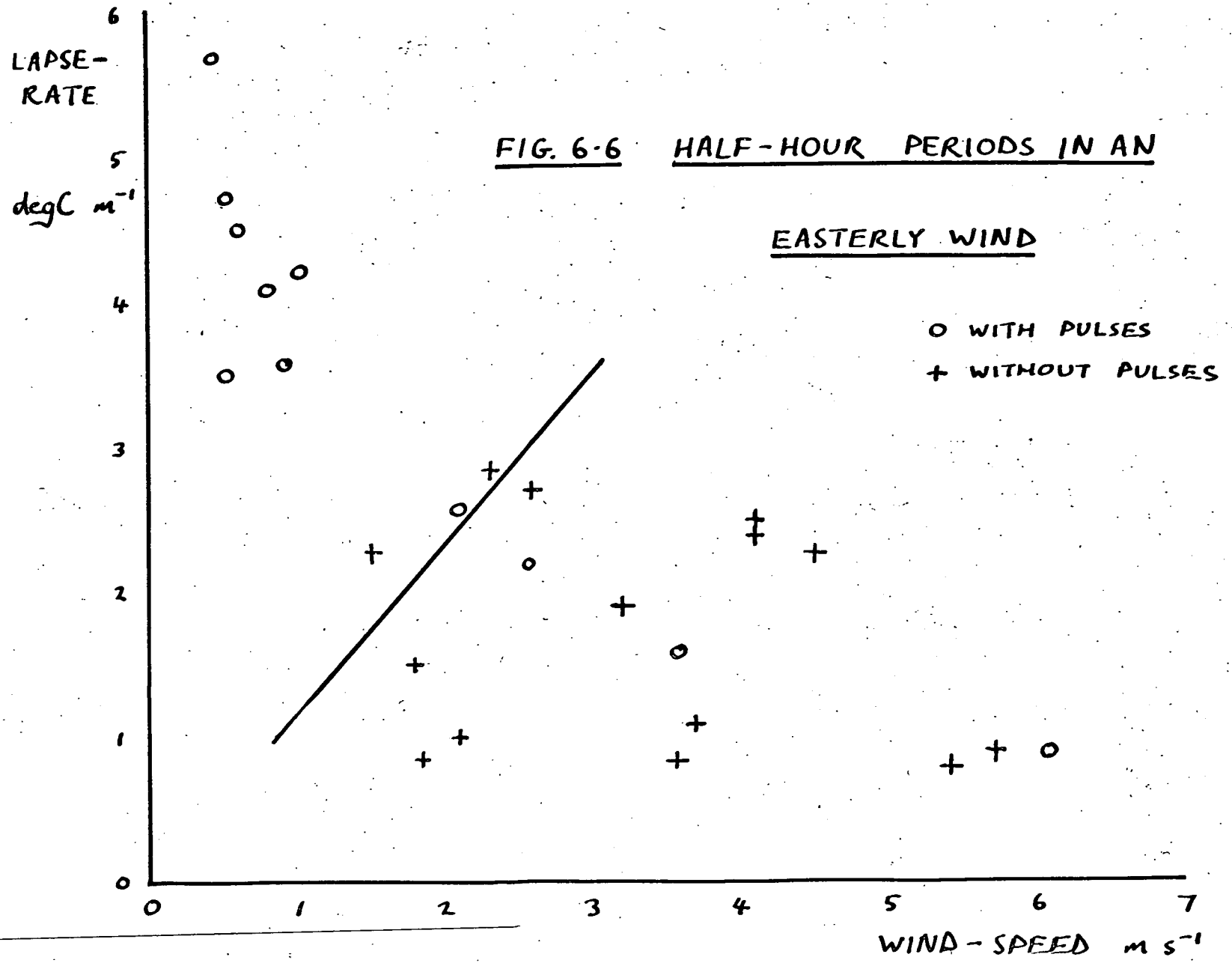

FIG. 6·6 HALF-HOUR PERIODS IN AN EASTERLY WIND

another for other winds. The distributions are shown in figs. 6.5 and 6.6. It will be seen that, generally speaking, the pulses were more likely to occur in lower wind-speeds and higher lapse-rates, and that the threshold wind-speed was lower when the wind had an easterly component. There were three periods which were exceptions in the westerly case. In each of these half-hour periods, only one pulse occurred, and the same applies to the exceptions in the easterly case, except for the period at 2.6 m s^{-1}, 2.7 deg C m^{-1}, which had three pulses. Fig. 6.5 does not show many points for wind-speeds less than 2 m s^{-1}, because in convective conditions with low wind-speeds, a sea-breeze often sets in at Durham in the late morning, giving an easterly wind.

The monthly distribution of the nine days with pulses was: March (1), April (1, with positive pulses), May (3, of which one gave positive pulses), June (1), August (2), and September (1). In addition, one set of measurements was made with the apparatus of Bent and Hutchinson, in late January, which showed positive space-charge pulses in shape more similar to those described by them than to the pulses shown here.

The distributions shown in figs. 6.5 and 6.6 will be discussed further in section 6.5, and those

characteristics which the Observatory pulses showed in common with the ones observed at Mordon will be discussed in section 6.4. It was thought, however, that the distributions indicated the pulses might be some sort of free-convection phenomenon, and it was hoped simultaneous records of small temperature changes might prove this. When these became available, it was sometimes possible to pick out periods of free convection, although at this height the air movement is still very turbulent, and these often coincided with periods in which pulses occurred, but there was clearly no correspondence at all between the space-charge peaks and the temperature peaks. Fig. 6.4 (a) is an example of such a record; on this occasion the thermistor was put at 1.5 m to try to ensure it was really in the free-convection zone. Measurements of temperature variations with the aspirated thermistor accompanied space-charge measurements at the Observatory on three days, during which eleven space-charge peaks were recorded.

6.3 Measurements at Mordon

The Mordon measurements detected a total of thirteen space-charge pulses, very like those at the Observatory, on three days, on two of which the pulses were predominantly negative. On the day with positive pulses,

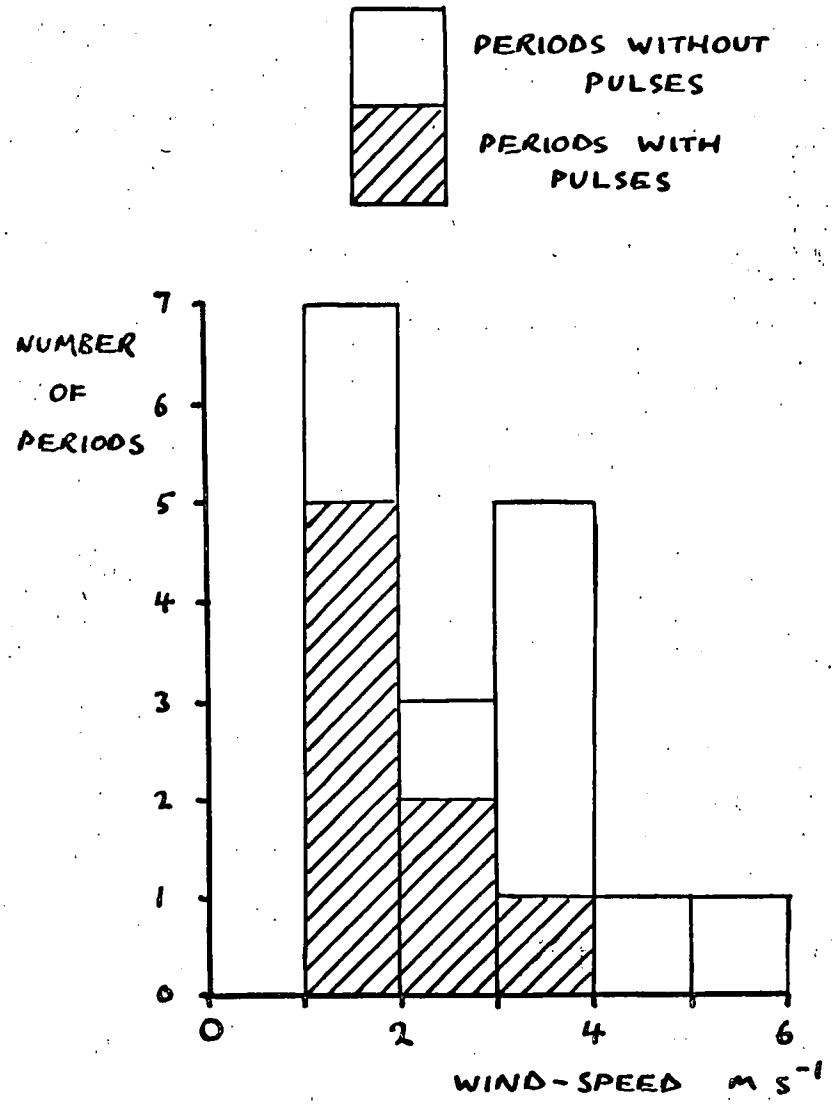

FIG. 6·7 DISTRIBUTION OF HALF-HOUR PERIODS AT MORDON

there was one negative pulse, which occurred before all the others, and on one of the days with negative pulses, there was a positive pulse over an hour after the others. Both of these anomalous pulses were rather uneven in shape, however, and may have been spurious. Fig. 6.4 (c) shows three of the Mordon pulses.

It was hoped originally to measure wind-speed gradient and temperature gradient during the Mordon readings, and to calculate the corresponding Richardson's numbers (section 1.3.3), in the hope of relating these to the conditions under which space-charge pulses occurred. Unfortunately, however, the procedure that had to be adopted to measure the temperature gradients (section 5.3.3) took so long that it was impossible to repeat it every half hour. It was therefore decided that this measurement should not be attempted, especially as the Observatory results had shown wind-speed to be the more important parameter, and measurements were made only of wind-speed at 2.2 m, either by continuous measurement on the recorder, or by running the anemometer on the electromagnetic counter for the whole half hour.

Fig. 6.7 shows how the half-hour periods of measurement in bright sunshine were distributed with wind-speed. It is clearly unwise to draw firm conclusions from such

scant data, but the distribution does suggest the pulses were more likely at low wind-speeds, with a cut-off wind-speed of about 3 m s^{-1}. In comparing this value with the Observatory result of about 4.5 m s^{-1} in a westerly wind, we must remember that the Mordon wind measurement was made at 2.2 m. If we assume a logarithmic wind-profile, although this strictly applies only to neutral stability, we can correct this value to 10 m. As was discussed in section 2.4.1 , the wind-speed

$$u \propto \log \frac{z}{z_o}$$

where Zo is the "roughness length". The surface in the field at Mordon was thin grass about 15 cm high, so it seems reasonable to take Zo = 0.01 m (see table 2.1), which gives the ratio of wind-speed at 10 m to that at 2.2 m as 1.28, and the approximate maximum 10 m wind-speed for plumes at Mordon as 3.8 m s^{-1}.

In most cases, the sensitive thermistor was in operation during the space-charge pulses, but, as at the Observatory, there was no correspondence in the traces. On two days, the propeller anemometer was used to measure vertical wind-speed at 1 m, the dial showing total run of wind being read every minute. The average runs of wind for the minute periods varied between +3 and -3 m. During the three hours for which this procedure was carried out,

only four space-charge pulses were observed, of which one was of doubtful validity, and these did not coincide with any striking event onthe vertical velocity record.

Potential gradient was also measured during all the Mordon pulses. For two pulses, there were possible coincident peaks of potential gradient 5 V m^{-1} high, but for all the others there was no correspondence. In general the potential gradient was fairly steady, and on only one occasion were short period variations observed anything like those described by Whitlock and Chalmers (1956). This occasion was in a wind-speed of about 5 m s^{-1}, too great for space-charge pulses at 1 m, and five peaks, each about 50 V m^{-1} high and lasting for two or three minutes, were measured. They had an average separation of about 15 minutes. Since a potential gradient deflection of 5 V m^{-1} would probably have been noticed, and this would be given by a uniform horizontal layer only 1 m thick of space charge of density 40 pC m^{-3}, it is clear that the pulses could not have had much vertical extent.

Since the pulses could apparently be detected only with the space-charge collector, it proved impossible to compare measurements at two places simultaneously.

The sign of the potential gradient did not seem to

affect whether the pulses were positive or negative.

6.4 Other General Properties of the Pulses

The remarks in this section apply to the results at both the Mordon and the Observatory sites, unless otherwise stated.

6.4.1 Intersection-Length and Wind-Speed

If we assume that the space-charge pulses are carried along by the wind, we can obtain a horizontal length for each pulse by multiplying the time it lasts on the record by the mean wind-speed. The time interval used was the "half-peak duration", i.e. the time for which the space-charge density was more than half-way from its quiescent value to the peak. The duration of each pulse thus measured was multiplied by the mean wind-speed for that half-hour period to give an "intersection length" of the pulse. For each half-hour period, the mean value of this quantity was calculated, and compared with the mean wind-speed. At Mordon, the 10 m wind-speed calculated as above was used. The results are shown in fig 6.8. Half-hour periods with only one pulse were not included because of the increased likelihood of random error. As already mentioned, Bent and Hutchinson's apparatus was used for one period of measurement, lasting

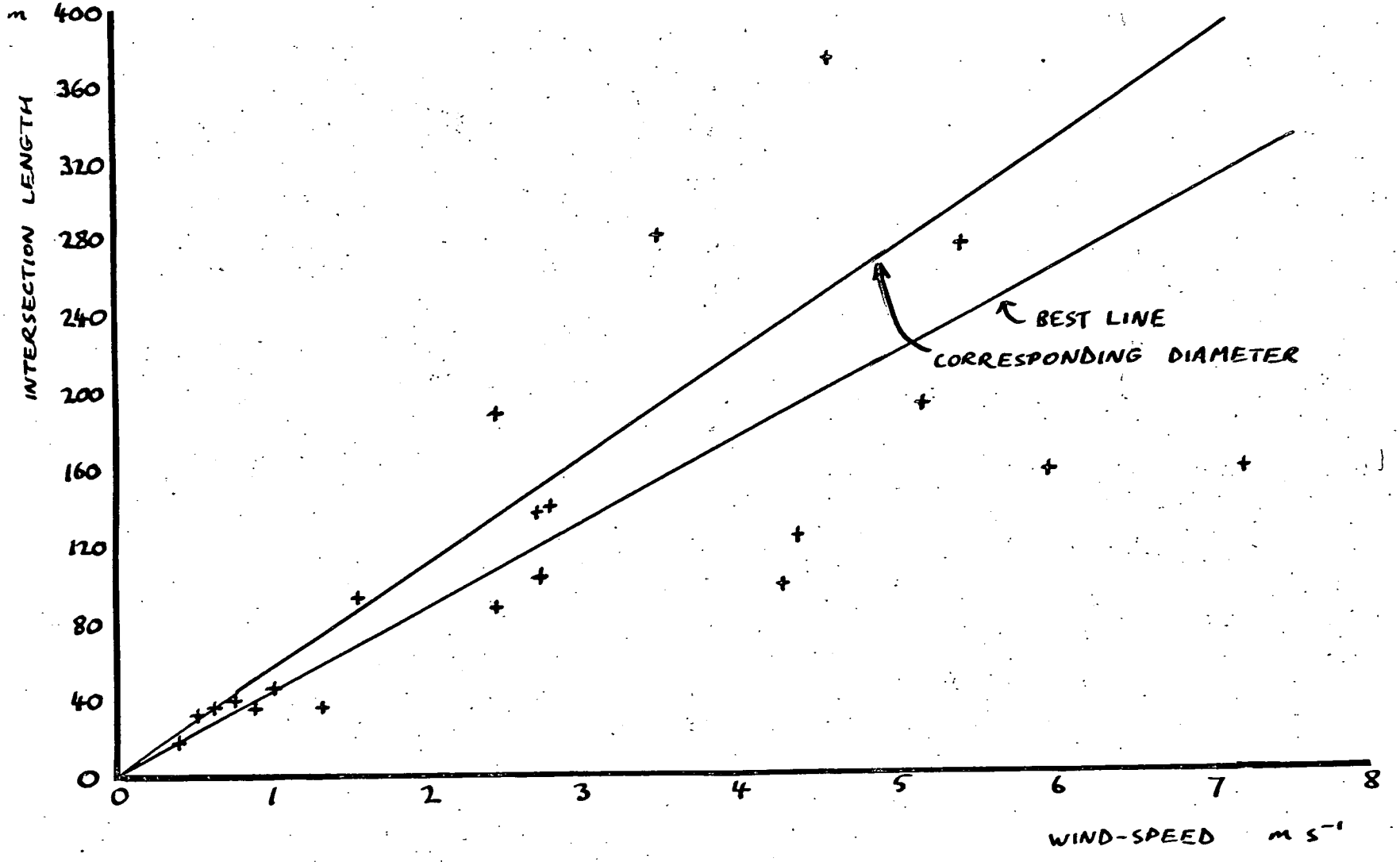

FIG. 6·8. VARIATION OF PULSE INTERSECTION LENGTH WITH WIND-SPEED

about 1½ hours and including eleven pulses, and this is shown on the graph as one point, at 3.5 m s^{-1}, 280 m.

The graph appears to be best represented by a straight line almost through the origin, and the least-squares best-fitting line through the origin is shown. The correlation coefficient r between intersection-length and wind-speed is about 0.7 (22 results), significant beyond the 0.1% level.

If we assume the space-charge pulses to represent vertical columns of space charge of circular horizontal cross-section, then the intersection-lengths measured will represent random chords of the circle, and, even if the cross-section had a fixed diameter for a particular wind-speed, a distribution of intersection-lengths between this diameter and zero is to be expected. It is easily shown that the average chord-length of a circle is $\pi/4$ x diameter, and a ~~dotted~~ line is shown on the graph which has $4/\pi$ x the slope of the best line. This should represent the mean diameter variation with wind-speed on this model. Of course, even ifthis picture of the pulses were true, a random distribution of diameters about a mean would be expected for each wind-speed.

Although some such model may represent the physical

picture, and we may indeed be discussing a physical element whose diameter increases with wind-speed, all that the linear relationship of fig. 6.8 tells us directly is about the time interval we multiplied by wind-speed to get the intersection length, which we then found proportional to wind-speed. Clearly, the half-peak duration of the pulses is independent of wind-speed, and the slope of the best line on fig. 6.8 shows its mean value to be 43 s.

6.4.2 Distribution and Mean Value of Intersection-Lengths

The distribution of individual pulses by intersection length showed a peak at about 30 m, and a gradual tail-off to zero pulses at about 500 m. This presumably represents only the distribution of wind-speeds during measurement, but it is mentioned because it showed quite a close resemblance to the distributions found for his temperature pulses by Vul'fson (1964) (section 1.5). For this reason, attempts were made to fit functions of the form

$$F(R) = a\left(\frac{R}{R_0}\right)^b e^{b\left(1-\frac{R}{R_0}\right)}$$

as suggested by Vul'fson, but, not surprisingly, the distribution could not be represented in this way.

The mean intersection-length of all the pulses

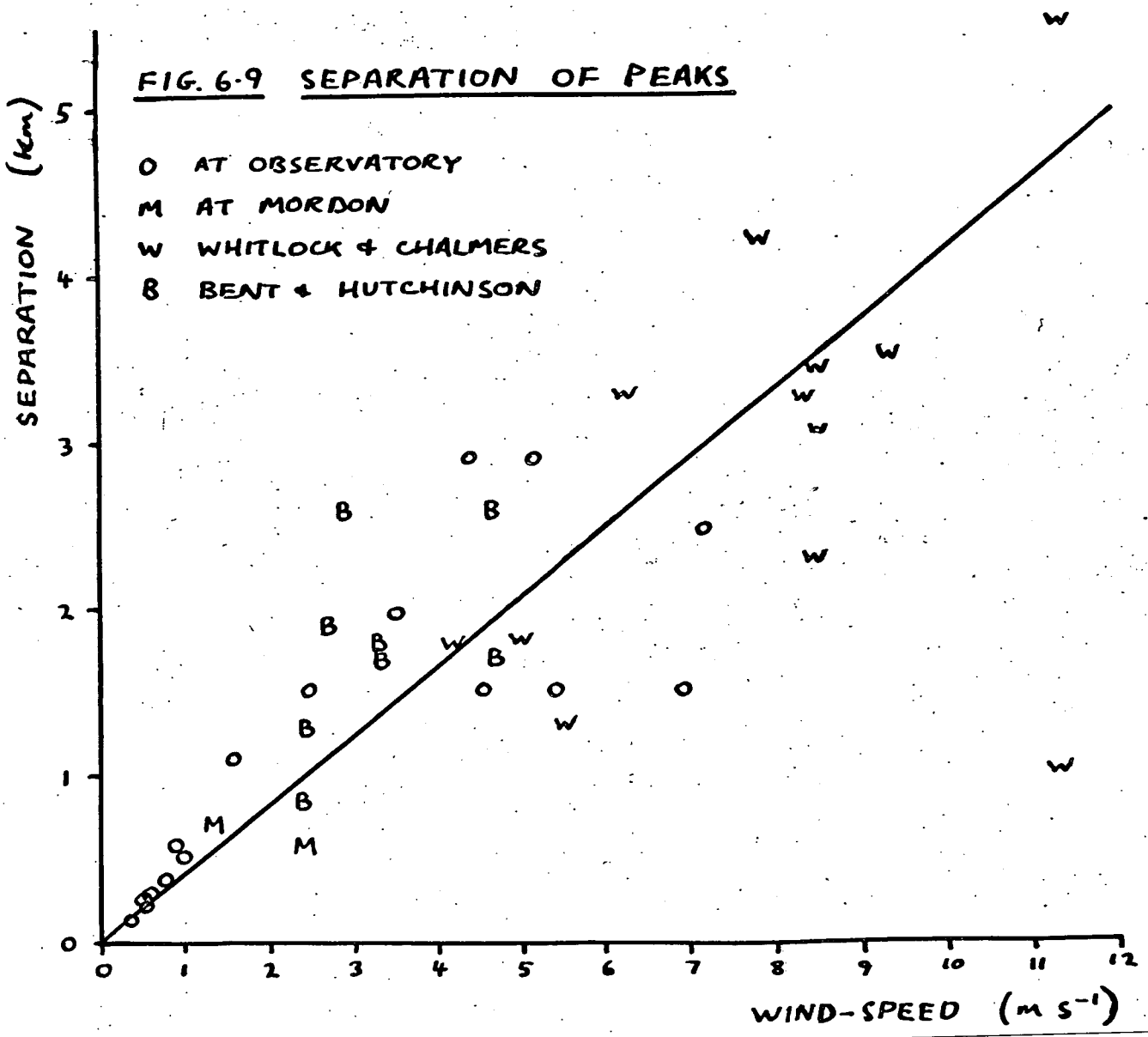
FIG. 6·9 SEPARATION OF PEAKS
O AT OBSERVATORY
M AT MORDON
W WHITLOCK & CHALMERS
B BENT & HUTCHINSON
SEPARATION (km)
WIND-SPEED (m s⁻¹)
0
1
2
3
4
5
6
7
8
9
10
11
12

measured was 143 m.

6.4.3 Pulse Separation and Wind-Speed

The time intervals between the sharp leading edges of successive pulses were treated in the same way as the half-peak durations, and the spatial separations obtained are shown plotted on fig. 6.9. The points from the Mordon measurements are distinguished from the Observatory points. Rather more scatter might be expected on this graph than on fig. 6.8, because there was no clear way of telling whether or not a pulse was in any way associated with its predecessor. An exceptionally long gap might have represented a period during which conditions had changed slightly to prevent pulses. However, all such gaps were included in the averages, unless it was quite clear that the pulses occurred in two separate groups with a long interval between them.

Because of the supposed relationship of these results with those of Bent and Hutchinson (1966) and of Whitlock and Chalmers (1956), their measurements are also included on the graph. Some adjustment of both these other sets of results was necessary to make a fair comparison. Whitlock (1955) gave the mean separations of the "field pulses" reported by him and Chalmers, but

calculated these using the speed of the pulses measured by correlating the records from two separated field mills. Fortunately, he also gave the ratio of this speed to the 10 m wind-speed, and so it is possible to calculate the 10 m wind-speed and corresponding mean separation for each set of pulses. Bent and Hutchinson calculated the separations of their pulses in the same way as the author, but used the 17 m wind-speed measured on the mast. We can very roughly reduce this to 10 m by multiplying by $\log 10 / \log 17$ which equals 0.81, although this neglects the roughness length Zo, and the fact that lapse conditions were not neutral. The state of the grass in the field (in the author's recollection) might justify putting Zo = 0.03 m, giving a correction factor of 0.92, but since the site generally was not horizontally uniform, any such estimate of roughness length is speculative. In any case, the factor chosen does not affect the ratio of wind-speed to spatial separation. The factor used was 0.81.

The author's results are grouped in half-hour periods, as before, but the other workers in general took an average for each day's readings.

It can be seen that all three sets of results seem to relate separation and wind-speed in the same way. There is some evidence of non-linearity, but a straight

line through the origin fits the results quite well. The correlation coefficient r is about 0.75 (38 results), which is significant beyond the 0.1% level. The mean intervals between pulses calculated from the points on the graph are as follows: author's results 7.58 min, results of Bent and Hutchinson 8.75 min, results of Whitlock and Chalmers 6.22 min, all results 7.40 min.

6.4.4 Pulse-Height Variation with Wind-Speed

No variation was apparent.

6.4.5 Consideration of Further Analysis

Some thought was given to whether the results justified a more rigorous statistical analysis than given above. Each point shown on figs. 6.8 and 6.9 is subject to error on both variables. The wind-speed measurement is a mean over half an hour, during which there is always short-period turbulent variation and often a slower change. To represent roughly the error due to the random variation, at the Observatory, one-sixth of the width of the wind-speed trace on the anemogram was taken, based on the argument that if the distribution about the mean were normal, three standard deviations on either side of the mean would enclose almost all the distribution. The error on the length was taken as the square root of the variance of the

distribution within each half hour. In this way, some idea, albeit very rough, was obtained of the errors for each point.

Fitting the best straight line to data with errors on both variates is a problem for which no general solution is known. Morgan (1960) and Davies (1957, section 7.6) suggest different methods of solution for special cases. Davies' treatment requires the errors on the variates to be independent, and this is probably true for Morgan's method also. Since the lengths plotted in both graphs were obtained by multiplying a time interval by the wind-speed, the error on the wind-speed clearly would have affected the error on the distance. This difficulty could be overcome. For example, if the intersection-length l were related to the mean wind-speed $\bar{u}$ by

$$l = a\bar{u} + b \qquad (6.1)$$

where a and b were constants, the half-peak duration t would be related to $\bar{u}$ by

$$t = a + \frac{b}{\bar{u}} \qquad (6.2)$$

The variables t and $\bar{u}$ should have independent errors, and so the method of either Morgan or Davies could be used to determine a and b and their probable errors in regression (6.2), and these substituted in (6.1).

There are more formidable difficulties, however, Both methods effectively assume that the ratio of the errors on the variates does not vary from point to point. This is certainly not so in this case. Also, the errors on a point calculated as above appear to bear no relation to the distance of the point from the best straight line. Finally, on graph 6.9, there is some evidence that the slope of the best fit should decrease with increasing wind-speed.

Taking into account all these objections, it was felt that there was little justification for applying either method to the analysis, and it was decided merely to show the least-squares lines of best fit through the origins, without attempting to calculate their confidence limits.

The author is grateful to Dr. M. Stone, Reader in Mathematical Statistics at this University, for his advice in this matter.

6.5 Interpretation of Results

6.5.1 Summary of Properties of Pulses

The following is a summary of the properties of the space-charge pulses observed at 1 m.

(a) They form distinctive peaks on the space-charge

density records, having a very sharp leading edge, and a slow decay with a time constant of the order of one minute.

(b) They can be of either sign, although about two-thirds are negative-going, and the shapes of negative and positive peaks are identical. Positive and negative pulses do not generally occur both on the same day. The sign of the pulses does not apparently depend on either the sign of the potential gradient or the sign of the quiescent space charge.

(c) Their magnitude is variable, does not depend noticeably on wind-speed, and is usually about 30 to 40 pC m^{-3}, but may exceed 100 pC m^{-3} (625 e cm^{-3}). Their vertical depth is probably less than 1 m.

(d) The peaks occur both at the Observatory and at Mordon, and pulses from the two places are indistinguishable.

(e) The pulses only occur in sunny weather, and are more likely in low wind-speeds and high lapse-rates.

(f) The maximum wind-speed at which they usually occur is lower when the wind blows over an obstruction before reaching the apparatus.

(g) The duration of the pulses is independent of wind-speed, indicating that, if the charge is blown along with the wind, the horizontal diameter of the charged volume is proportional to wind-speed. The mean duration is about

43 s.

(h) The interval between pulses is also independent of wind-speed, indicating that their spatial separation is proportional to wind-speed. The interval is about equal to those observed by Whitlock and Chalmers (1955) and Bent and Hutchinson (1956), and the average of all these results is 7.4 minutes.

(i) The pulses do not seem to be related to variations of temperature, or, with less certainty, vertical air velocity.

6.5.2 Comparison with the Results of Bent and Hutchinson (1966), and Whitlock and Chalmers (1956)

The phenomena observed on all three occasions have one fundamental similarity. They all probably represent discrete concentrations of space charge occurring only in sunny weather. Also, the magnitudes of the concentrations, and their mean separations, are about the same. However, there are important differences.

The first of these is the shape of the pulses. The peaks of Bent and Hutchinson, from the illustration they give, were straight-sided, and they do not report any asymmetry. Also, both sets of workers report only positive peaks, but in the present work negative ones were usual. This may be an accident of sampling, perhaps

aggravated by failure to recognize the negative peaks as the same phenomenon when the workers had become accustomed to looking for positive ones, but this explanation seems unlikely.

One possible explanation of the shape of the pulses is that this is an instrumental effect. The recorder cannot have been at fault, or it would not have responded so quickly to the leading edge of the pulse. Similarly, the V.R.E. should react symmetrically to the pulse. Its time constant is irrelevant, because we are not considering a decay from an imposed signal to zero, but from one imposed signal to another, as can be clearly seen by considering the cases where the peak took the space-charge density negative from a quiescent positive value. The possibility that this shape was a characteristic of the collector cannot be eliminated - a somewhat similar decay was noticed in one or two other measurements - but once again it seems unlikely that the collector should react asymmetrically to the square-edged pulses, especially as the virtually identical collectors of Bent and Hutchinson did not.

Secondly, although the observations of Whitlock and Chalmers were solely of potential gradient peaks, there were none observed to coincide with the space-charge peaks in the present case. It is possible that the

space-charge columns reach sufficient height only at the Observatory to affect the potential gradient, although this seems unlikely. Although neither Bent and Hutchinson (1966) nor Bent (1965) mention potential gradient measurements in this connection, Dr. Bent was kind enough to let the author have the computer print-outs of his results for three of the days on which he detected peaks, and these show simultaneous potential gradient peaks sometimes 30 - 40 V m^{-1} high.

Also, in the present case, no coincident temperature variations were observed. This agrees with the result of Whitlock (1955), but disagrees with Bent and Hutchinson who detected marked variations down to 0.5 m, the variations at the lowest level being, in fact, the most marked. Unwilling to neglect any possibility, the author considered whether Bent's temperature and humidity peaks might be an instrumental effect: Mr. M.J. Smith (personal communication), who took over Bent's apparatus, found that, due to a faulty biassing arrangement, the channels on the recorder sometimes influenced one-another, but consideration of the sampling sequence which connected the apparatus to the recorder showed that the space-charge peaks could not have influenced the temperature.

Although the importance of the difficulties cannot

be underrated, it seems probable that the three sets of measurement are related in some way. It would be surprising if three workers on the same site, however irregular in topography, could each find a phenomenon involving peaks of space charge in convective weather, and that all three phenomena were different, and no worker detected either of the phenomena reported by the others. Clarification of the relationship of the three sets of records must await further measurements. Meanwhile, some limited conclusions can be drawn about the nature of the peaks.

6.5.3 Relation of the Results to Convection Models

As was discussed in chapter 1, the best supported model of convection in the first few metres is a layer of forced convection, with fully-turbulent temperature variations, overlain by a region in which freely convective plumes are present. It is clear that figs. 6.5 and 6.6 invite the explanation that the space-charge pulses occur in the free convection region, but not in the forced convection layer. This would mean that the forced convection layer was about 1 m deep for a 4.5 m s^{-1} wind (at 10 m) blowing up the Observatory field from the west, but reached this depth at the apparatus in a wind of only 1.5 m s^{-1} when the air had to blow across a

five-metre hedge, which, of course, would increase the depth of turbulence downwind. The lower cut-off wind-speed over open ground at Mordon of 3.8 m s^{-1} is to be expected from the longer grass there.

If this interpretation is correct, it is important in showing the depth of the fully-turbulent layer over land much more uneven, and much more typical of this country, than the very flat countryside over which, for example, the measurements of Swinbank (Priestley 1955) or Taylor (1956) were made. There seem to be no previous data on the likely depth of the forced convection layer over uneven topography. Comparison of the measurements on the relatively flat country at Mordon with those at the Observatory shows, on this interpretation, that gentle slopes, and obstacles like trees within a few hundred metres, make little difference to the depth of forced convection, and the disturbance caused by the Observatory building and the hedge is surprisingly little. For comparison, Webb (1964) quotes 1.5 m as a typical depth of forced convection in a 5 m s^{-1} wind over flat grassland on a "clear summer day in middle latitudes". Webb is presumably referring to Australia, where the heat flux will be greater and the forced convection layer therefore shallower than in this country.

If the space-charge pulses are associated with the free convection layer, then they provide a very much better indicator of the layer than temperature or vertical velocity measurements. Near the boundary, the temperature pulses are much less marked, as is shown by the example given by Priestley (1959, P. 54), and was certainly found in the temperature records taken in this experiment, from which it was often very difficult to distinguish the free convection periods from the fully turbulent records.

However, the relation of the space-charge pulses to buoyant elements remains obscure. It was shown in section 2.4.3 that Priestley's plumes would be expected to give space-charge peaks, but two orders of magnitude smaller than those measured. The other principal objection is the failure to detect coincident temperature peaks, although, in view of the measurements of Bent and Hutchinson (1966), it is possible that there is some other undetected reason for this. Also, in a leaning plume, the air from nearest the ground, being warmest, and presumably carrying most space charge, would be expected to concentrate on the upper, upwind side of the plume, as is shown in temperature measurements. This would give a sharp edge to the space-charge pulse at the back edge, and not the front. Finally, both the diameters and the separations of the pulses are greater than would

be expected for convection plumes, judging from the measurements of Vul'fson (1964). As far as the author is aware, variation of the dimensions and separation of plumes with wind-speed has never been reported.

One interesting possibility is that the plumes carry up from the ground not only space charge, but air of greater conductivity. The discontinuity of conductivity at the upper, sharp edge of the plume might give a very local space charge, as described in section 2.2.2, which would account for the sharp leading edge of the space-charge pulse, which would then coincide with the back of the plume. The magnitude of the pulse would depend on the conductivity gradient and the extent to which an electrical quasi-static state, with a conduction current, would be set up across the back face of the plume during its lifetime. Inspection of the records showed that the space-charge pulses coincided no more regularly with a sharp fall in temperature than they did with a sharp rise, and the other objections listed above remain.

6.5.4 Other Possible Explanations

The convection interpretation, despite all its faults, seems to provide a better explanation of the pulses than any other. A local pollution source might explain

the constant duration and interval of the pulses, but cannot explain why they are only found in low wind-speeds in sunny weather, and why they are negative on most days, but positive on others. It would also be remarkable for such a source to be present both at the Observatory and at Mordon.

Another possibility is that electrode effect produced space charge at the Observatory mast or other objects, as described by Bent and Hutchinson (1966), and this blew off at intervals. This would only occur at low wind-speeds, but does not explain the association with sunny weather, the presence of the pulses in the open country at Mordon, and, most telling of all, why the sign of the pulses is independent of the sign of the potential gradient.

The possibility of some weather-dependent instrumental effect, such as those described in section 4.6, cannot be entirely eliminated, of course, although it is hard to imagine what sort of phenomenon it could be, and why it should produce negative pulses on some days and positive on others.

6.6 Conclusion

The circumstantial evidence strongly suggests that the space-charge pulses are associated with free convective

conditions; if this is true, it shows that the depth of the forced convection layer is about the same in broken countryside as over very flat ground. The relation of the pulses to buoyant elements is, however, obscure. It seems unlikely that they coincide with convective plumes. The origin of the space charge is also a complete mystery. Space-charge gradients usually observed do not seem sufficient to account for the pulses, even assuming the peaks are in some way related to vertical motion. It is hard to imagine a pollution source which would give identical pulses at both the Observatory and Mordon, especially taking into account variation of the sign of the pulses, and the weather conditions under which they occur. Perhaps in solving the mystery of where the space charge originates, and how long the pulses last, some light might be shed on the cause of their relation to free convection conditions. More will be said on this in chapter 10.

CHAPTER 7

SPACE CHARGE OVER MELTING SNOW

7.1 Charge Released from Melting Snow

Bent and Hutchinson (1965) measured a marked space-charge gradient over melting snow on the ground in moderate winds, indicating that negative charge was being released to the air at the surface. This chapter describes attempts to repeat their measurements, and includes estimates of the convection current and rate of charge separation required to explain their results.

Some workers report that when ice sublimes, it releases positive charge to the air, which probably accounts for the positive space charge observed near blowing snow, and has been explained in terms of temperature gradients by Latham (1964). The negative space charge often observed near melting snow may originate from water becoming negative with respect to ice at the interface. In melting snow, some of the melt-water might be scattered in the air as small droplets, which would evaporate, or be themselves trapped in the charge measurement apparatus. The magnitude of the effect depends on many factors, however. The presence of carbon dioxide maybe important, perhaps because of its relatively high solubility and ionization in solution,

and other impurities also affect results. There is evidence to suggest that the rate of melting is also important. Magono and Kikuchi (1963 and 1965), using natural and artificial snowflakes, have found that the charge released to the air depends very much on the number of air bubbles breaking as the ice melts, presumably because this governs the number of droplets scattered into the air, and the charge therefore depends on the dimensions and complexity of the crystals.

In view of these many variable factors, it is not surprising that there is wide disagreement amongst measurements of the amount of charge released to the air when ice melts. Most measurements have given results of the order of 1 esu gm^{-1} of ice (0.33 $\mu C\ kgm^{-1}$) but results vary from 0.3 esu gm^{-1} (MacCready and Proudfit 1965, for natural hailstones melting in the laboratory) to 1.1×10^{8} esu gm^{-1} (Magono and Kikuchi (1963 and 1965) for snow crystals).

7.2 Space-Charge Gradients over Melting Snow

7.2.1 General Theory

It was shown in section 2.4.2 that a convection current density i_2 in forced convection in horizontally uniform conditions is linked to the space-charge density gradient by equation (2.15):

$$\frac{\partial \sigma}{\partial z} = i_2 / k z u_* \qquad (7.1)$$

This was derived for neutral stability, since it assumes $\frac{\partial u}{\partial z} \propto \frac{1}{z}$, but, as Priestley (1959, P.39) has pointed out, in forced convection buoyancy plays no part in heat transfer, and this wind-speed gradient relation therefore applies. Using equation (2.3) for the conduction current i_1, we can write the total current i at a particular height as

$$\begin{aligned} i &= i_1 + i_2 \\ &= F\lambda + k z u_* \frac{\partial \sigma}{\partial z} \end{aligned} \qquad (7.2)$$

Since (equation 2.11)

$$u_* = k z \frac{\partial u}{\partial z}$$

$$i = F\lambda + k^2 z^2 \frac{\partial u}{\partial z} \frac{\partial \sigma}{\partial z} \qquad (7.3)$$

Hence, by measurement of potential gradient, conductivity, wind gradient, and space-charge density gradient at a particular height, the total upward current density could be calculated, and this would be equal to the rate of charge-release to the air per unit area of snow surface.

By a method analogous to that used to derive (7.1), and detailed by Priestley (1959, chapter 3)[a4], the heat flux H can be shown to be related to the potential temperature gradient $\frac{\partial \theta}{\partial z}$ by

$$H = -\rho C_p k^2 z^2 \left(\frac{\partial u}{\partial z}\right)\left(\frac{\partial \theta}{\partial z}\right) \qquad (7.4)$$

For explanation of the difference of sign, the reader is once again referred to the conventions described in the Foreword. Also

$$\frac{\partial \theta}{\partial z} = \frac{\partial T}{\partial z} + \Gamma$$

where Γ is the dry adiabatic lapse-rate. If L is the latent heat of melting of ice, then a heat flux H melts a mass of ice H/L per unit area per unit time. If the charge released to the air per kilogram melted is S, which we may call the "specific charge", then

$$i = SH/L \qquad (7.5)$$

Hence, from (7.2)

$$S = -\frac{L\left(\frac{F\lambda}{k^2 z^2 \frac{\partial u}{\partial z}} + \frac{\partial \sigma}{\partial z}\right)}{\rho C_p \left(\frac{\partial T}{\partial z} + \Gamma\right)} \qquad (7.6)$$

This treatment involves a number of assumptions, in particular that all the heat flux melts snow at the surface, and that all the heat reaching the surface is carried down from the warm air above by forced convection.

With the snow surface at 0°C, the first assumption is likely to be not much in error. With regard to the second, any heat from the ground will presumably melt snow at the bottom of the layer. A more serious error is likely to be the heat flux from radiation from the sun and the sky in clear conditions. This might be

calculable for a particular case - Sutton (1953, chapter 3) discusses this problem - but in this treatment we shall assume the radiative heat flux to be negligible, as might perhaps be the case under an overcast sky.

The treatment also assumes aerodynamically rough flow, which, over a smooth snow surface, requires justification. Priestley (1959) states that it occurs when

$$u_* > 2.5\,\nu / z_o \qquad (7.7)$$

where ν is the kinematic viscosity. For air around 0^oC, $\nu = 1.3 \times 10^{-5}\ m^2\ s^{-1}$. According to Priestley (1959, P.21), over smooth snow on short grass, $z_o = 5 \times 10^{-5}$ m, and so (7.7) becomes

$$u_* > 0.65\ m\ s^{-1}$$

The general condition becomes

$$u_* z_o > 3.25 \times 10^{-5}\ m^2\ s^{-1} \qquad (7.8)$$

Figures given by Priestley show that over smooth snow on short grass this would correspond to a wind-speed at 2 m of 18.5 m s^{-1}, which means that over such a surface the treatment could only be used in a strong wind. However, since the determination of S requires calculation of u_*, and z_o can easily be determined, a check can be kept on the applicability of the treatment.

It should be noted that (7.6) gives only the charge

released to the air. Much of the charge separated in melting is presumably carried in melt-water which percolates through the snow to the ground, and would not be measured by this method. The proportion released to the air in the form, initially at least, of small droplets, is likely to depend mainly on the texture of the snow surface, but also on the degree of turbulence in the air near the surface. This second factor suggests that there might be a relationship between S and u_*, to be determined experimentally.

7.2.2 Application to Measurements of Bent and Hutchinson (1965)

As already mentioned, Bent and Hutchinson report a period (their period "C") when they measured a positive space-charge density gradient over melting snow, in a mean wind-speed of 10.5 m s^{-1} at 10 m, and a mean temperature of 2.5°C at 1.2 m. Using these figures we can make a very rough calculation of the specific charge of the melting snow, although we have to make assumptions about the gradients. The calculation will, in any case, serve as an example of the application of the method.

In addition to the charge gradient, Bent and Hutchinson observed a high positive charge density at higher levels, which they attributed to blowing snow on

distant hills. Since it came from a distant source, this charge should have been uniformly mixed, and ought not to have affected the charge gradient. This will be assumed to be the case.

First, we must calculate $u_* Z_o$ to find whether the flow was aerodynamically rough. If we knew the wind-speeds at two heights this could be done by substituting both sets of figures in the wind profile

$$\frac{u}{u_*} = \frac{1}{k} \log_e \frac{z}{z_o} \qquad (7.9)$$

However, we must here assume a value for Z_o. Priestley (1959, P.21) gives $Z_o = 10^{-3}$ m over a snow surface on natural prairie. Taking u as 10.5 m s^{-1} and Z as 10 m, (7.9) gives $u_* = 0.46$ m s^{-1} and $u_* Z_o = 4.6 \times 10^{-4}$ m^2 s^{-1}, which fulfils the condition (7.8). The condition is fulfilled unless $Z_o < 10^{-4}$m, which seems unlikely.

As already mentioned,

$$H = -\rho C_p k^2 z^2 \frac{\partial u}{\partial z} \frac{\partial \theta}{\partial z} \qquad (7.4)$$

Putting $u_* = kz \frac{\partial u}{\partial z}$ and $\frac{\partial \theta}{\partial z} \simeq \frac{\partial T}{\partial z}$

$$H = -\rho C_p k z u_* \frac{\partial T}{\partial z}$$

If T = 0^oC at Z = 10^{-3}m, integration of this gives for the temperature difference between that height and 1.2 m

$$\Delta T = 7.1 \frac{H}{C_p \rho k u_*} \qquad (7.10)$$

The space-charge density difference between 1 and 2 m, $\Delta\sigma$,

is given by the integration of (7.1), assuming the convection current to be constant with height between these two levels:

$$\Delta\sigma = 0.695\, i_2 / k u_* \qquad (7.11)$$

The charge released S will be transferred upwards by conduction and convection. Let us call the part transferred by conduction S_1 and the part transported by convection S_2. Clearly,

$$S = S_1 + S_2$$

and, from (7.5), $S_2 = L i_2 / H$

whence, using (7.10) and (7.11)

$$S_2 = 10.2 L \Delta\sigma / C_p \Delta T$$

We shall take Cp = 1.01 x 10^3 J kgm^{-1} $degC^{-1}$, L = 3.34 x 10^5 J kgm^{-1}, and ρ = 1.28 kgm m^{-3}. Bent and Hutchinson obtained $\Delta\sigma$ = 250 e cm^{-3} (40 pC m^{-3}), and ΔT=2.5 degC. Hence

$$S_2 = 0.042\ \mu C\ kgm^{-1}$$
$$= 0.14\ esu\ gm^{-1}$$

This, of course, only represents the charge which is released at the surface and carried upwards by convection between 1 and 2 m. The convection current is shown by (7.11) to be equal to 1.06 x 10^{-11} A m^{-2}, assuming u_* = 0.46 m s^{-1}.

The potential gradient at 1 m during the measurement was

+ 500 V m^{-1}, and if we assume the conductivity at 1 m measured at the Observatory by Higazi and Chalmers (1966), 8.4 x 10^{-15} Ω^{-1} m^{-1}, from

$$i_1 = F\lambda$$
$$i_1 = 4.2 \times 10^{-17} \text{ A m}^{-2} \qquad (2.3)$$

This is a little under half the convection current value, and S_1 might therefore be about half S_2, if the value taken for the conductivity were realistic. However, the melting of the snow may be accompanied by the production of small ions, which will increase the conductivity. As is shown by fig 2.2, this would not by itself increase the conduction current, but the space charge present has increased the potential gradient, so the current will be greater. Clearly, if this method is to be useful, measurements of conductivity and potential gradient are essential.

As regards errors on the heat flux, the Observatory records show the sky to have been overcast all day. One source of error not yet considered is the heat used up in vaporizing any small droplets produced at the surface. Some kind of estimate of this can be made by measuring the water vapour pressure gradient, and hence the flux of vapour. The report by Bent and Hutchinson gives a gradient of relative humidity, but when the temperature gradient is taken into account, it is found

that this represents an insignificant gradient of water concentration. It would seem that in this case at least, the error from this source is small.

We can conclude that, to the nearest order of magnitude or so, the charge released to the air by the melting snow in the case considered was 0.5 esu gm^{-1} (0.16 $\mu C\ kgm^{-1}$), which compares well with measurements by the other methods already mentioned.

7.3 Measurements

Although apparatus for measuring conductivity was not available, it was felt worthwhile to try to measure the convection current from snow, if only to define more closely the melting conditions under which charge separation might be expected. Preliminary measurements were made in the winter of 1965-66, but this was done before the above theory was worked out, and the measurements were not accompanied by wind and temperature gradient determinations. In any case, a possible charge density gradient was detected on only one occasion.

Unfortunately, the winter of 1966-67 was almost entirely without snow at Durham. Two days of measurements were obtained there, and three more on trips into the Pennines, but even there snowfall was comparatively light. The temperature gradient was measured, as described in

section 5.3.3, and the wind at 0.5 and 1 m. Space-charge density measurements were made at the same heights, but, as only one collector was available, these had to be made successively and not simultaneously.

On no occasion was any space-charge density gradient observed. For all the sites, $u_* Z_o$ exceeded the critical value at the wind-speed used, but for the three sites in the Pennines the value of Z_o calculated was found to be ridiculously small (less than 10^{-7} m), indicating either that the ground was too rough to apply the equations, or that one of the anemometers was faulty. The satisfactory readings were taken on a football pitch at Durham.

For one, u_* was 0.46 m s^{-1}, the 1 m wind-speed 0.83 m s^{-1}, and the temperature difference between 0.5 and 1 m was 4.18 degC; for the other, u_* was 0.32 m s^{-1}, the 1 m wind-speed 0.49 m s^{-1}, and the temperature difference 0.07 degC, which is probably not significantly different from zero, bearing in mind the probable error on the thermistor measurements.

7.4 Proposed Experiment

Measurement of charge separation on melting by any method is beset by difficulties, and so it is not out of the question that this method should yield information useful in evaluation of thunderstorm electrification

theories. However, the effects of dissolved gases and of crystal structure make it clear that the most useful results would come from snow which melts soon after it falls, and in an unpolluted region. The site would also need to be level for a distance upwind of perhaps a few hundred metres to ensure reasonable horizontal uniformity in the air, and smooth. The problem in this country would be to find such a site with snow-fall that could be relied upon, but which remained accessible through the winter.

The measurements required would be:

(a) Wind-speed at two heights (say 0.5 and 1 m);

(b) Temperature at the same heights;

(c) Space-charge density at the same heights;

(d) Total conductivity and potential gradient at about 0.75 m;

(e) Humidity at the two heights.

From (a) and (b) could be calculated the heat flux to the snow surface, from (a) and (c) the convection current, from (d) the conduction current, and from (a) and (e) the water vapour flux, from which could be determined the proportion of the heat flux evaporating the melt-water, and the proportion melting the snow.

In the author's opinion, this would be a worth-while experiment on a suitable accessible site with predictable

snow-fall and melting conditions, but is probably unsuitable for the climate of England, although it might conceivably be possible elsewhere in Britain.

CHAPTER 8

POINT DISCHARGE AND FOG MEASUREMENTS

This chapter describes measurements made of point discharge currents and in fog. They are grouped together because in both cases the space charge is emitted from an elevated source, and blown away, diffusing sideways as it goes. The possibility of using such a situation in diffusion measurements is considered.

8.1 The Point-Discharge Experiment

8.1.1 Point Discharge from Trees

Since the first suggestion that corona discharge from points connected to the ground might make a significant contribution to atmospheric electrical processes, various attempts have been made to measure the current in high potential gradients from living trees, which probably constitute the majority of such points over land, and to assess the total current from a large area. Milner and Chalmers (1961) attempted to by-pass the current down the trunk of a tree by inserting electrodes at different heights, and found that a lime tree in leaf, about 15 m high and the same distance from the nearest other trees, began to discharge when the ambient

potential gradient reached a threshold value of about 1000 V m^{-1}. Ette (1966), and Jhawar and Chalmers (1967) have shown that this method does not measure the total current down the tree, and so the measurement by Milner and Chalmers of about 2 μA in a potential gradient of 2500 V m^{-1} is presumably an under-estimate. Maund and Chalmers (1960), measuring the depression of potential gradient downwind of trees, calculated that a 12 m sycamore in full leaf gave less than 1 μA of space charge in a potential gradient of 7000 V m^{-1}. Using the same technique on a line of poplar and ash trees, Maund (1958) showed that these had a threshold potential gradient of about 1100 V m^{-1}, and that the current in summer, with the trees in leaf, was about one-third the winter value. Bent, Collin, Hutchinson and Chalmers (1965) measured directly the space charge during a thunderstorm downwind of a line of ash trees in bud, and estimated the current per tree required to produce it to be of the order of 1 μA. Their potential gradient measurements were made in the region heavily influenced by the space charge they measured, and cannot therefore be related to measurements by other workers.

Jhawar and Chalmers (1967) insulated a small living tree, and placed it between two metal plates to

which a voltage difference was applied. They found the relation of the current i to the voltage V when this had reached a threshold value V_o to have the form

$$i \propto V(V - V_o)^2 \qquad (8.1)$$

This experiment makes it seem likely that the current from a tree in a thunderstorm follows a cubic relation with potential gradient, although Milner and Chalmers (1961) found a linear relation for their tree, and so did Maund (1958) for his line of trees.

The measurements on individual living trees, although few in number, agree in showing that discharge begins when the potential gradient reaches about 1000 V m^{-1}, with the measurement of Maund and Chalmers on the sycamore as a notable exception. When we consider the total charge transported from a large area during a storm, there is more room for doubt. Experiments with artificial points have found ratios of negative charge to positive charge brought to earth over periods of months between 1.3:1 and 2.9:1, and point discharge current would therefore contribute to the "charging current" of the Earth's field. However, the problem of extrapolating from a single point to a large area containing many trees of different exposures makes estimation of the total current from this source difficult. Most workers have

obtained charge transfer rates in England of roughly 100 C km^{-2} yr^{-1} or rather more, in which case point discharge makes up the greater part of the charging current. Such figures are based on estimates of the "effective separation" of points, derived either by counting trees, making allowance for their exposure, or from rain currents. The extrapolation from individual trees to a large area is still a matter of doubt. Wormell (1930) pointed out that the total point-discharge current was likely to be governed by the cloud and not the nature of the surface, and this idea has been developed by Chalmers (1952a, and 1967 section 9.25). The vertical current over a thundercloud has been shown to be of the order of 1A, and the current underneath the cloud must be the same. In the absence of any other charge transfer process likely to be of sufficient magnitude, point discharge must provide most of this current, and if the points on the ground are small, the potential gradient at the ground will increase until the total current they give is equal to the current above the cloud.

The measurement described here, although unconfirmed, must apparently be explained by point discharge at a small clump of trees, and forms an addition to the sparse

experimental data on this subject.

8.1.2 Outline of Method

Maund and Chalmers (1960) have shown that the space charge flowing from an isolated point at height h has virtually the same effect on the potential gradient at a horizontal distance of downwind from the point as an infinite line of charge, provided that $d < \sqrt{3}h$. This case has been treated by Davis and Standring (1947) who obtained an expression for the potential gradient due to the charge

$$F = \frac{i}{2\pi\epsilon_0 u h}\left(1 + \frac{d}{(d^2+h^2)^{\frac{1}{2}}}\right) \qquad (8.2)$$

where ϵ_0 is the permittivity of free space, and u the wind-speed.

A group of trees can be considered as a large number of discharging points, each of which will produce this potential gradient reduction directly downwind. The field mill can only be directly downwind of one part of the clump, however, and the field contribution at the mill from other points will be less. Maund (1958) stated that if the wind blows at an acute angle ϕ to the line joining the point to the mill, the expression (8.2) becomes

$$F = \frac{i\,h}{2\pi\epsilon_0 u\left(h^2+d^2\sin^2\phi\right)}\left\{1 + \frac{d\cos\phi}{(h^2+d^2)^{\frac{1}{2}}}\right\} \qquad (8.3)$$

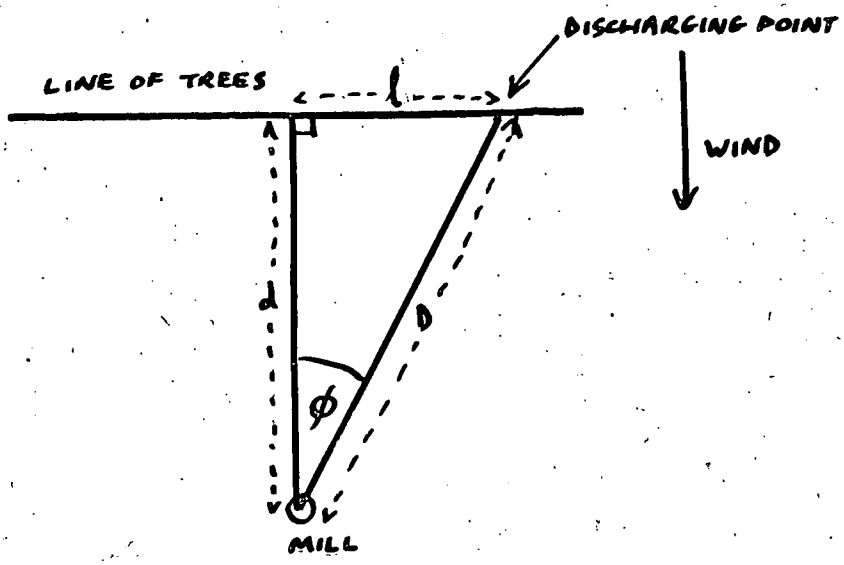

FIG. 8·1 EFFECT OF FINITE SIZE OF GROUP OF TREES

This is not quite equivalent to the case under consideration, because for a point in a group of trees the distance D must be substituted for d in (8.3) (see fig 8.1), giving

$$F = \frac{ih}{2\pi\varepsilon_0 u\left(h^2+d^2\tan^2\phi\right)}\left[1+\frac{d}{\left(h^2+d^2\sec^2\phi\right)^{\frac{1}{2}}}\right] \qquad (8.4)$$

Using this formula, the effect of the finite size of the clump can be assessed for a particular case.

8.1.3. The Experiment

During May 1967, an unusually long spell of thundery weather occurred at Durham, and the opportunity was taken to carry out an experiment similar to those of Maund and Chalmers. The three field-mills were used, with their ranges extended as described in section 5.2.3, with one placed upwind and another downwind of a group of three deciduous trees in full leaf. There was an ash tree in bud nearby, and the third mill was placed downwind of this, in the hope that it might be possible to compare its characteristics with those of the clump. Unfortunately, on the only occasion for which a useful record was obtained, the wind was blowing roughly from the clump to the ash tree.

A plan of the group of trees is shown in fig 8.2, where A is a hawthorn 10.7 m high, B a 15.9 m lime tree,

FIG. 8·2

PLAN OF THE SITE

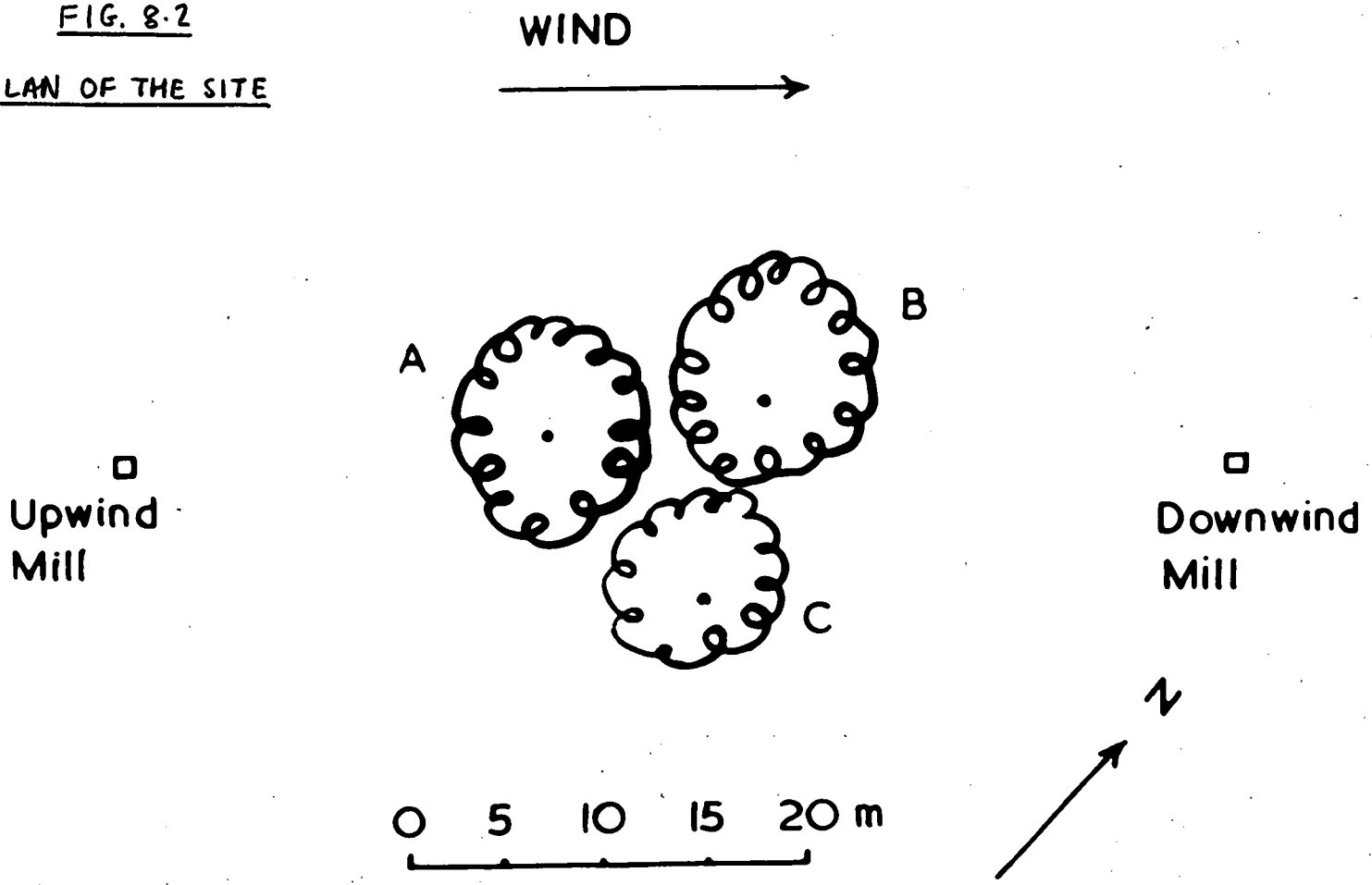

and C a 14.2 m plane tree. The nearest trees upwind were in a small group about 12 m high to the north of the Observatory, which was 130 m SW. The record of the 10 m anemometer at the Observatory was used for wind-speed information.

8.1.4 Results and Discussion

Fig. 8.3 shows part of the record obtained when two or three decaying cumulonimbus clouds passed nearby, the full line showing the upwind mill record, and the dotted line the downwind. It can be seen that at low potential gradients the outputs of the two mills generally agreed to within 50 V m^{-1} - the accuracy to which the records could be read. On three occasions of high potential gradient (at 1141, 1147, 1226), however, the downwind mill read substantially less than the upwind, and the difference was especially well-marked for the peak at 1141, where the difference exceeded 200 V m^{-1} for over 3 min. The only explanation for this seems to be a source of space charge between the mills, and, although it is unwise to be too dogmatic on the basis of one record, point discharge at the trees obviously provides the best explanation.

The clump was 20 m wide perpendicular to the wind direction. Referring to fig 8.1, what appeared from the

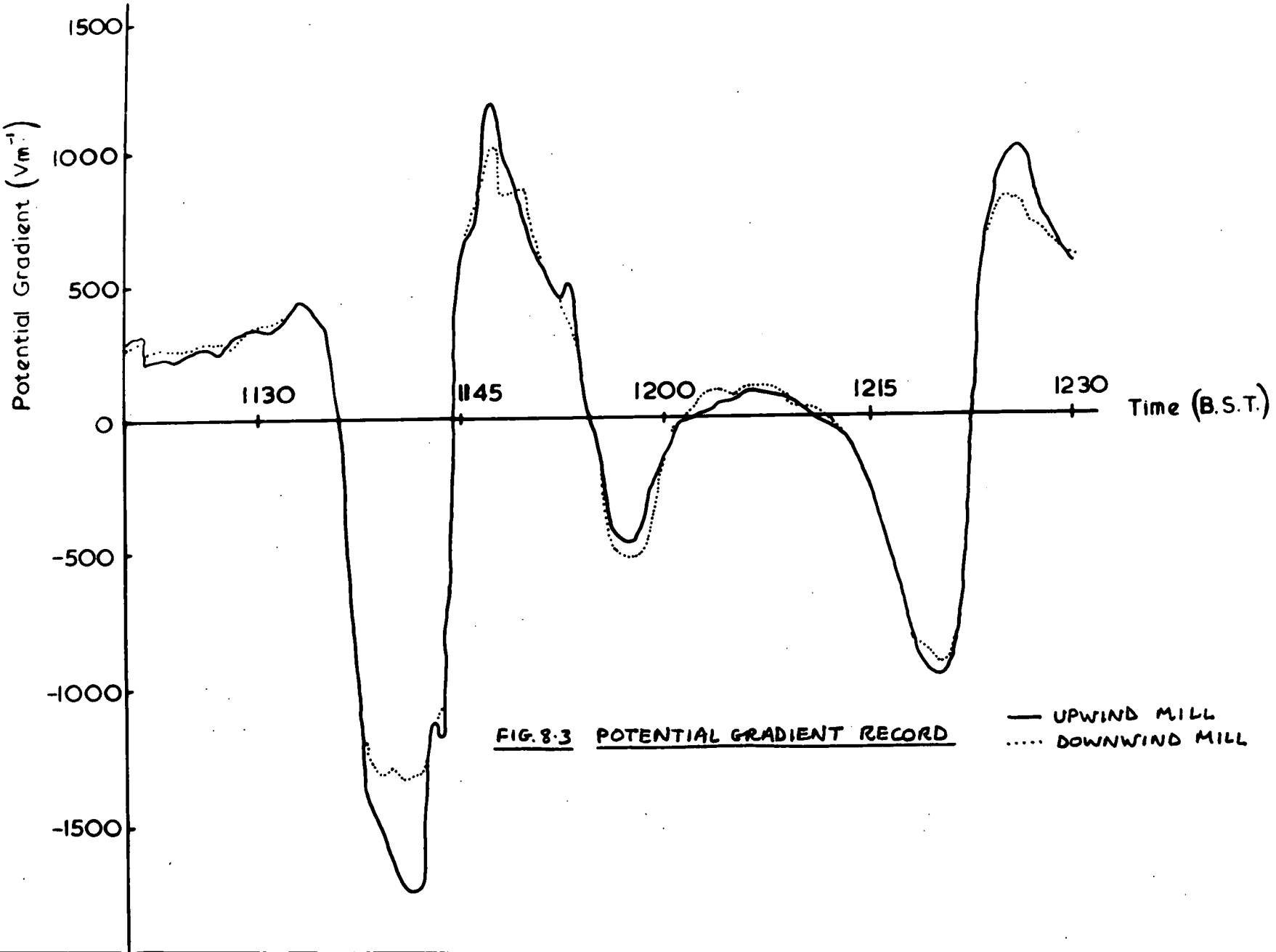

FIG. 8·3 POTENTIAL GRADIENT RECORD

mill to be the edge of the clump would make an angle ϕ of about 22°. Comparing equations (8.2) and (8.4), it follows that the potential gradient decrease on the downwind mill due to discharge at the edge will be only about 60% of what would be measured if the mill were directly downwind from the edge. We can therefore expect the value of the current for the whole group derived from (8.2) to be too low by not more than two-fifths, and probably by much less than that, since the highest parts of the trees were near the centre.

Table 8.1 shows the current calculated from (8.2) for the four main peaks, taking d as 26 m, and h as 14 m. (It will be noticed that for these dimensions d is slightly greater than $\sqrt{3}$ h; d was originally set by the height of the tallest tree, 15.9 m, but it seems reasonable to take the centre of the space-charge plume as a little below that. In any case, the error will not be great.)

Table 8.1 The four potential gradient peaks

Time	Upwind P.G.	Reduction	Mean Wind-Speed	Current
1220	- 950 V m^{-1}	0 V m^{-1}	2.5 m s^{-1}	0 μA
1226	+ 1000	170	3.1	0.22
1147	+1150	150	2.5	0.16
1141	- 1650	300	3.4	0.42

It seems probable that the 1141 current at least is

significant. As already mentioned, the calculated value must be increased to allow for the finite size of the clump.

8.1.5 Conclusion

The record seems to show that the group of trees starts to discharge at slightly less than $\pm$ 1000 V m^{-1}, and gives a total current of about 0.5 μA at an ambient potential gradient of -1650 V m^{-1}. It seems likely that most of the charge originated at the two taller trees, which overshadowed the hawthorn. This result is consistent with all others for trees in leaf, except that of Maund and Chalmers (1960) on the sycamore, which remains unexplained.

8.2 Fog Measurements

8.2.1 Power-Line Insulation Breakdown

Chalmers (1952b) showed that negative potential gradients observed in fog were associated with overhead power lines, and proposed that space charge produced by partial breakdown at the insulators was responsible.

Several workers have since confirmed the observation, and have shown that the charges can survive for miles downwind. Bent and Hutchinson (1966) showed that the charges persisted even after the mist had evaporated,

and also attributed negative space charges on humid nights to the formation of dew on the insulators. Groom and Chalmers (1967) showed that the charge was indeed produced at the pylons, and suggested that discharges resulting from the breakdown of surface insulation would produce electrons. If these were produced at the negative peak of line voltage, they would be repelled from the line, and might then form negative small ions before they could be attracted back to the line in the positive half of the voltage cycle. The ions, having a lower mobility than the electrons, would not be attracted back all the way to the line, and could be blown away by the wind.

The problem of surface breakdown on damp insulators is well-known to electrical engineers, and much effort has been put into designing insulators that will not form a damp layer over the whole surface and are easy to clean, for the problem arises not from a layer of pure water, but the moistening of a deposit of pollution, forming a conducting layer. The problem is reviewed from this point of view by James (1965). According to James, insulators are designed to give a uniform voltage drop down from the cable to earth. A conducting surface layer means that the lines of force ending on the insulator will be perpendicular to the surface rather than oblique to it,

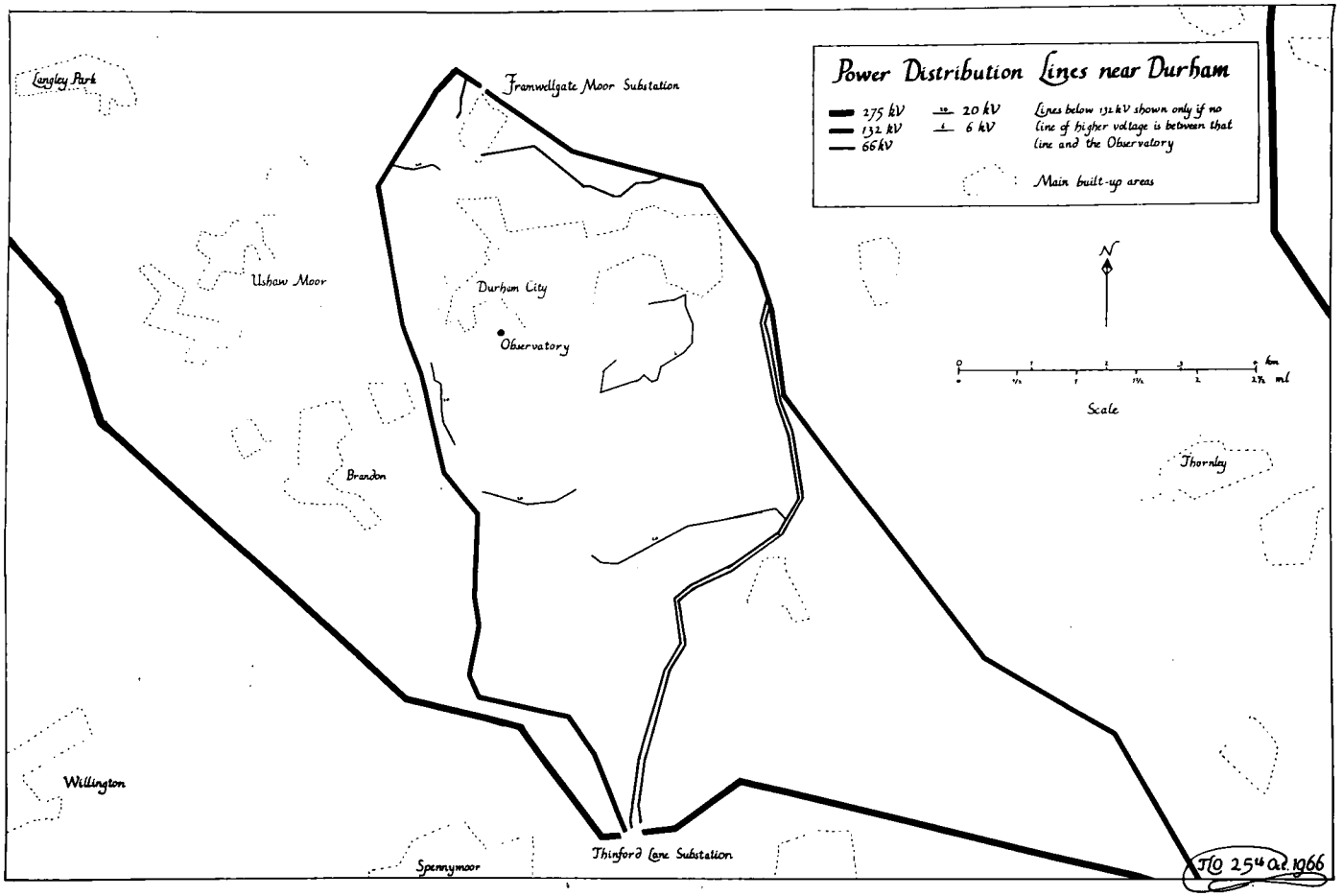
Power Distribution Lines near Durham
275 kV
132 kV
66 kV
20 kV
6 kV
Lines below 132 kV shown only if no line of higher voltage is between that line and the Observatory
Main built-up areas
Langley Park
Framwellgate Moor Substation
Ushaw Moor
Durham City
Observatory
Brandon
Thornley
Willington
Spennymoor
Thinford Lane Substation
N
km
mi
Scale
JIO 25th Oct 1966

FIG. 8.4

leading to concentration of the lines of force and perhaps corona discharge on the more highly curved parts of the surface. The current flowing in the moist layer may be several milliamperes and so there is quite sufficient charge flow to sustain a corona discharge current of some microamperes. In addition, the heating produced by the current may dry part of the current-path, leading to a discharge along the surface.

It is clear that the electrons produced will be influenced by the field at the insulator surface, and not by a simple radial field from the cable. The principle of the theory of Groom and Chalmers is not affected, however.

Dr. J.S. Forrest, F.R.S., of the Central Electricity Research Laboratories, (personal communication to Groom) has pointed out that on the higher voltage cables, operating at 275 and 400 kV, corona discharge occurs on the conductors themselves, and has suggested that this might contribute to space charge, especially as wind-speed is observed to affect the phenomenon.

8.2.2 Measurements

Throughout the experiments, negative space charge was observed to be generally associated with mist. Durham is now surrounded by power lines (fig 8.4) and the wind

direction makes little difference. At Mordon, on one occasion, a change within half an hour from positive space charge and potential gradient to negative was associated with the passage of a sea breeze front, the wind bringing mist from the coast, and passing a 275 kV line on the way.

As regards the minimum voltage required to produce appreciable charge, it was found that lines of 66 kV and above gave negative charge in mist whenever measurements were made. On two occasions, attempts were made to detect charge from 20kV lines, by measuring the space charge upwind and then downwind of the lines. On the first, the wind was about 10 m s^{-1} (at 10 m) and the visibility about 4 km; on the second, the wind was about 15 m s^{-1} and the visibility 1½ km. No significant charge production was measured on either occasion.

During mist in a north-easterly wind of less than 1 m s^{-1}, the opportunity was taken of measuring the space-charge density in mist blowing off the sea. This mist, of course, would not have had contact with power lines. The charge density at the Observatory was about - 8 pC m^{-3}, but on the sea-front at Marsden (NZ 403645), about 26 km NE, the charge was + 9.5 pC m^{-3}: a normal fair-weather value. By a fortunate chance, the period of

measurement coincided with the passage of a front, and within an hour the wind at the coast was blowing off the land, although still very light, and the charge had changed to - 14.5 pC m^{-3}. Although conditions are perhaps not really comparable, the space-charge density in a cloud was also measured on one occasion, and found to be positive. This was during one of the snow measurements at 650 m above sea level in the Pennines, when descending nimbostratus enveloped the apparatus, and the charge density was observed to be indistinguishable from just below the cloud, viz. + 24 pC m^{-3}.

Attempts were also made to measure how the ratio of the concentrations of small and large ions depended on the distance from the pylons, as suggested by Groom (1966). The small ion filter (section 4.5.1) was used. A measurement was made in mist not particularly close to any lines, and when this failed to detect any small ion concentration at all, the measurement was repeated immediately underneath the support pole of a 66 kV line in a visibility of 1 km, and no detectable wind. Like most of the fog measurements, this was carried out at night, and the sparking on the line insulators could be seen. However, there was still no detectable difference between the total space-charge density andthe large ion space-charge density. A subsequent laboratory test confirmed

that the small ion filter was still functioning. Although this unexpected result needs confirmation, it seems that the lifetime of a small ion in mist must be considerably less than a minute.

An attempt was also made to measure systematically another sort of variation with distance. It was noticed that in light winds there was a decrease in the negative space-charge density with distance downwind from the pylons, and, since this was presumably due to the diffusion upwards of the charge, measurements were made to see if this could be used to investigate the actual diffusion processes themselves. The experiment was usually carried out at night, when the mist was thicker, the wind conditions steadier, and the traffic pollution less. It was, of course, impossible to conduct simultaneous measurements at different distances, and the shortness of the lifetime of the collector before insulation breakdown under these conditions added to the problems. In fact, the decrease of density with distance did not seem to be related systematically to the wind-speed. In a typical case, in a visibility of 4 km and a wind-speed of about 1 m s^{-1}, the space-charge density decreased from -23 pC m^{-3} 130 m downwind from the pylons to-1 pC m^{-3} at 1750 m. As would be expected, in these

light winds measurements near the lines showed rapid variations with time, presumably as the wind-direction changed slightly, blowing the plumes of charge from the pylons towards or away from the apparatus.

Also in an attempt to see how the dilution rate varied with wind, measurements at the Observatory in mist were examined to see if space-charge density values could be related to wind-speed and direction, but once again there was no apparent regularity. Presumably other factors, such as traffic pollution, are more important.

8.2.3 Conclusions

The measurements generally confirmed what was already known about space charge produced at pylons in mist. It seems that lines of 20 kV and below do not give appreciable charge, but that lines of 66 kV and higher give negative charge even when the visibility is 4 km: it is probably the relative humidity that matters. Measurements suggest that if the negative charge is initially in the form of small ions, it is captured by large ions in less than a minute. The amount of charge produced at a line would be expected to be related to the pollution deposit on the insulators.

The possibility of using space-charge measurements

in diffusion studies will now be considered further.

8.3 Possible Diffusion Experiment

The decrease of space-charge density with increasing distance downwind of pylons suggests that it might be possible to use such measurements to carry out studies on the diffusion of pollution from a point source, such as has been done with smoke from factory chimneys. An elevated point charged to a high potential could provide the space charge by point discharge, as in the experiment of Large and Pierce (1957). The current flowing could easily and accurately be controlled and monitored, this perhaps providing the chief advantage over conventional methods of study. The height of the point could also be changed at will. Downwind, it might be possible to use potential gradient measurements at the ground, like those of Maund and Chalmers (1960), or a more direct method of space charge measurement. Close to the point, it might be possible to erect a filtration space-charge collector on a derrick, which would have to be of insulating material, to avoid interference from the electrode effect, as observed by Bent and Hutchinson (1966). This would probably still give trouble by charge separation near the earthed electrostatic shield of the collector. Such an arrangement would be clumsy, however, and useful measurements are more likely to be feasible

at a greater distance from the source, where the apparatus could be mounted nearer the ground without appreciable error or could be used on an aircraft. The diffusion rates could be investigated by measuring the decrease of charge density with distance directly downwind of the point, and the density cross-section perpendicular to the wind direction. Because a discharge current of a few microamperes would provide a large amount of space charge (Chalmers(1952b) estimated the current from each pylon to be about 1 μA), useful measurements should be feasible from this point of view for perhaps a dozen kilometers downwind.

Account would have to be taken of the effect on charge movement of the ambient fair-weather potential gradient, and the radial potential gradient produced by the plume itself. The radial potential gradient would be strongest near the source, of course. Analytical calculation is difficult, but the test experiments of Maund and Chalmers (1960) on their theory seem to show that its effect should be negligible near the source. As was pointed out in section 2.4.1, the movement of even small ions in the fair-weather potential gradient is much slower than their movement by diffusion, and it is probable that the ions produced by the discharge

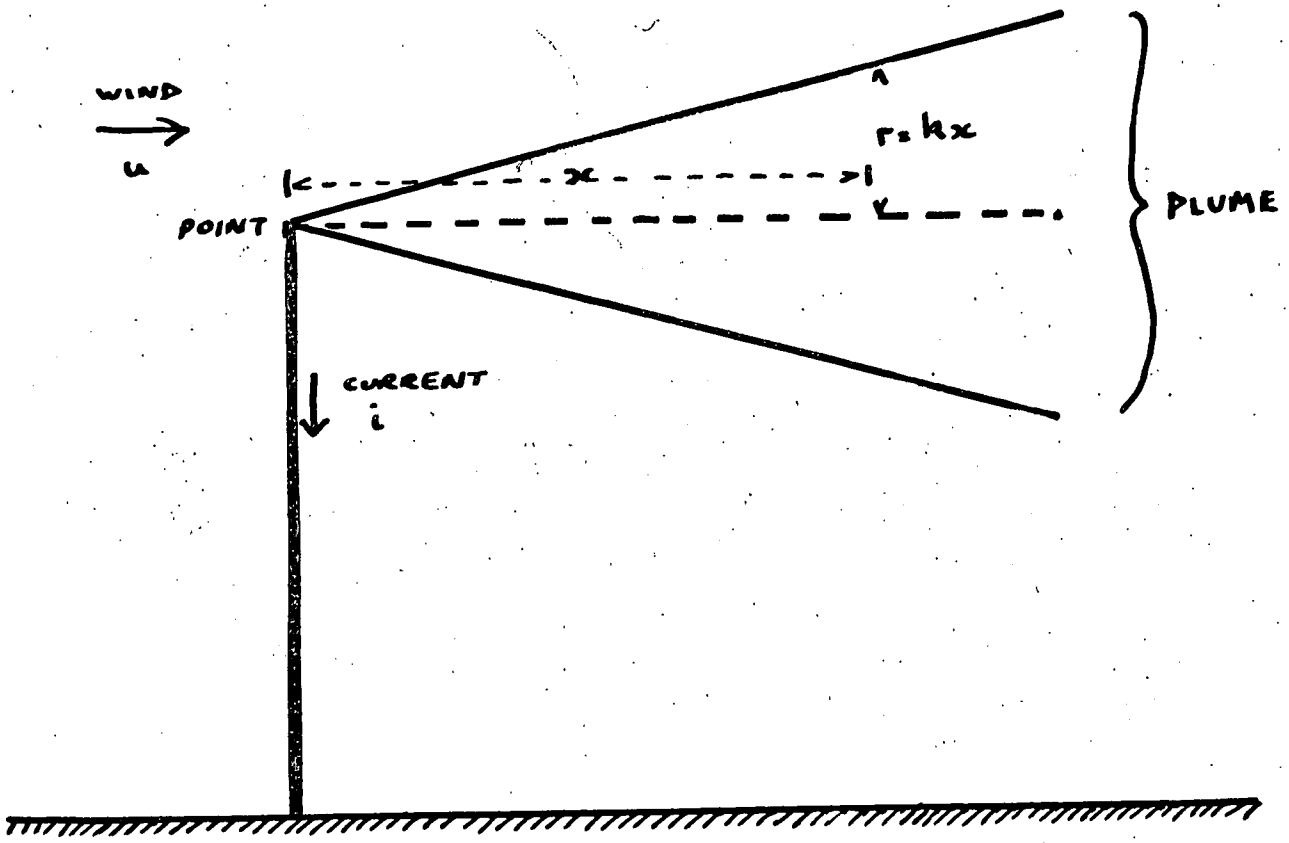

FIG. 8·5 DIFFUSION OF SPACE-CHARGE FROM POINT

would not stay as small ions very long. However, the potential gradient produced by the plume and the ordinary atmospheric potential gradient would probably produce an appreciable effect over large distances, although it might be possible to allow for this.

The time for which the ions produced at the source would remain small can be roughly calculated by considering how far the plume would have travelled before the volume it occupied contained as many nuclei as small ions. Referring to fig 8.5, suppose the point-discharge current is i, the wind-speed u, the number of nuclei per unit volume is χ and the ratio of r to x is k. The number of small ions of charge e in unit length of the plume is clearly i/eu, and in length x is ix/eu. The number of nuclei in this volume is $\pi k^2 x^3 \chi/3$, and these numbers are equal when

$$x^2 = 3i/\pi k^2 e u \chi$$

Taking i = 1 μA, k = 10^{-1}, e = 1.6 x 10^{-19} C, u = 5 m s^{-1}, χ = 10^3 cm^{-3} = 10^9 m^{-3}, this gives x = 450 m approximately. This is only a rough calculation of course, but it indicates that we can expect the plume to consist mainly of large ions at something like 1 km from the source.

The feasibility of this experiment clearly requires further investigation, especially from the point of view

of the influence of the potential gradients on the ion concentrations at the ground. The influence of this factor on the spread of pollution from conventional sources does not seem to have been taken into account. The principle consideration is, however, whether any useful new information could be obtained by such a technique. A comprehensive survey and bibliography of diffusion from a point source is given by Pasquill (1962).

The experiment would clearly require a site with no other space charge sources for a large distance.

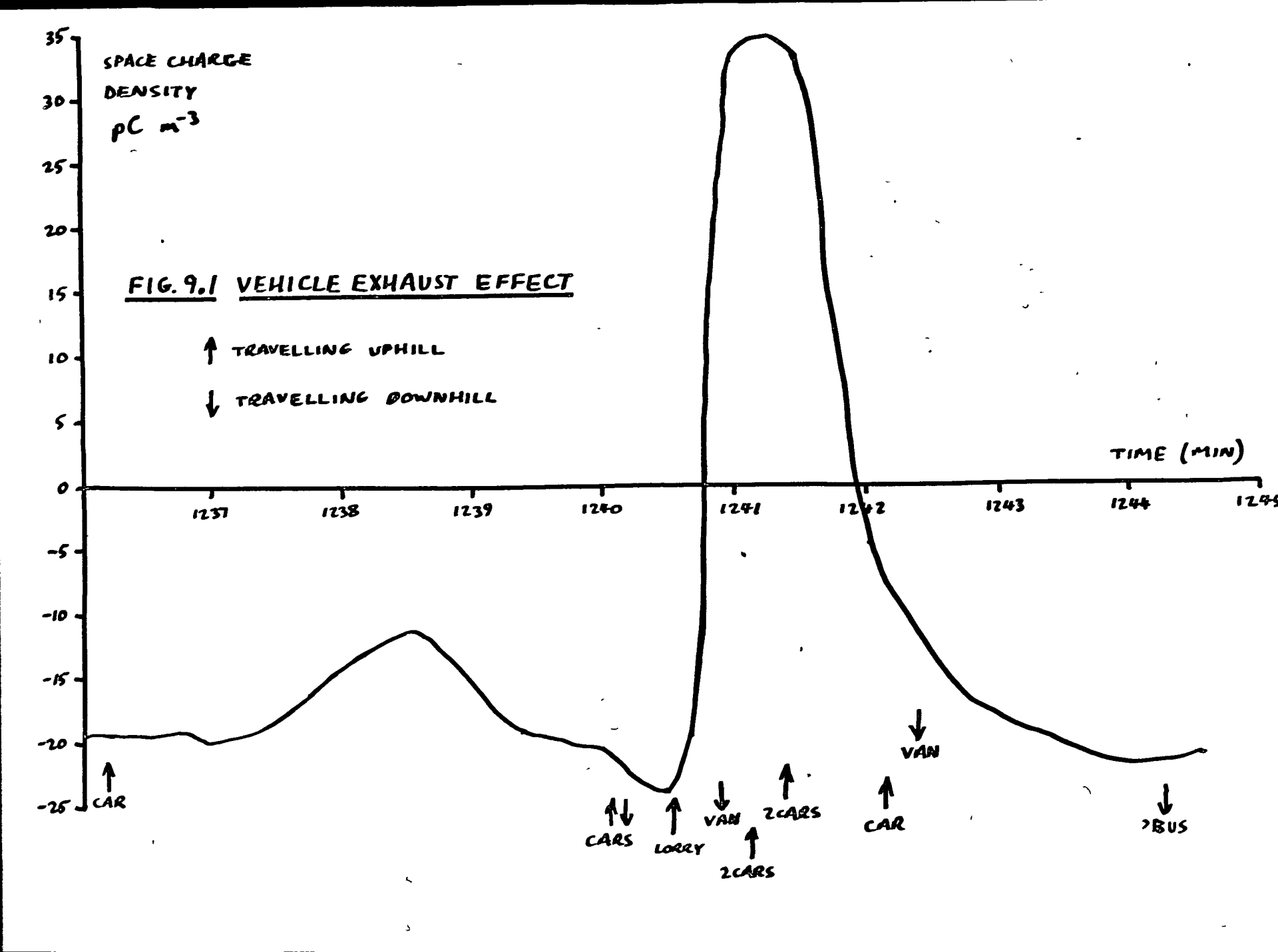

FIG. 9.1 VEHICLE EXHAUST EFFECT

CHAPTER 9

OTHER MEASUREMENTS

9.1 Normal Fair-Weather Space Charge

In fair weather, the space-charge density at 1 m almost always lay in the range 0 - 25 pC m^{-3} (0-150 e cm^{-3}). Since this charge probably comes for the most part from artificial sources, it is unsafe to draw any conclusions about the presence of natural processes.

9.2 Pollution Effects

It has been noted by various workers that the exhaust of road vehicles sometimes gives positive space charge. This was noticed on several occasions, and the impression was gained that cars passing along a road had little or no effect, and neither did heavy vehicles going downhill, but that lorries or buses going uphill, with their engines working hard, produced copious positive charge. This may indicate that the charge is produced primarily by diesel engines, which was the finding of Mülheisen (1953). Fig 9.1 is a copy of part of a record taken during fog measurements. The Land-Rover was parked beside a road with a slight slope, It can be seen that the only effect certainly attributable to a vehicle was due to a lorry going uphill, which produced a space-charge

density peak about 55 pC m^{-3} high. In principle, it should be possible to estimate the current flowing from the vehicle, but in this case it is difficult because the wind was blowing almost directly along the road. If we assume that the component perpendicular to the road was 0.5 m s^{-1}, then the time the charge pulse took to pass (50 s) corresponds to an "intersection length" of 25 m. If we assume the lorry produced a plume of space charge 25 m in diameter with its axis horizontal, and was travelling at 15 m s^{-1}, the volume of space charge produced every second was π x 12.5^2 x 15 m^3, corresponding to a current the order of 0.5 μA.

As was remarked in chapter 2, it is well known that steam trains produce space charge, but there seem to be less data on diesel locomotives. At Mordon, as already noted, trains could be seen passing about 0.5 km away, but, even with the wind blowing directly from the line, there was never any fluctuation of potential gradient or space charge density which could be associated with them.

On one occasion at Mordon, with clear skies and a slight haze giving a visibility of 4 - 5 km, the potential gradient was steady at about + 300 V m^{-1} - much higher than usual - although the space-charge density had a normal fair-weather value. The wind was blowing from the

east, and the effect may have been due to pollution from Imperial Chemical Industries' petrochemical plant at Billingham, 12 km upwind.

9.3 Precipitation current

During the point-discharge experiment (section 8.1.3), when the three field-mills were spread out roughly in a line, with about 50 m between each and the next, a period of heavy rain and hail was experienced. The field-mills, although not inverted, continued to operate, and gave an output with very rapid fluctuations in both directions. On all three mills, the same fluctuations occurred simultaneously: the way in which the three recorder pens moved together was very striking. Precipitation current, caused by the rain-drops giving their charge to the vanes of the mills, would give negligible output, and wind-blown charge would not have affected all three mills simultaneously. The field changes seem likely to be due to charge carried on the precipitation above the mills, and the fact that the changes were simultaneous indicates that on this occasion of heavy rain and hail, fluctuations of precipitation current occurred with periods of less than one second, and the changes were simultaneous over horizontal distances of about 100 m. Similar observations might be useful in precipitation studies.

CHAPTER 10

SUGGESTIONS FOR FURTHER WORK

Section 4.7 gives recommendations about the design of future space-charge collectors, and further possible experiments on the charge released by melting snow and on diffusion are discussed in sections 7.4 and 8.3 respectively.

10.1 General Observations

As has been indicated in chapter 4, the space-charge measurement apparatus used was found to be not very satisfactory for transport, and the author would not recommend attempting an experiment of this type with mobile apparatus. Breakdowns were frequent - it often seemed that three days in the field were necessary for one day of useful readings - and the equipment took a long time to set up and dismantle. Apart from the time taken for travel, it usually took about an hour to set up the apparatus at Mordon and to get it working, and another to take it down again. If there is any choice in the matter, an experiment on a fixed site is much to be preferred. If the recommendations of section 4.7 were adopted, space-charge measurement from a vehicle could become fairly reliable, but to attempt to run a whole

experiment with much apparatus on a mobile basis means much time wasted.

10.2 The Space-Charge Pulses

As was mentioned in chapter 6, the most obvious approach to the problem of the space-charge pulses is to attempt to trace the source of the charge. It appears it would be necessary to use two collectors, of which one at least would have to be mobile. With these, attempts could be made to detect the same pulse at different places perhaps a few hundred metres apart, to confirm that the pulses do move with the wind. It could be seen whether their magnitude changes with time, and perhaps whether they have an identifiable source.

On a suitable site, simultaneous measurements of Richardson's number (section 1.3.3) could confirm that the pulses are indeed associated with free convection. The surprising lack of correspondence with temperature or potential gradient fluctuations needs to be confirmed.

10.3 Point Discharge

As potential gradient is so easy to measure accurately, it is surprising that the method of Maund and Chalmers (1960) has not been used more widely, especially as their result on the sycamore was so un-

expected and possibly very important in computation of the charge "balance sheet" of the Earth. It should be easy to apply the method to a wood, since by integrating equation (8.4) the potential gradient due to discharge from an extensive width of trees could be calculated. This is an interesting and complicated problem, since the trees are not only shielded by the presence of their fellows, but by the space charge they produce upwind.

In a place like Durham, with relatively few thunderstorms, such an experiment might have to wait a long time for readings, but as it would be very simple to perform and would require little apparatus, this is not a great problem. The study of a single tree, or of a clump like that discussed in chapter 8, over a considerable period, might give valuable information of the relation of current with potential gradient.

REFERENCES

The abbreviations of titles of journals are those used in the "World List of Scientific Periodicals", 4th Edn. (Butterworth, London, 1960).

ANGELL J.K., 1964. Q.JL.R. Met. Soc. 90, 307-312. "Correlations of the vertical component of the wind at heights of 600, 1600 and 2600 ft. at Cardington."

ATLAS D., 1964. Adv. Geophys. 10, 317-478. "Advances in radar meteorology". Section 8, "Angel Echoes", pp. 432-457.

BENARD H., 1900. Revue Gen. Sci. Pur. Appl. 11, 1261-1271 & 1309-1328. "Tourbillons cellulaires dans une nappe liquide."

BENT R.B., 1964. J. Atmos. Terr. Phys. 26, 313-318, "The testing of apparatus for ground fair-weather space-charge measurements."

BENT R.B., 1965. Ph.D. Thesis, Durham Univ. "The electrical space charge in the lower atmosphere."

BENT R.B., and HUTCHINSON W.C.A., 1965. J. Atmos. Terr. Phys. 27, 91-99. "Electric space charges over melting snow on the ground".

BENT R.B., and HUTCHINSON W.C.A., 1966. J. Atmos. Terr. Phys. 28, 53-73, "Electric space charge measurements and the electrode effect within the height of a 21 m mast."

BENT R.B., COLLIN H.L., HUTCHINSON W.C.A., and CHALMERS J.A., 1965. J. Atmos. Terr. Phys. 27, 67-72. "Space charges produced by point discharge from trees during a thunderstorm."

BRUNT Sir David, 1925. Nature, Lond. 115, 300-301. Letter

BRUNT Sir David, 1937. Q.JL.R. Met. Soc. 63, 277-288. "Natural and artificial clouds."

BUNKER A.F., 1953. J. Met. 10, 212-218. "Diffusion, entrainment and frictional drag associated with non-saturated buoyant air parcels rising through a turbulent air mass."

CHALMERS J.A., 1952a. J. Atmos. Terr. Phys. 2, 301-305. "Point Discharge Currents."

CHALMERS J.A., 1952b. J. Atmos. Terr. Phys. 2, 155-159. "Negative electric fields in mist and fog."

CHALMERS J.A., 1957. "Atmospheric Electricity", 1st Edn. Pergamon Press, London.

CHALMERS J.A., 1966-1967. I, J. Atmos. Terr. Phys. 28, 565-572; II, J. Atmos. Terr. Phys. 28, 573-579; III, J. Atmos. Terr. Phys. 28, 1029-1033; IV, J. Atmos. Terr. Phys. 29, 217-219. "the theory of the electrode effect."

CHALMERS J.A., 1967. "Atmospheric Electricity", 2nd Edn. Pergamon Press, London.

CHANDRASEKHAR S., 1961. "Hydrodynamic and Hydromagnetic Stability." O.U.P.

COLLIN H.L., GROOM K.N., and HIGAZI K.A., 1966. J. Atmos. Terr. Phys. 28, 695-697. "The memory of the atmosphere."

DAVIES O.L.(Ed.), 1957. "Statistical Methods in Research and Production," 2nd Edn. Oliver and Boyd, London.

DAVIS R., and STANDRING W.G., 1947. Proc. R. Soc. A 191, 304-322. "Discharge currents associated with kite balloons."

DINGER J.E., and GUNN R., 1946. Terr. Magn. Atmos. Elect. 51, 477-494. "Electrical effects associated with a change of state of water."

DURST C.S., 1932. Met. Off. Geophys. Mem., No. 54. "Structure of wind over level country," by M.A. Giblett and others. Chapter 3: "A theory of Eddies," by C.S. Durst.

EINSTEIN A., 1905. Annln. Phys. 17, 549-560. "Über die von der molekularkinetischen Theorie der Warme gelforderte Bewegung von in ruhenden Flüssigkeiten suspendierten Teilchen."

ETTE A.I.I., 1966. J. Atmos. Terr. Phys. 28, 295-302. "Measurement of electrode by-passing efficiency in living trees."

FINDLATER J., 1959. Sailpl. Gliding 10, 134. "Wind shear and dry thermals."

FRENZEN P., 1962. Tellus 14, 173-176. "On the origin of certain symmetrical patterns of atmospheric convection."

GARROD M., 1966. Sailpl. Gliding 17, 8-9. "How far to the next thermal?"

GRANT D.R., 1965. Q. JL. R. Met. Soc. 91, 268-281. "Some aspects of convection as measured from aircraft."

GROOM K.N., 1966. Ph.D. Thesis, Durham Univ. "Disturbed weather measurements in atmospheric electricity using an instrumented van."

GROOM K.N., and CHALMERS J.A., 1967. J. Atmos. Terr. Phys. 29, 613-615. "Negative charges from high-tension power cables in fog."

HANKIN E.H., 1913. "Animal flight: a record of observation." Iliffe, London.

HIGAZI K.A., and CHALMERS J.A., 1966. J. Atmos. Terr. Phys. 28, 327-330. "Measurements of atmospheric electrical conductivity near the ground."

HIGUCHI K., 1963. J. Met. Soc. Japan, 2nd Series 41, 53-70. "The band structure of snowfalls."

HIRTH W., 1933. "Die Höhe Schule des Segefluges." Klasing, Berlin.

JAMES A.G., 1965. Students Q. J. Instn. Elect. Engrs. 35, 182-190. "A review of the problem of polluted insulation."

JAMES D.B., 1960. Sailpl. Gliding 11, 155-156. "Prospects of distant thermal detection."

JAMES D.G., 1953. Q.JL.R. Met. Soc. 79, 425-428. "Fluctuations of temperature below cumulus clouds."

JEFFREYS H., 1928. Proc. R. Soc. A 118, 195-208. "Some Cases of instability in fluid motion."

JHAWAR D.S., and CHALMERS J.A., 1967. J. Atmos. Terr. Phys. (In press). "Point-Discharge Currents Through Small Trees in Artificial Fields."

JONES J.I.P., and BUTLER H.E., 1958. Q.JL.R. Met. Soc. 84, 17-24. "The measurement of gustiness in the first few thousand feet of the atmosphere."

KASEMIR H.W., 1950. Arch. Met. Geophys. Bioklim. A 3, 84-97. "Zur Strömungstheorie des luft-elektrischen Feldes, I."

KEARON P., 1965. Sailpl. Gliding, 16, 406-409. "World contest - 1965. 'Flying to no avail'."

KRUEGER A.F., and FRITZ S., 1961. Tellus 13, 1-8. "Cellular cloud patterns revealed by TIROS 1."

KUETTNER J.P., 1959. Tellus 11, 267-294. "The band structure of the atmosphere."

LANGWELL P.A., 1948. J. Met. 5, 243-246. "Inhomogeneities of turbulence, temperature and moisture in the West Indies trade-wind region."

LARGE M.I., and PIERCE E.T., 1957. J. Atmos. Terr. Phys. 10, 251-257. "The dependence of point-discharge currents on wind as examined by a new experimental approach."

LATHAM J., 1964. Q. JL. R. Met. Soc. 90, 91-95. "The electrification of snowstorms and sandstorms."

LAW J., 1963. Q. JL. R. Met. Soc. 89, 107-121. "The ionization of the atmosphere near the ground in fair weather."

MACCREADY P.B. Jr., 1961. Schweizer Aerorevue 36, 403-407. "Improving thermal soaring flight techniques."

MACCREADY P.B. Jr., and PROUDFIT A., 1965. Q. JL. R. Met. Soc. 91, 54-59. "Self-charging of melting ice."

MAGONO C., and KIKUCHI K., 1963. J. Met. Soc. Japan, 2nd Series 41, 270-277. "On the positive electrification of snow crystals in the process of their melting."

MAGONO C., and KIKUCHI K., 1965. J. Met. Soc. Japan, 2nd Series 43, 331-342. "On the positive electrification of snow crystals in the process of their melting (II)."

MALKUS J.S., and SCORER R.S., 1955. J. Met. 12, 43- "Erosion of cumulus towers."

MAL S., 1930. Beitr. Phys. Atmos. 17, 40. "Forms of stratified cloud."

MAUND J.E., 1958. Ph.D. Thesis, Durham Univ. "Point discharge in atmospheric electricity."

MAUND J.E., and CHALMERS J.A., 1960. Q. JL. R. Met. Soc. 86, 85-90. "Point-discharge currents from natural and artificial points."

MILNER J.W., and CHALMERS J.A., 1961. Q. JL, R. Met. Soc. 87, 592-596. "Point discharge from natural and artificial points (Pt.II)."

MOORE C.B., VONNEGUT B., SEMONIN R.G., BULLOCK J.W., and BRADLEY W., 1962. J. Geophys. Res. 67, 1061-1071. "Fair weather atmospheric electric potential gradient and space charge over central Illinois, summer 1960."

MORGAN W., 1960. Q. JL. R. Met. Soc. 86, 107-113. "Determination of the straight line of best fit to observational data of two related variates when both sets of values are subject to error."

MORTON B.R., TAYLOR G.I., and TURNER J.S., 1956. Proc. R. Soc. A 234, 1-23. "Turbulent gravitational convection from maintained and instantaneous sources."

MÜHLEISEN R., 1953. B. Geophys. 29, 142-160. "Die luftelektrischen Elemente in Grossstadtbereich."

NOLAN P.J., and KENNY P.J., 1953. J. Atmos. Terr. Phys. 3, 181-185. "Anomalous loss of condensation nuclei in rubber tubing."

NORTON K.A., RICE P.L., and VOGLER L.E., 1955. Proc. Inst. Radio Engrs. 43, 1488-1526. "The use of angular distance in estimating transmission loss and fading range for propagation through a turbulent atmosphere over irregular terrain."

PAGE L., and ADAMS N.I., 1958. "Principles of Electricity," 3rd Edn. Van Nostrand, Princeton, N.J.

PASQUILL F., 1962. "Atmospheric Diffusion." Van Nostrand, London.

PEARSON T., 1966. Sailpl. Gliding 17, 462-465. "Rhodesian championships - October 1966."

PIERCE E.T., 1959. "Recent Advances in Atmos. Elect." Pergamon, N.Y. (Proc. of second Wentworth Conf., May 1958) pp. 5-16. "Some topics in atmospheric electricity."

PLUVINAGE P., and STAHL P., 1953. Annls. Géophys. 9, 34-43. "La conductibilité électrique de l'air sur l'inlandsis Groenlandais."

PRIESTLEY C.H.B., 1954. Aust. J. Phys. 7, 176-201. "Convection from a large horizontal surface."

PRIESTLEY C.H.B., 1955. Q. JL. R. Met. Soc. 81, 139-143. "Free and forced convection in the atmosphere near the ground."

PRIESTLEY C.H.B., 1956. Proc. R. Soc. A 238, 287-304. "Convection from the Earth's surface."

PRIESTLEY C.H.B., 1959. "Turbulent Transfer in the Lower Atmosphere." Chicago U.P.

PRIESTLEY C.H.B., and BALL F.K., 1955. Q. JL. R. Met. Soc. 81, 144-157. "Continuous convection from an isolated source of heat."

RAINEY R.C., 1947. Q. JL. R. Met. Soc. 73, 437-452. "Observations on the structure of convection currents; meteorological aspects of some South African gliding flights."

RAYLEIGH, Lord, 1916. Phil. Mag., 6th series 32, 529-546. "On convection currents in a horizontal layer of fluid, when the higher temperature is on the underside."

RUHNKE L.H., 1962. J. Geophys. Res. 67, 2767-2772. "Electrical conductivity of air on the Greenland Ice Cap."

RUMFORD Count, 1870. "Complete Works" 1, 239. (American Acad. of Arts & Sciences, Boston, Mass.) "Of the propagation of heat in fluids."

SAGALYN R.C., 1960. "Handbook of Geophysics." Macmillan, N.Y., for U.S.A.F. Fig. 9.2.

SCORER R.S., 1954a. Met. Mag., Lond. 83, 202- . "Bubble Convection."

SCORER R.S., 1954b. Q. JL. R. Met. Soc. 80, 68-77. "Nature of convection as revealed by soaring birds and dragonflies."

SCORER R.S., 1957. J. Fluid Mech. 2, 583- . "Experiments on the convection of isolated masses of buoyant fluid."

SCORER R.S., 1958. "Natural Aerodynamics". Pergamon, London.

SCORER R.S., and LUDLAM F.H., 1953. Q. JL. R. Met. Soc. 79, 94-103. "Bubble theory of penetrative convection."

SCORER R.S. and RONNE C., 1956. Weather, Lond. 11, 151-154. "Experiments with convection bubbles."

SLATER A.E., 1965. Sailpl. Gliding 16, 506-507. "Can vultures smell thermals?"

SMITH A., 1963. "Throw out Two Hands." George Allen and Unwin, London.

SUTTON O.G., 1953. "Micrometeorology" McGraw-Hill, N.Y.

TAYLOR R.J., 1956. Q. JL. R. Met. Soc. 82, 89-91. "Some measurements of heat flux at large negative Richardson number."

TAYLOR R.J., 1958. Aust. J. Phys. 11, 168-176. "Thermal structures in the lowest layers of the atmosphere."

THOMSON J., 1881. Proc. Glasgow Phil. Soc. 13, 464-468. "On a changing tesselated structure in certain liquids."

VONNEGUT B., and MOORE C.B., 1958. Rept. on contract AF 19 (604) 1920, Arthur D. Little, Inc. "A study of techniques for measuring the concentration of space charge in the lower atmosphere."

VUL'FSON N.L., 1964. "Convective Motions in a Free Atmosphere." Israel Program for Scientific Translations, Jerusalem. Orig. pub. in Russian in 1961 by Acad. Sci. USSR.

WARNER J., and TELFORD J.W., 1963. J. Atmos. Sci. 20, 313-318. "Some patterns of convection in the lower atmosphere."

WEBB E.K., 1958. Q. JL. R. Met. Soc. 84, 118-125. "Vanishing potential temperature gradients in strong convection."

WEBB E.K., 1962. Nature, Lond. 193, 840-842. "Thermal convection in wind-shear."

WEBB E.K., 1964. Appl. Optics 3, 1329-1336. "Daytime thermal fluctuations in the lower atmosphere."

WELCH L., 1953. Q. JL. R. Met. Soc. 79, 429-430. "Thermals as seen by glider pilots."

WHITLOCK W.S., 1955. Ph.D. Thesis, Durham Univ. "Variations in the Earth's electric field."

WHITLOCK W.S., and CHALMERS J.A., 1956. Q. JL. R. Met. Soc. 82, 325-336. "Short-period variations in the atmospheric potential gradient."

WILLIAMSON J., 1966. Sailpl. Gliding 17, 48-50. "Teaching thermal soaring."

WILLS P., 1961. "Where no Birds Fly."

WOODCOCK A.H., 1940. J. Mar. Res. 3, 248-253. "Convection and soaring over the open sea."

WOODCOCK A.H., and WYMAN J. 1947. Ann. N.Y. Acad. Sci. 48, 749- . "Convective motion in air over the sea."

WOODWARD B., 1959. Q. JL. R. Met. Soc. 85, 144-151. "The motion in and around isolated thermals."

WORMELL T.W., 1930. Proc. R. Soc. A 127, 567-590. "Vertical electric currents below thunderstorms and showers."

YATES A.H., 1953. Q. JL. R. Met. Soc. 79, 420-424. "Atmospheric convection; the structure of thermals below cloud-base."